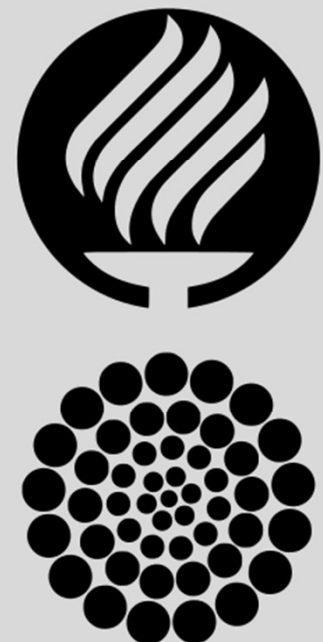


Fabrication of graphitic-carbon suspended nanowires through mechano-electrospinning of photo-crosslinkable polymers



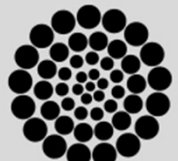
Osamu Katagiri-Tanaka
A01212611@itesm.mx

Principal Advisor: **Dr. Héctor Alán Aguirre Soto**
Co-advisor and Director of Program: **Dra. Dora Iliana Medina Medina**

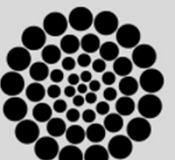
02 Dec 2020

Agenda

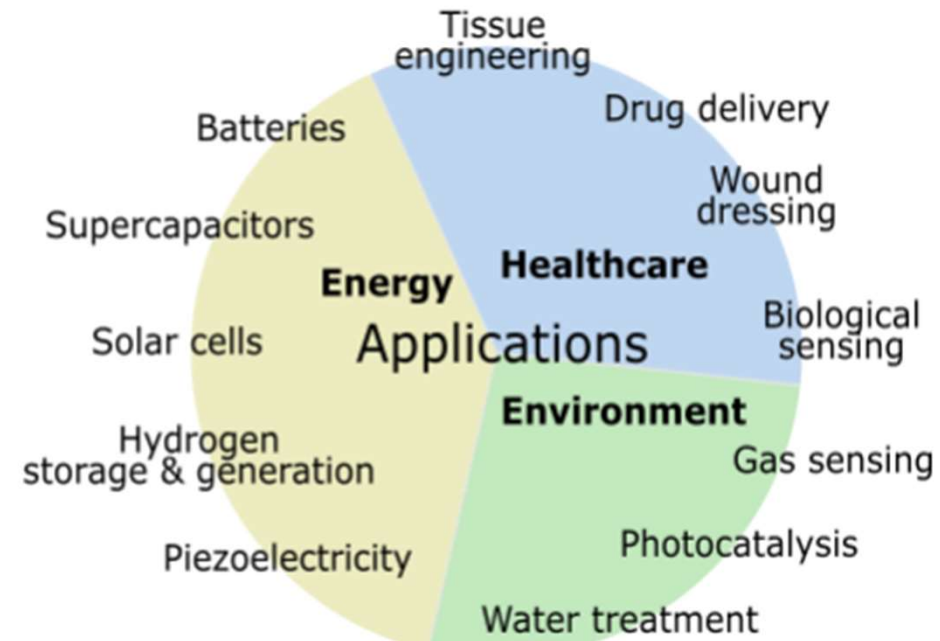
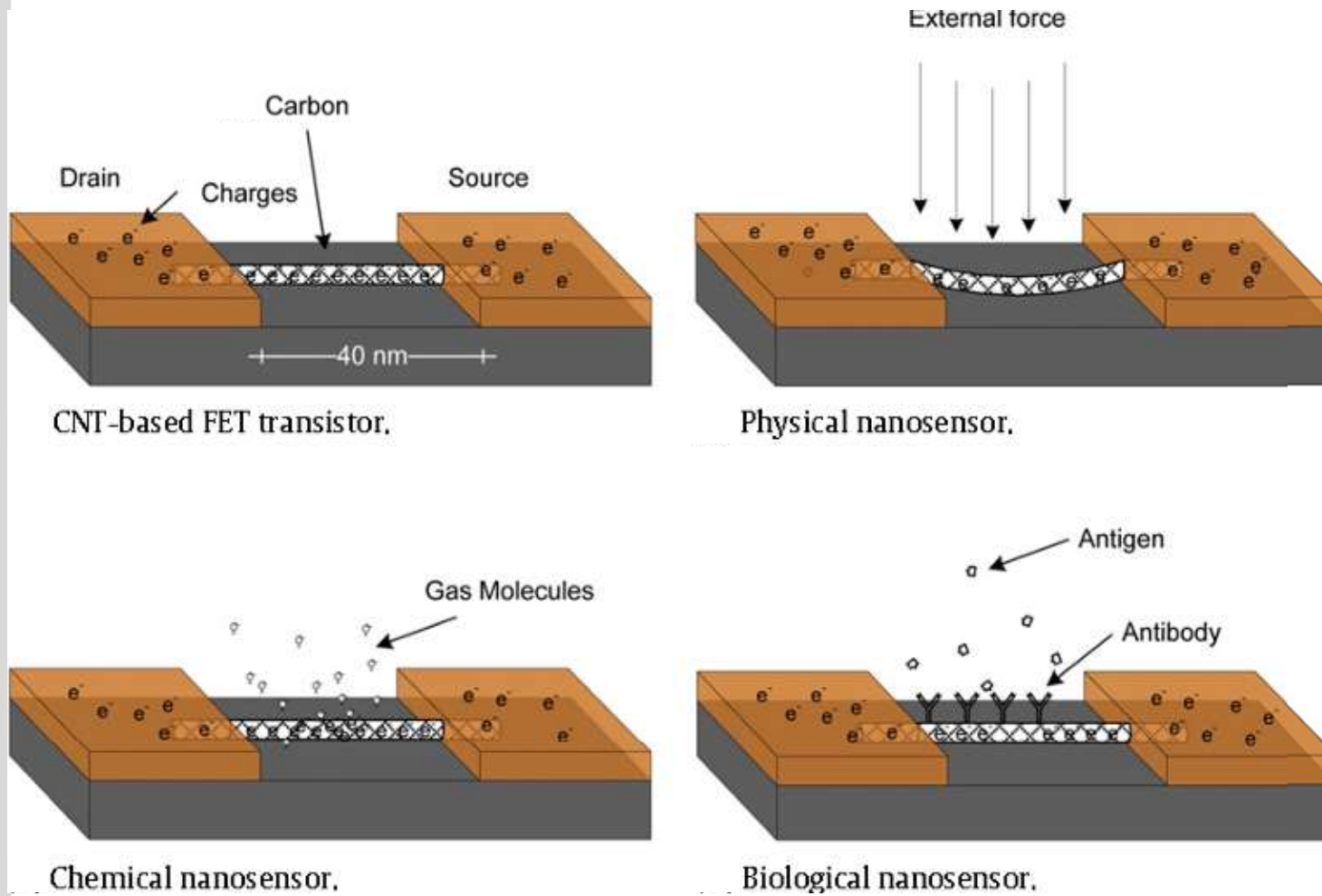
1. Motivation & Problem Statement : 10 min
2. Objectives : 3 min
3. NFES literature review : 10 min
4. Rheology Analyses : 10 min
5. Fabrication & Characterization : 5 min
6. Conclusions & Future Work : 3 min



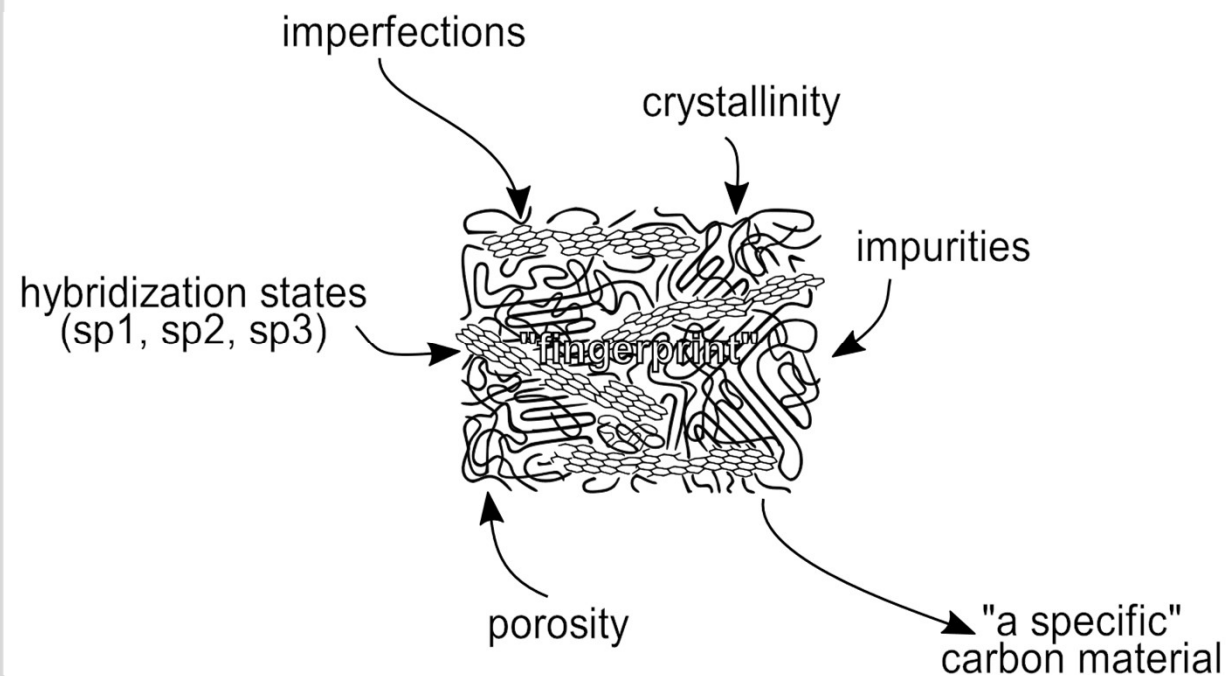
Motivation & Problem Statement



Glass-like Carbon NWs: Applications

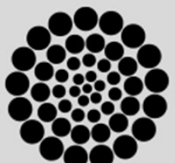


Carbon Based Nanomaterials (CBNs)

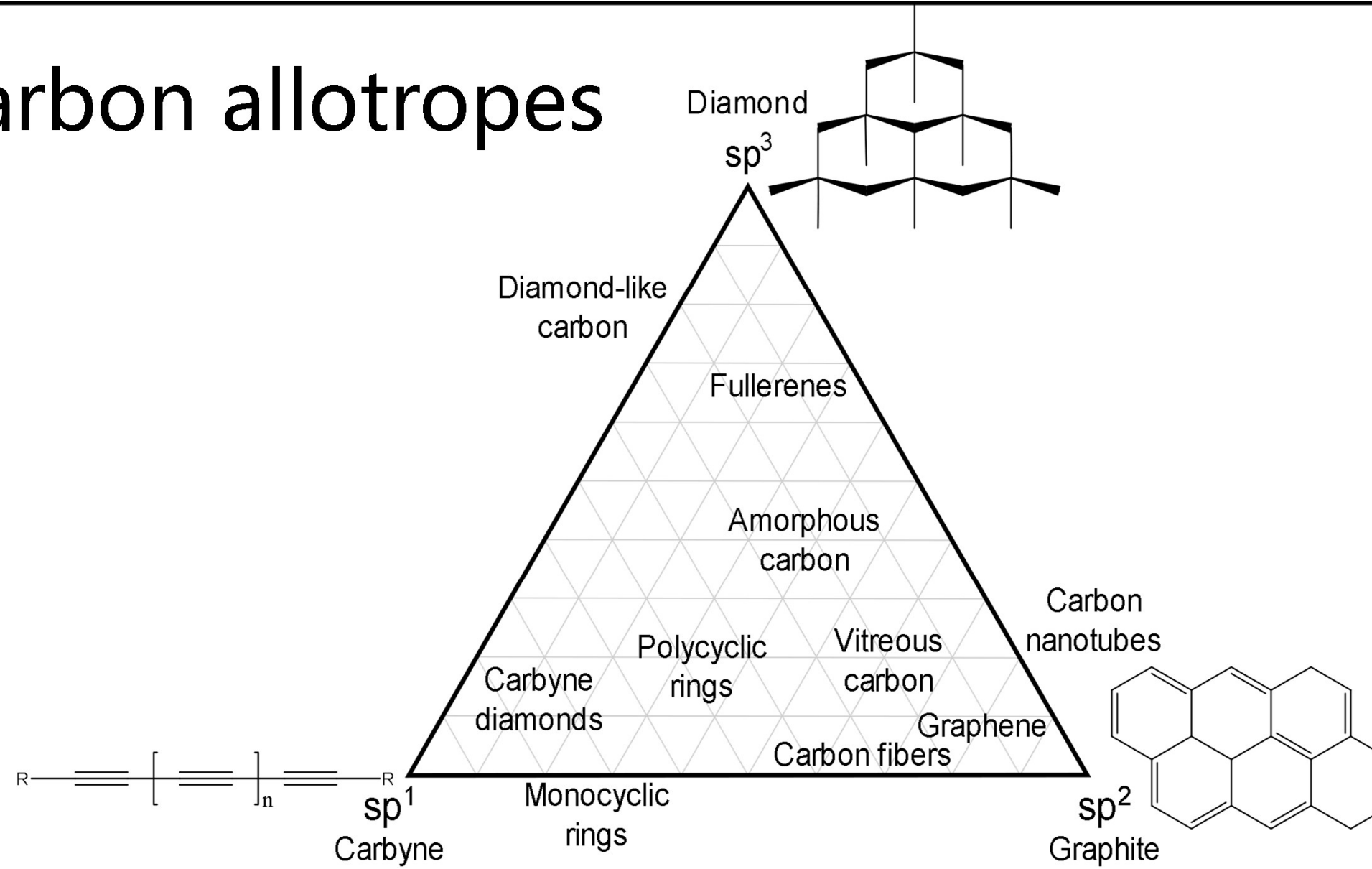


The crystallite size, molecular arrangement, and anisotropy determine the material's properties.

The interminable collection of CBNs range from soft, conductive lubricants to very hard, low conductivity solids; and from black colour, bulks to transparent, disordered thin films



Carbon allotropes



R.B. Heimann, S.E. Evsvukov, Y. Koga, Carbon N. Y. 35 (1997) 1654–1658. [https://doi.org/10.1016/S0008-6223\(97\)82794-7](https://doi.org/10.1016/S0008-6223(97)82794-7).

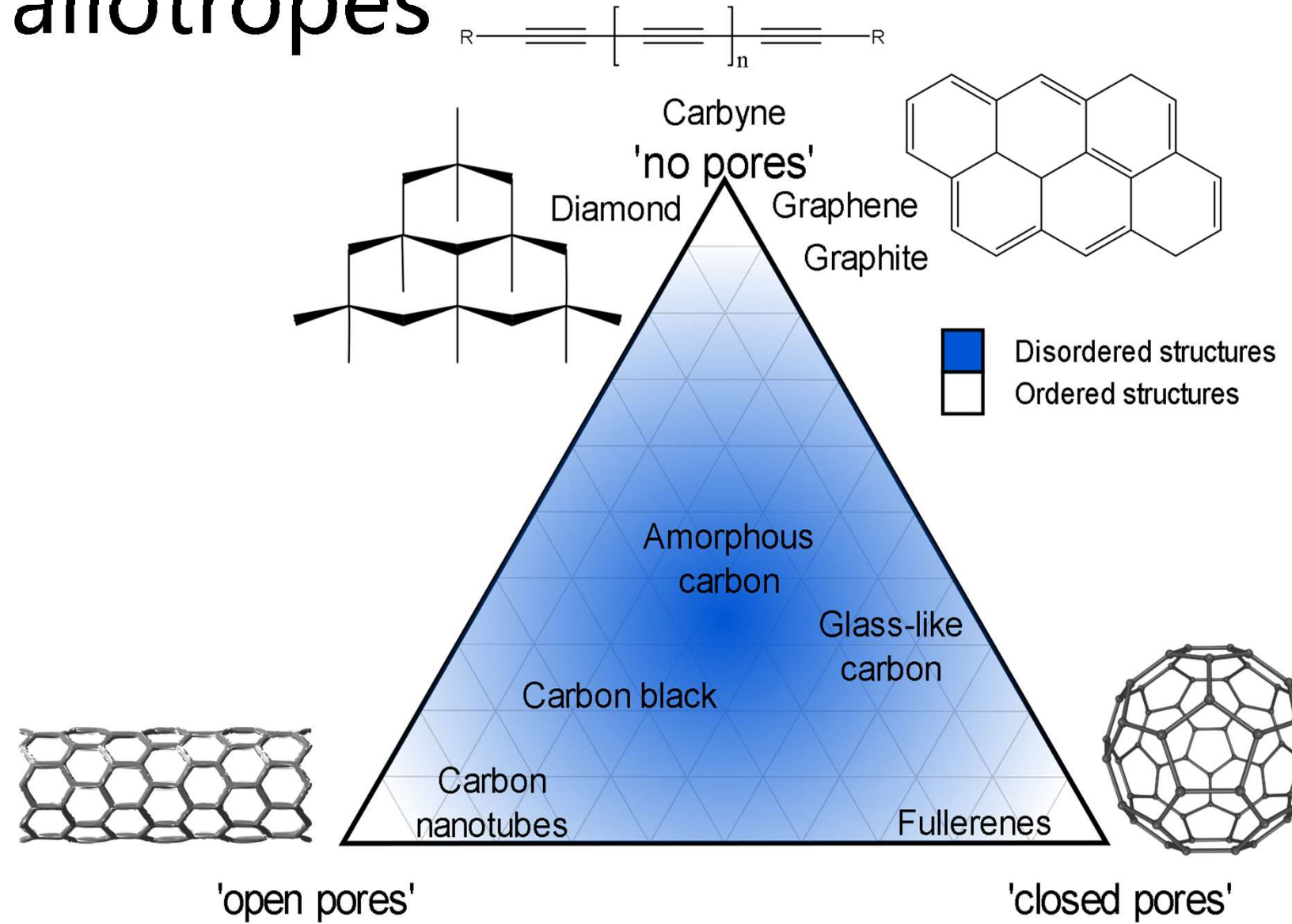
E.A. Belenkov, Chelyabinsk State University, Chelyabinsk, Russia, 2003: p. 5.

M. Fedel, Elsevier, 2013: pp. 71–102. <https://doi.org/10.1533/9780857093516.1.71>.

M. Razeghi, Springer International Publishing, Cham, 2019. <https://doi.org/10.1007/978-3-319-75708-7>.

K. Alstrup Jensen, J. Bøgelund, P. Jackson, N. Raun Jacobsen, R. Birkedal, P. Axel Clausen, A. Thoustrup Saber, H. Wallin, U. Birgitte Vogel, The Danish Environmental Protection Agency, 2015.

Carbon allotropes



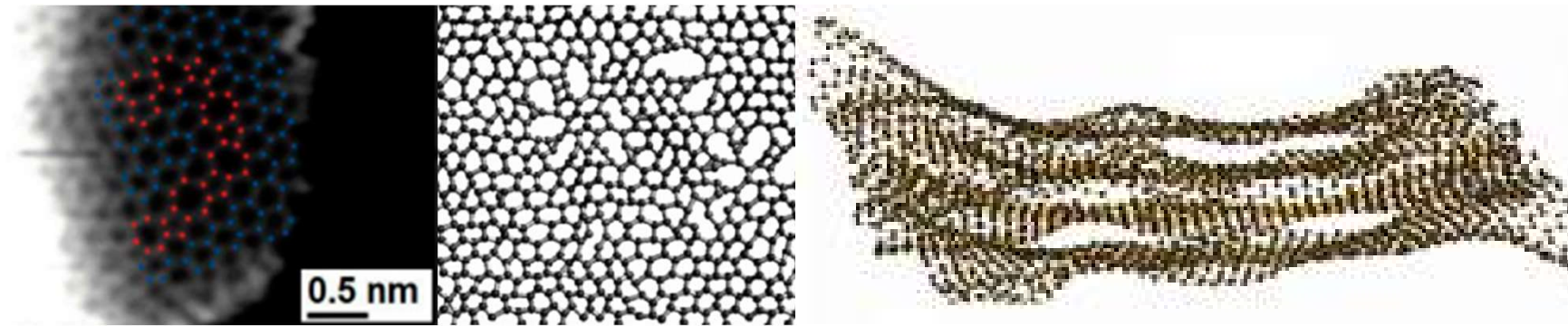
R.L. McCreery, Chem. Rev. 108 (2008) 2646–2687. <https://doi.org/10.1021/cr068076m>.

S. Beigi-Boroujeni, O. Katagiri-Tanaka, B. Cardenas-Benitez, S.O. Martinez-Chapa, A. Aguirre-Soto, Mater. Today Proc. (2020). <https://doi.org/10.1016/j.matpr.2020.10.014>.

Harry Marsh. Elsevier, Apr. 1989, p. 43. ISBN: 9780408038379. DOI: 10.1016/C2013-0-04111-4. URL: <https://linkinghub.elsevier.com/retrieve/pii/C20130041114>.

Pierson Hugh. Elsevier, 1994, p. 419. ISBN: 9780815513391.

Glass-like Carbon



Attractive for its electrochemical stability, thermal resistance, electrical conductivity, biocompatibility and is gas impermeable.

- It is used in the manufacture of semiconductors.

MicroChem's SU-8 & Tokai's recipe

Electrical resistivity, comparison:

highly oriented
pyrolytic graphite
(HOPG)

$\times 10^3$

TOKAI Glassy
carbon

$\times 4$

SU-8 glass-like
carbon



Tokai's recipe is a secret ...

MicroChem's SU-8 & Tokai's recipe

SU-8
glass-like carbon
resistivity:

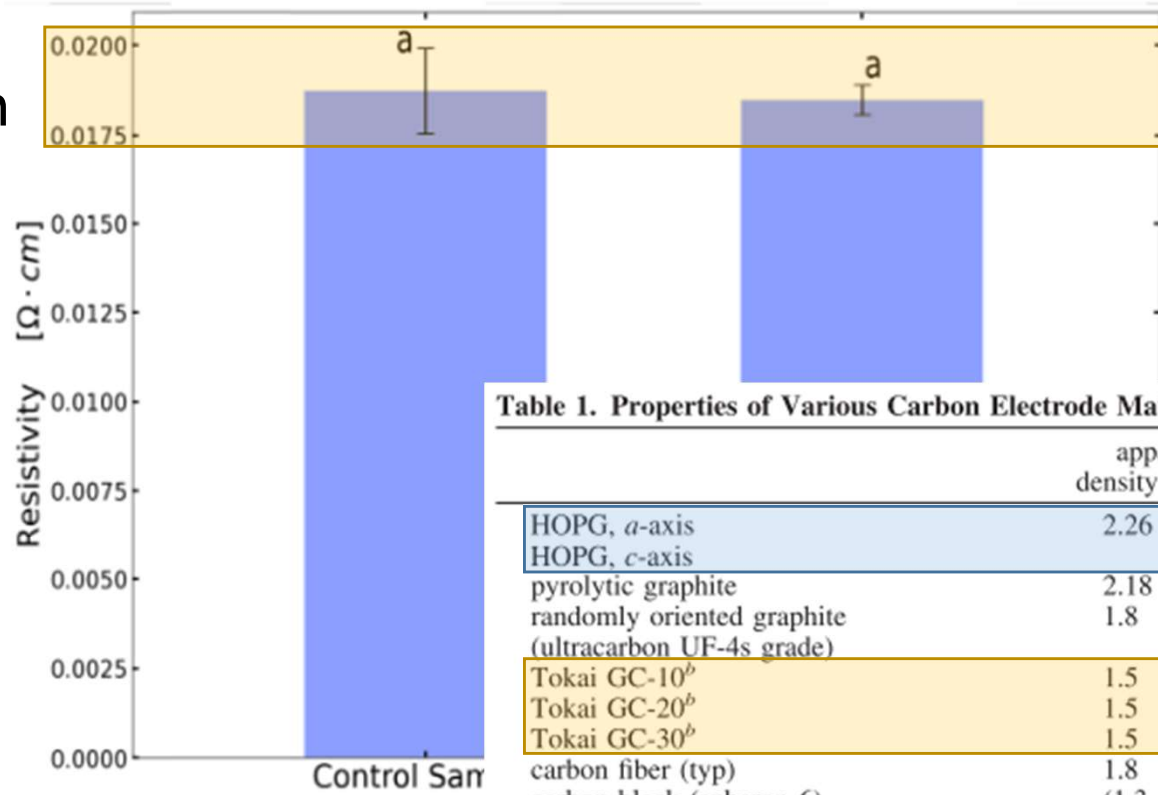


Table 1. Properties of Various Carbon Electrode Materials³

	apparent density (g/cm^3)	d_{002} (\AA)	ρ ($\Omega \cdot \text{cm}$)	L_a (\AA)	L_c (\AA)
HOPG, <i>a</i> -axis	2.26	3.354	4×10^{-5}	> 10000	
HOPG, <i>c</i> -axis			0.17		> 100000
pyrolytic graphite	2.18	3.34		1000 (typ) ^a	1000 (typ)
randomly oriented graphite (ultracarbon UF-4s grade)	1.8	3.35	1×10^{-3}	300 (typ)	500 (typ)
Tokai GC-10 ^b	1.5	3.49	4.5×10^{-3}	20 (typ)	-10
Tokai GC-20 ^b	1.5	3.48	4.2×10^{-3}	25 (typ)	12
Tokai GC-30 ^b	1.5	3.41	3.7×10^{-3}	55	70
carbon fiber (typ)	1.8	3.4	$(5-20) \times 10^{-4}$	> 100	40
carbon black (spheron 6)	(1.3–2.0) ^c	3.55	0.05	20	13
evaporated <i>a</i> -C	-2.0	>3.4	$\sim 10^3$	~ 10	~ 10
<i>a</i> -C:H	1.4–1.8		$10^7 - 10^{16}$		
pyrolyzed photoresist film (PFF)			0.006 ¹⁴⁹		
boron-doped diamond			0.05–0.5 ^d		
N-doped amorphous tetrahedral carbon			10–1000 ^e		

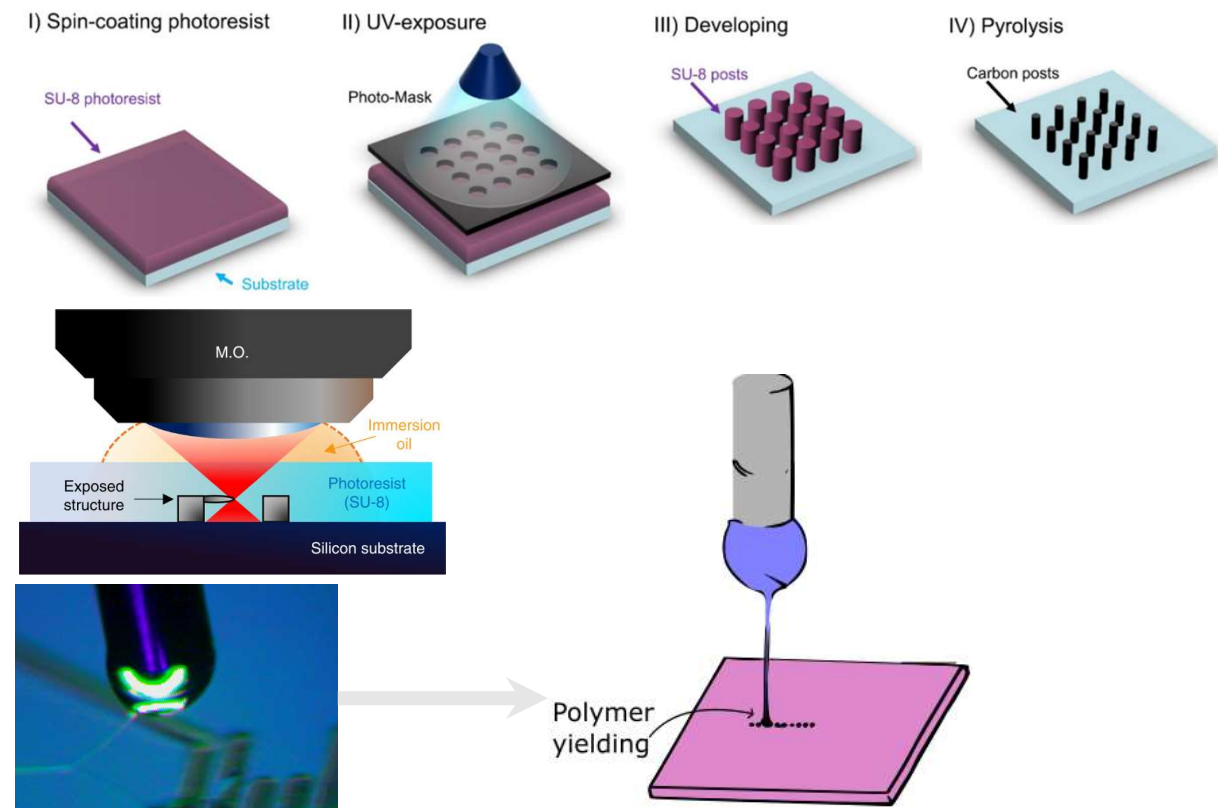
^a Entries marked "typ" may vary significantly with sample or preparation procedures. ^b Number refers to heat treatment temperatures, for example, GC-20 was treated at 2000 °C. ^c Depends on technique used to measure density. ^d Depends strongly on doping level. See ref 30. ^e See ref 35.

Current approaches

Photolithography Physical & Optical Limitations

Two-Photon Polymerization (TPP)
Slow (mm per sec) & **Expensive**

***Near-Field Electrosprining** (NFES)
Suspended Nanowires w/Spatial Control



V. Galstyan, M. Bhandari, V. Sberveglieri, G. Sberveglieri, E. Comini, Metal Oxide Nanostructures in Food Applications: Quality Control and Packaging, Chemosensors. 6 (2018) 16. <https://doi.org/10.3390/chemosensors6020016>.

D. Kluge, J.C. Singer, B.R. Neugirg, J.W. Neubauer, H.-W. Schmidt, A. Fery, Top-down meets bottom-up: A comparison of the mechanical properties of melt electrospun and self-assembled 1,3,5-benzenetrisamide fibers, Polymer (Guildf). 53 (2012) 5754–5759. <https://doi.org/10.1016/j.polymer.2012.10.016>.

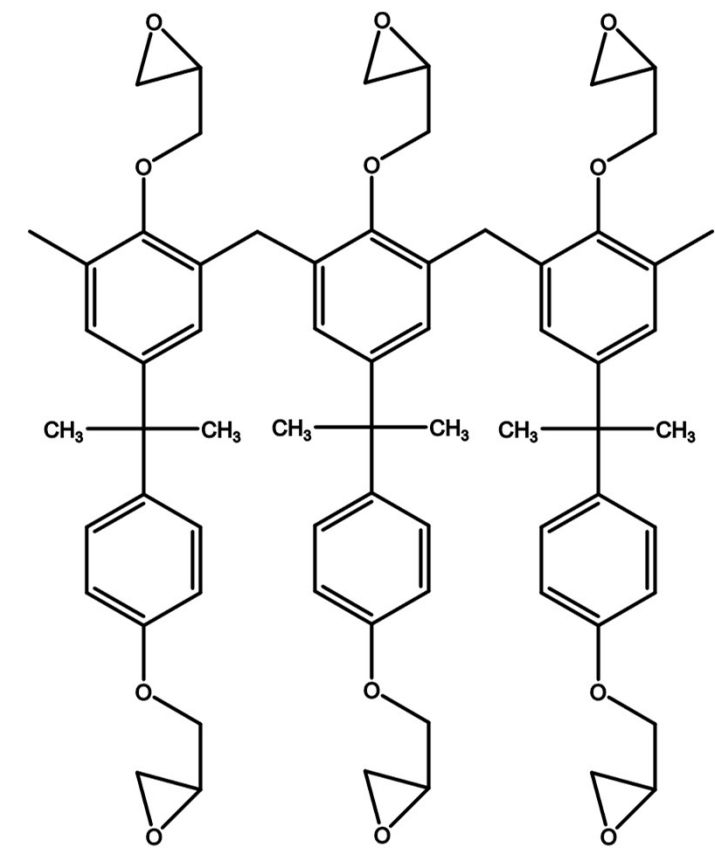
MicroChem's SU-8

Pyrolysis of SU8 is currently the typical method to produce glass-like carbon.

1. Polymer patterning through **photolithography**
2. Carbonization through **pyrolysis**

However, **photolithography generates waste** in the spin-coating and developing steps. Also, it presents **structural limitations**.

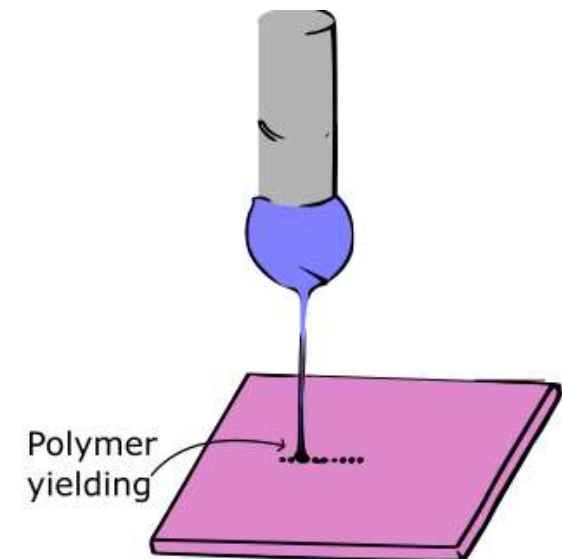
Limitations can be overcome with other fabrication techniques, such as **NFES**



Structure of SU-8 after UV exposure

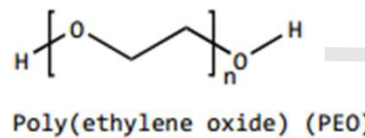
MicroChem's SU-8

However, **SU-8 as is not electrospinnable**
SU-8 does not have the right viscosity & solution conductivity.
SU-8 is design for photolithography.



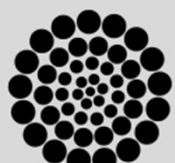
SU-8 + TBF + PEO formulation:
TBF to increase the **solution conductivity**

Tetrabutylammonium tetrafluoroborate (TBF)



& PEO to provided the required **viscosity**

... both needed for **smooth PEO flow** during electrospinning

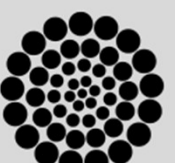


Problem Statement

- Properties of an electrospun fiber depend on many parameters,
- and each parameter also depends on the polymer-solvent system.

Solution Parameters: **Ambient Parameters:** **Process Parameters:**

- | | | |
|---------------------------|---------------|--------------------|
| • Concentration | • Humidity | • Applied Voltage |
| • Molecular weight | • Temperature | • Flow rate |
| • Viscosity | | • Working distance |
| • Electrical conductivity | | |



The interdependence between the process and solution parameters presents a **challenge** to predict the fiber diameter.

Best Results so far by NFES (previous work)

Fiber yield rate of 81 %

Fiber diameter before pyrolysis of 4.966 μm

Fiber diameter after pyrolysis of 204 nm

Fiber length of $60.5 \pm 4.3 \mu\text{m}$

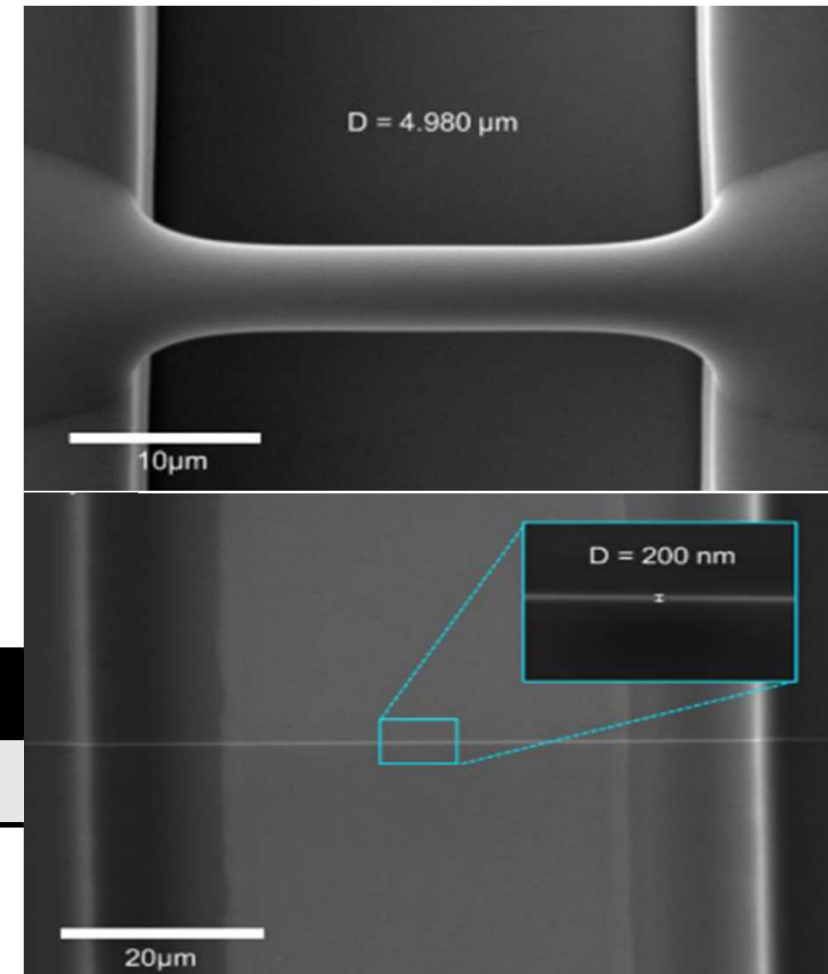
Fiber resistance from $407 \text{ K}\Omega$ to $1.727 \text{ M}\Omega$

wt% PEO
0.25

SU-8 2002 [mg]
2246

PEO [mg]
5.65

TBF [mg]
11.32

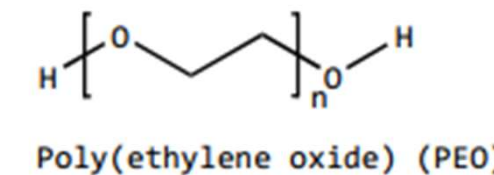


Implications of PEO

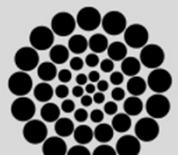
The **fiber yield rate** and **fiber conductivity** are impacted negatively as PEO introduces more oxygen to the solution

Some samples are destroyed during pyrolysis

High variance in the obtained conductivity across samples.



The addition of oxygen modifies the carbon structure.



Objectives



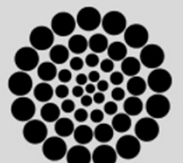
Objectives

- General. Formulate polymer/solvent combinations that have the greatest potential to replace or modify the SU-8/PEO formulation for the fabrication of microscopic polymer fibers that may be converted to conductive suspended carbon nano-wires.
- Specific1. Learn how the diameter of the electrospun polymer fiber can be controlled by appropriate tuning of the **NFES parameters and solution properties**.
- Specific2. Through **rheological analyses**, determine if polymer solutions have comparative viscoelastic properties to those of the SU-8/PEO benchmark, and if they can be easily electrospun by NFES.
- Specific3. Propose **alternatives to the SU-8/PEO benchmark** formulation for the production of microscopic polymer fibers with potential for the fabrication of carbon nano-wires.

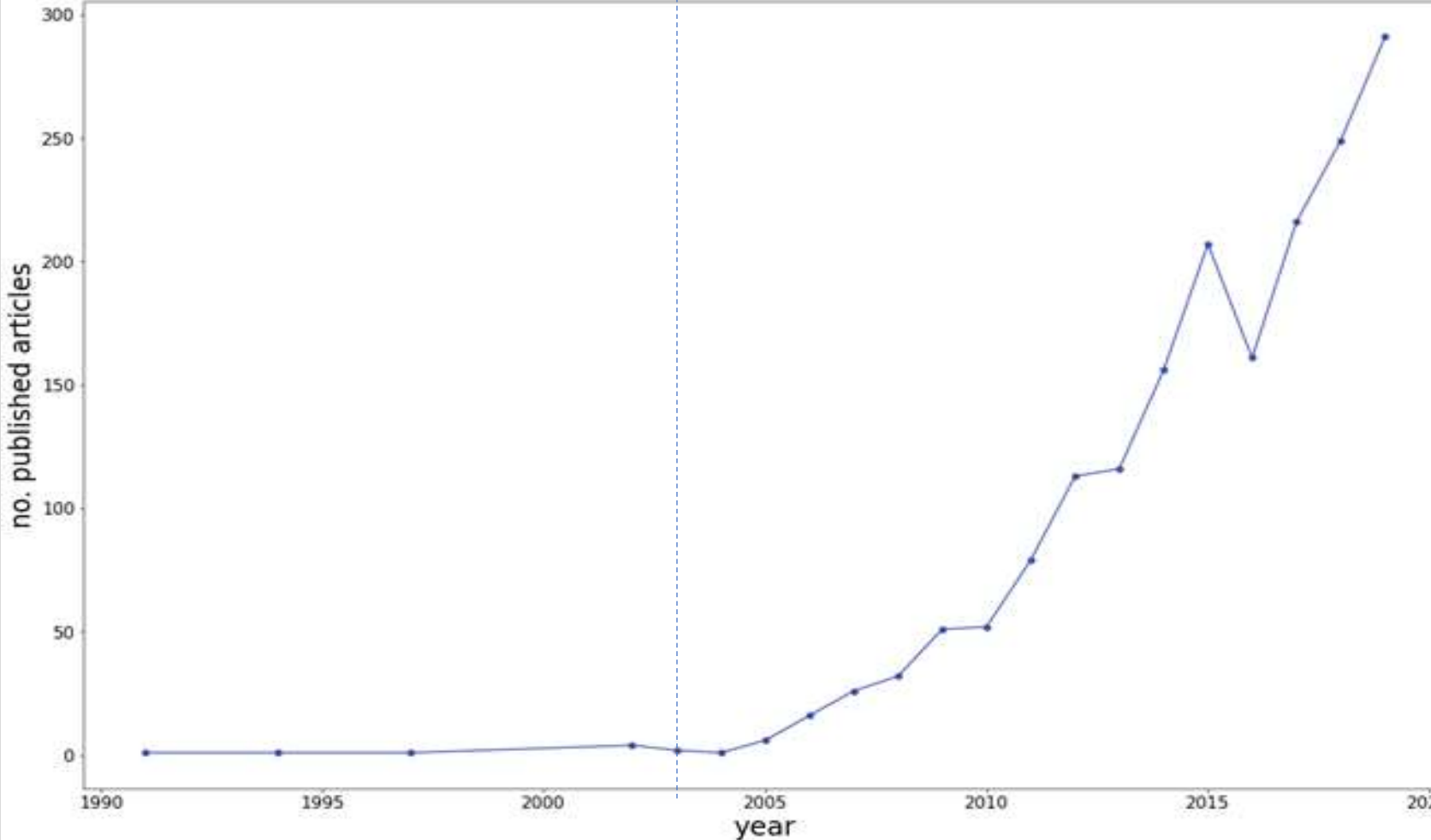


NFES literature review

Specific Objective 1. Learn how the diameter of the electrospun polymer fiber can be controlled by appropriate tuning of the **NFES parameters and solution properties.**

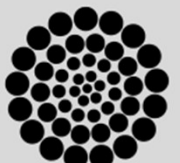


Methods: NFES literature
(first NFES apparatus built in 2003 by J. Kameoka et al.)



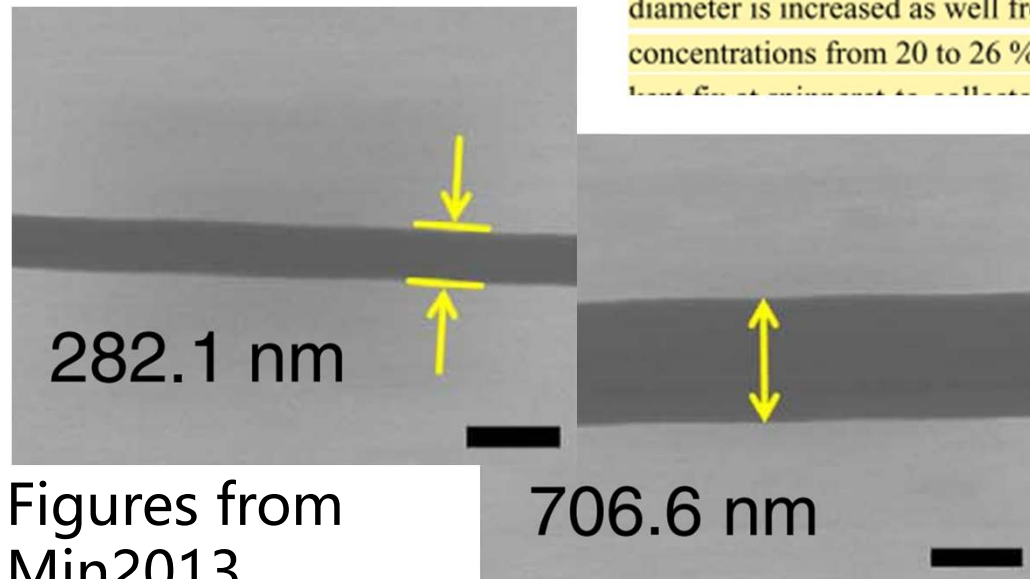
Thinnest fiber achieved
by C. Chang et al. with
~50 nm in diameter.
(PEO in water)

However, **fiber yield rate**
was not reported



Methods: Data collection (analysis of NFES articles from 2003 to 2020)

The author mentions the process parameters and fiber properties within the article **in writing**.



HHS Public Access

Author manuscript

Adv Healthc Mater. Author manuscript; available in PMC 2018 October 01.

Published in final edited form as:

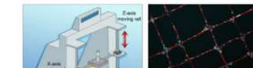
Adv Healthc Mater. 2017 October ; 6(19): . doi:10.1002/adhm.201700456.

Fattahi2017

3D Near-Field Electrospinning of Biomaterial Microfibers with Potential for Blended Microfiber-Cell Loaded Gel Composite Structures

PMMA microfibers. First, we varied the concentration of PMMA in nitromethane from 16 to 24 % (W/V) and observed as the PMMA concentration increased the polymer fiber diameter is increased as well from 1.86 ± 0.41 to 4.73 ± 1.40 μm corresponding to concentrations from 20 to 26 % (W/V, PMMA/nitromethane) while other parameters were

polymeric fibers in highly organized, controlled and reproducible manner. The research strategy described in this work offers several significant advantages including: 1) producing precise patterns of fibers on relatively large scale area with minimum material consumption, 2) ability to print in all three directions of X, Y and Z, 3) offering an inexpensive method with easy control over shape and orientation of fibers compared to other available methods, and 4) readily combines with other pre-patterned nanostructures or microstructures such as gels (e.g. collagen gel) to create multi-material composites.



Methods: Data collection

(analysis of NFES articles from 2003 to 2020)

The author provides the data in **plots and graphs**.

WebPlotDigitalizer (<https://github.com/ankitrohatgi/WebPlotDigitizer>):

panels a to c when the voltage is switched from 400 to 200 V in steps of 100 V. The light against the smooth Si surface. X-Y stage speed is 40 mm/s.

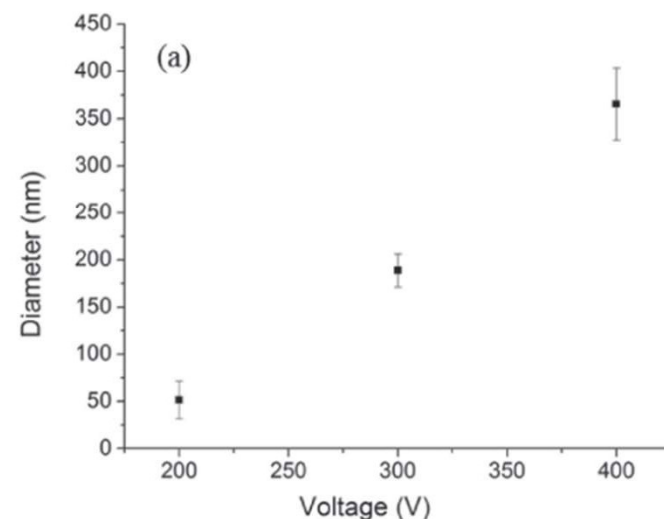
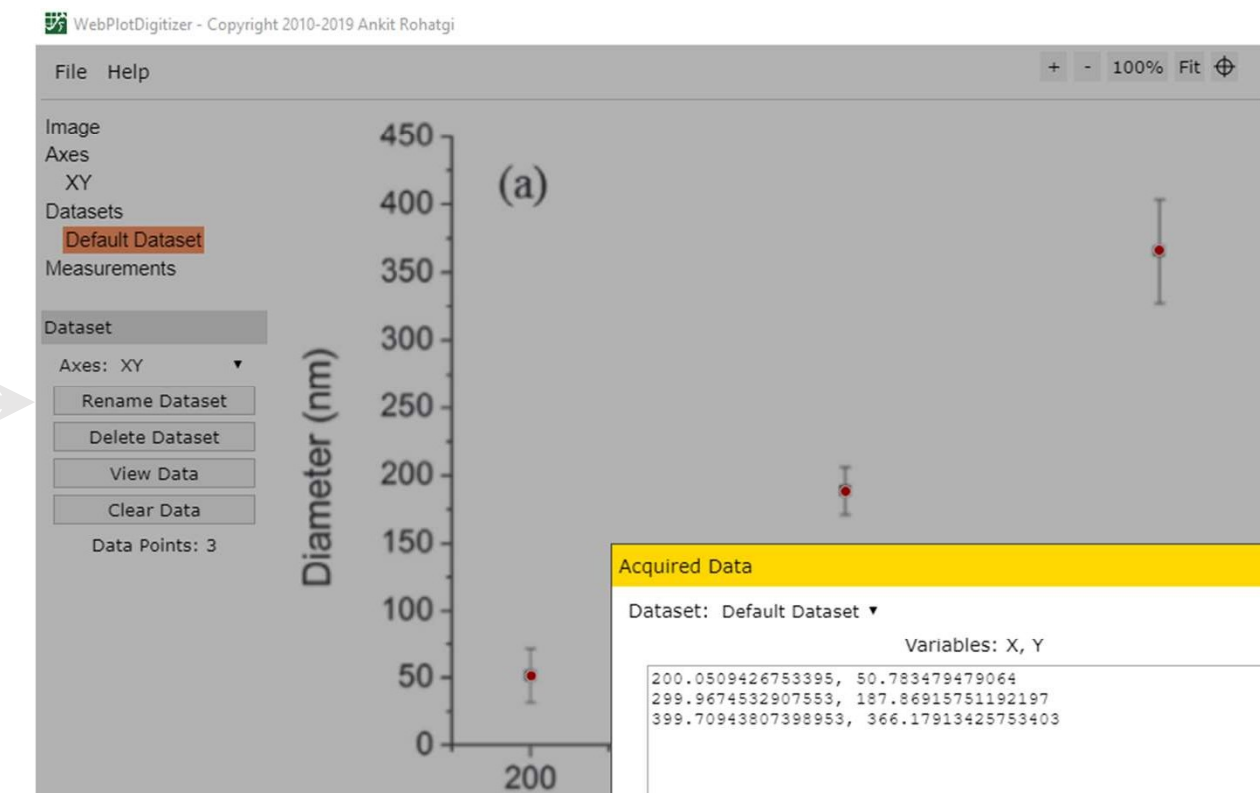


Figure 6. Correlation between nanofiber thickness and voltage applied between

M.J. Madou, D. Dunn-Rankin, L. Kulinsky, A. Mirsepassi, G.S. Bisht, S. Oh, G. Canton, Nano Lett. 11 (2011) 1831–1837. <https://doi.org/10.1021/nl2006164>.



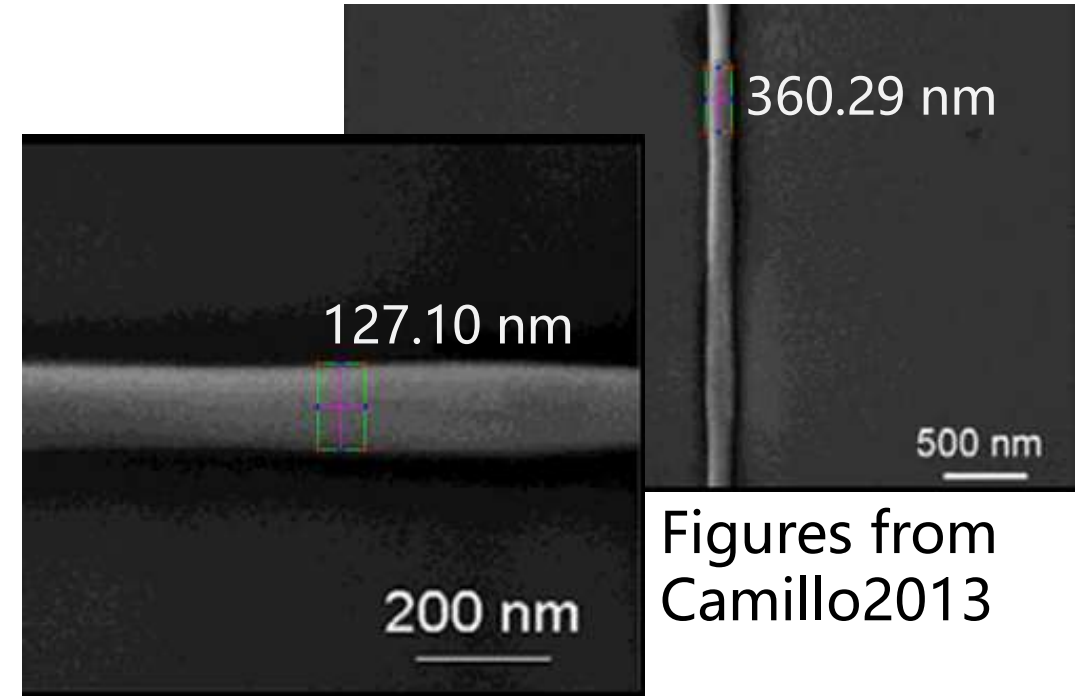
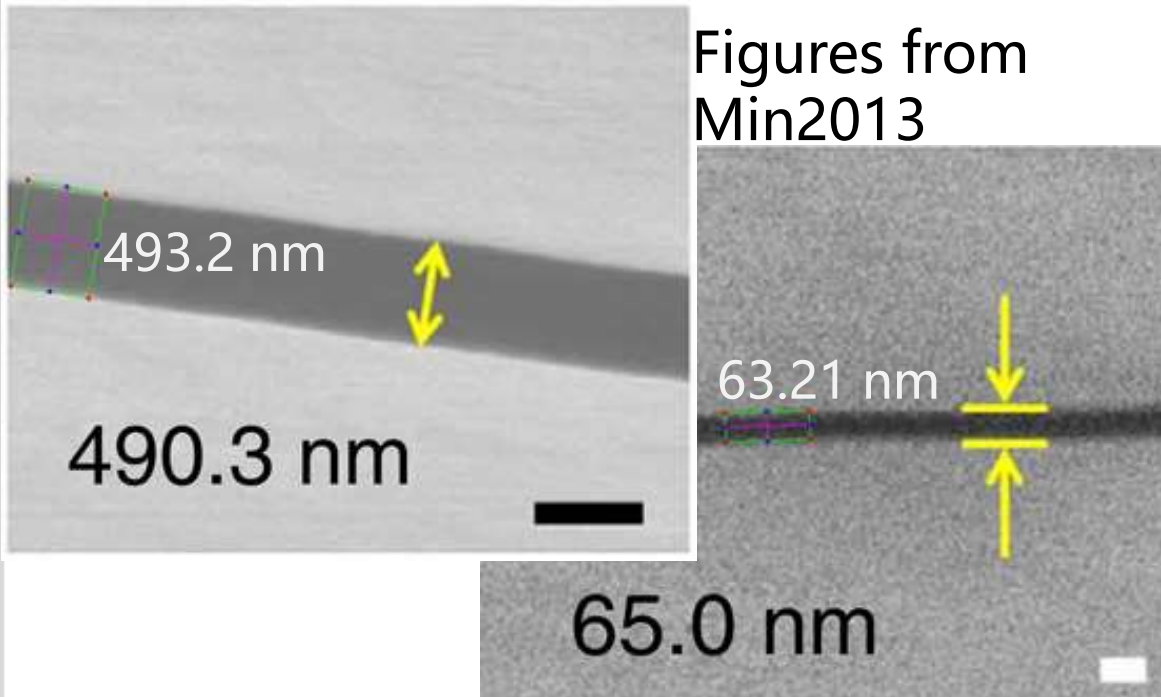
Applied voltage vs. fiber diameter by Madou2011

Methods: Data collection

(analysis of NFES articles from 2003 to 2020)

The author does not mention the fiber diameter in writing but provides a **EM characterization**.

Python Image Analysis (with a 3.2% error in avg.):



S.-Y. Min, T.-S. Kim, B.J. Kim, H. Cho, Y.-Y. Noh, H. Yang, J.H. Cho, T.-W. Lee, Nat. Commun. 4 (2013) 1773. <https://doi.org/10.1038/ncomms2785..>

<https://github.com/katagirimx/OpenCV-image-measuring>

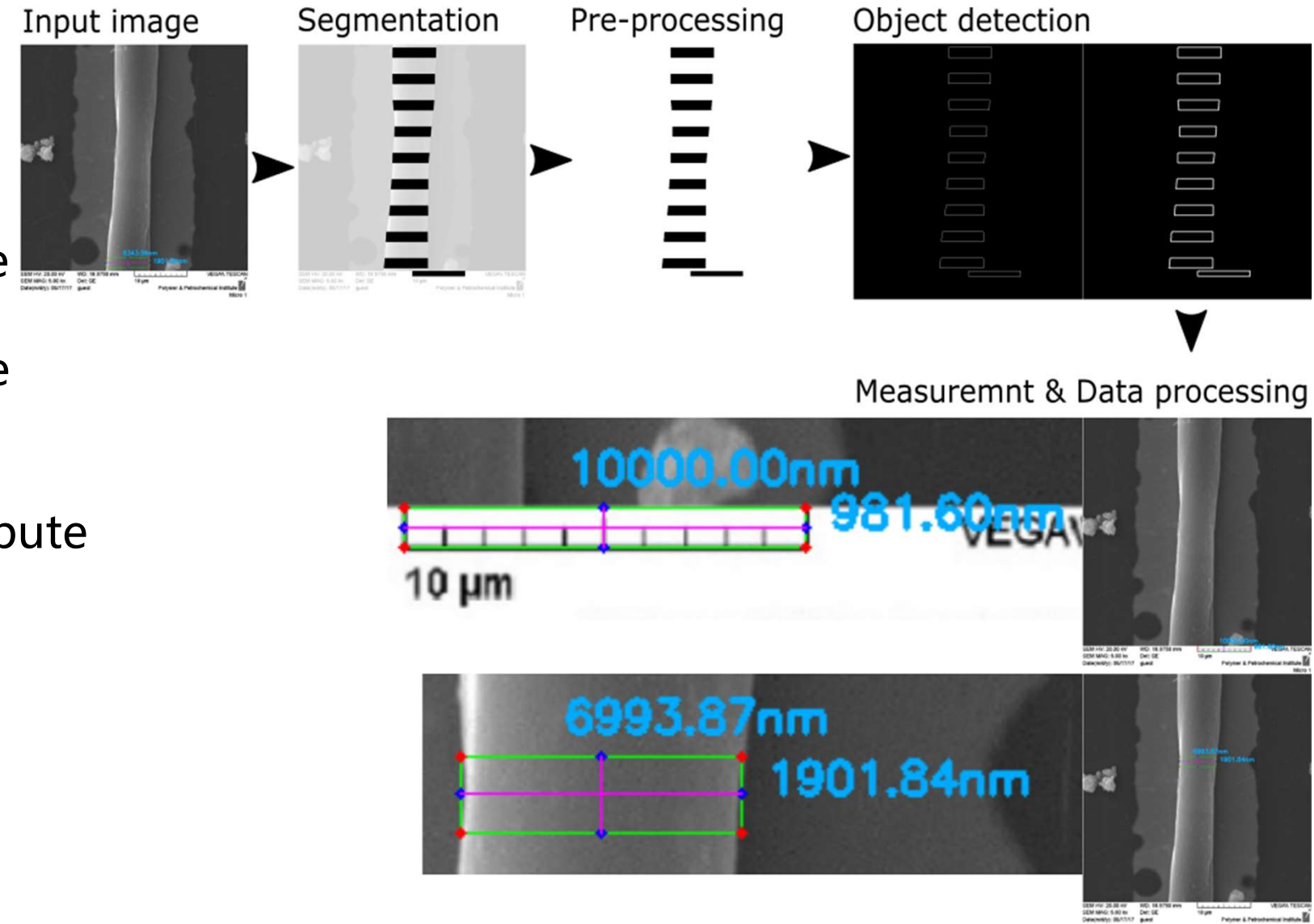
D. Di Camillo, V. Fasano, F. Ruggieri, S. Santucci, L. Lozzi, A. Camposeo, D. Pisignano, Nanoscale. 5 (2013) 11637–11642. <https://doi.org/10.1039/C3NR03094F>.

Methods: Data collection

(analysis of NFES articles from 2003 to 2020)

Image analysis algorithm:

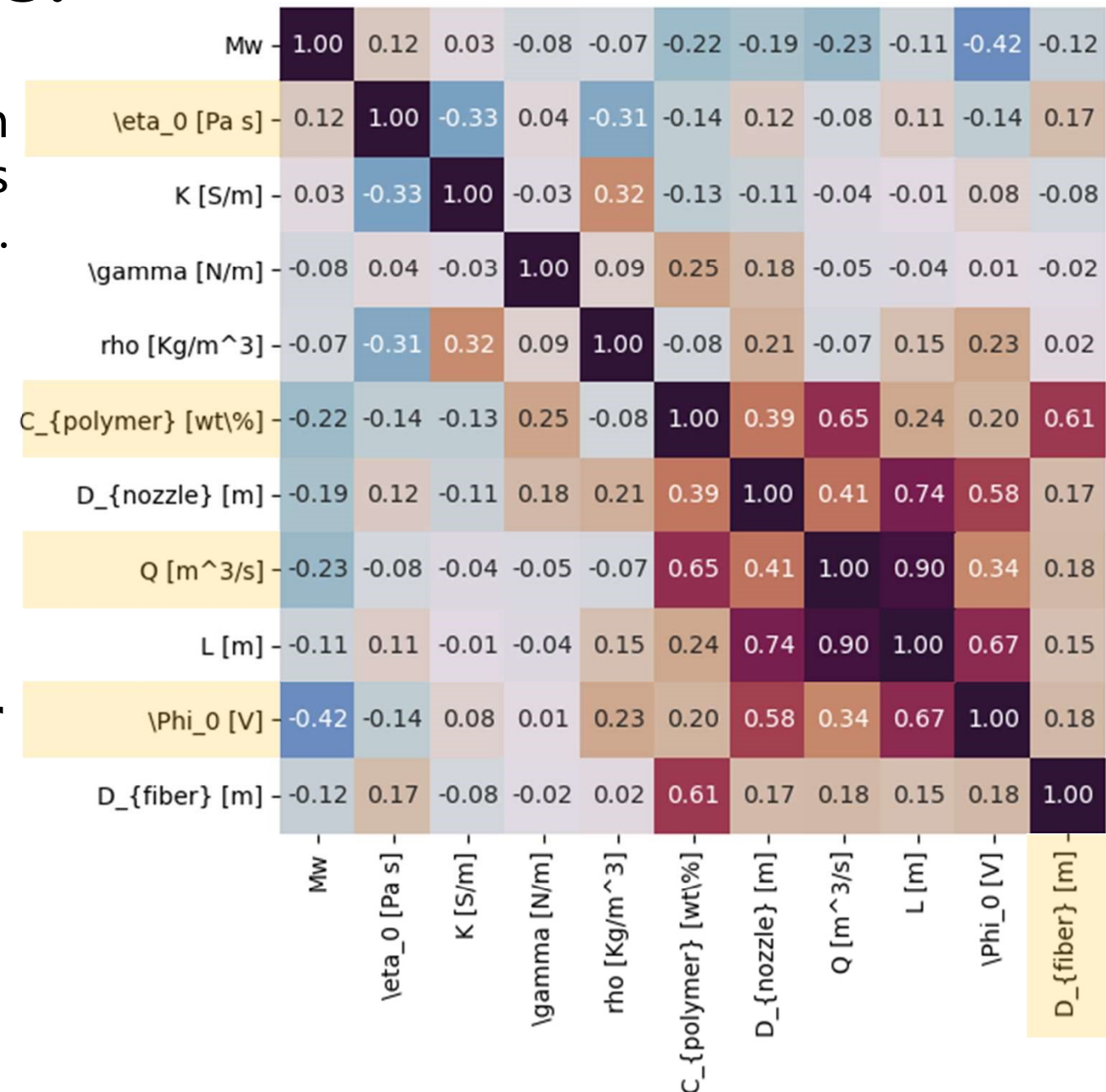
- Segmentation is done manually with a image processing software
- Pre-processing takes the binary image
- Object detection is done with the Sobel/Canny algorithm
- Measurement is to compute the pixel-to- metric proportions, using the scalebar as reference



Relevant Parameters:

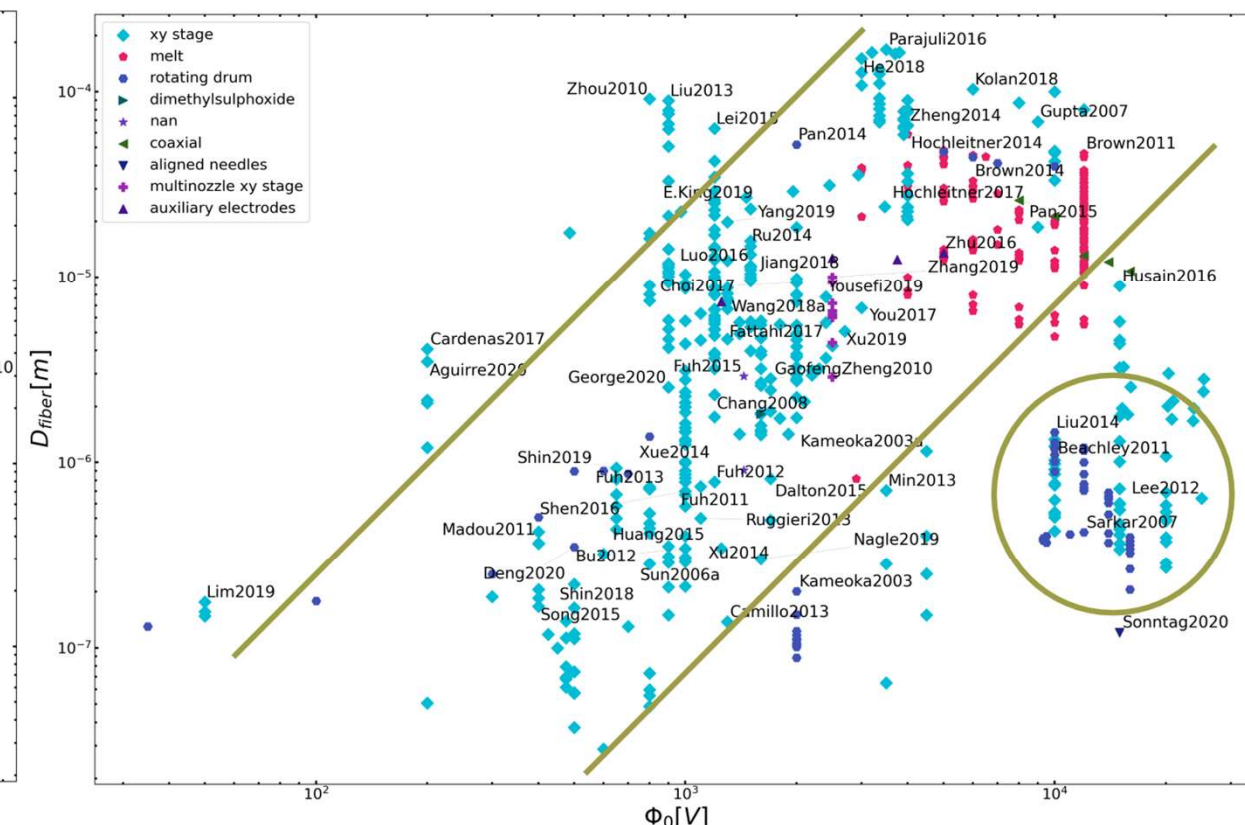
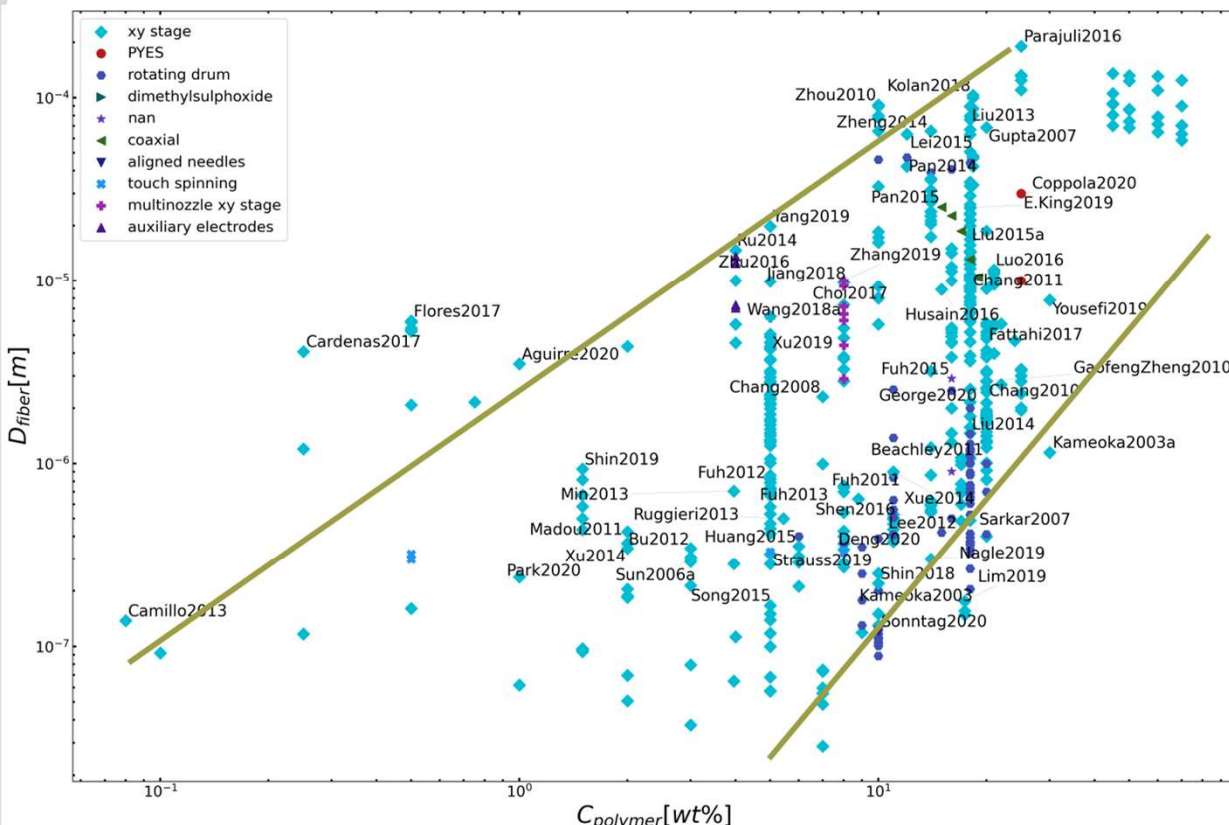
Matrix of Pearson linear correlation coefficients, built with Python's seaborn package.

- Zero-shear viscosity,
 - Polymer Concentration,
 - Solution Flow Rate,
&
 - Applied Voltage
- are the main drivers of the **final Fiber Diameter**



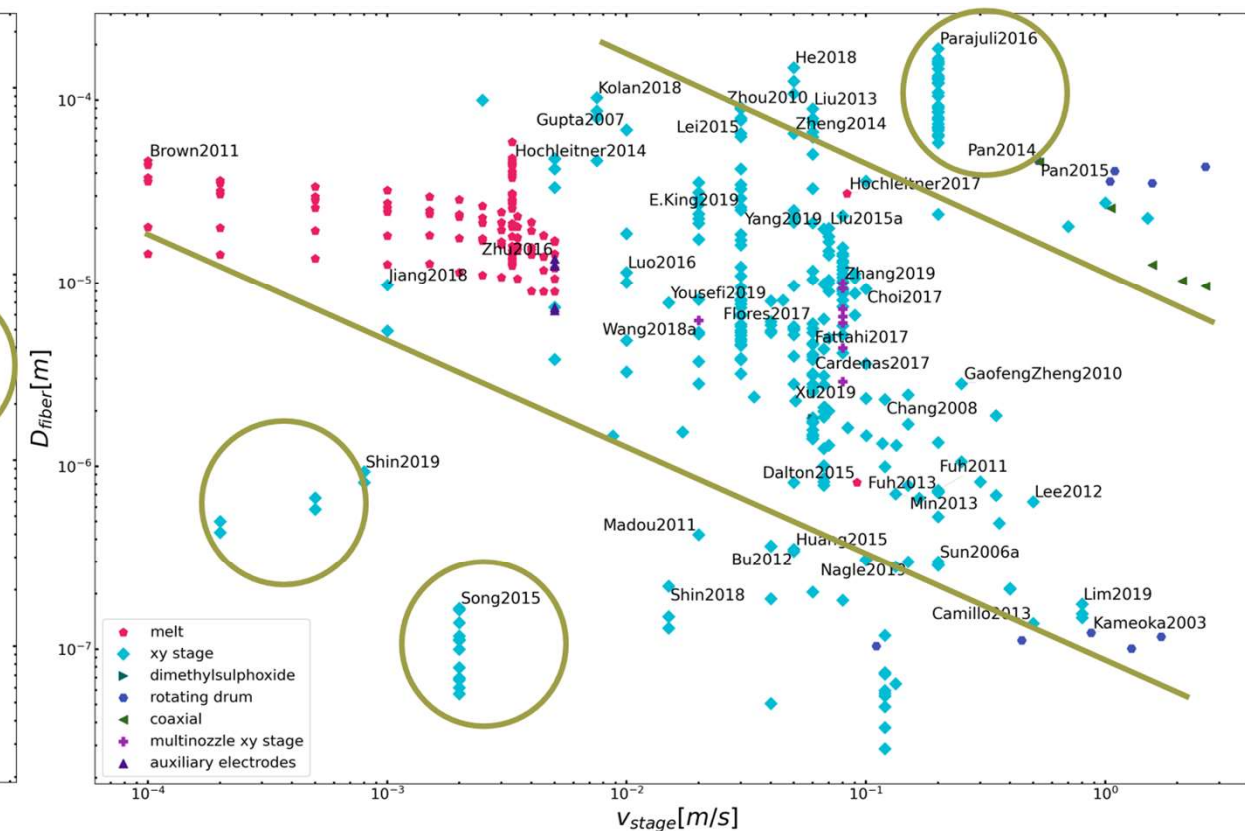
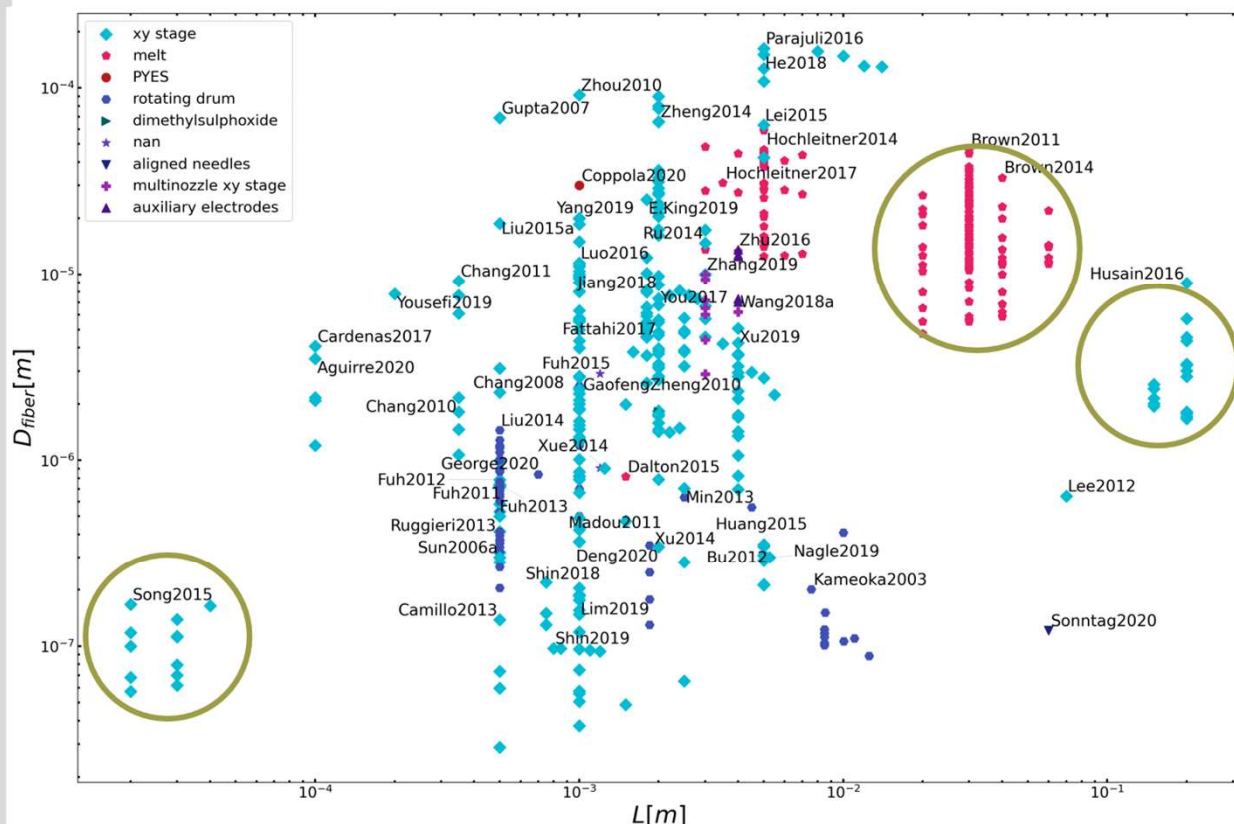
Conclusion 1.2: Let's focus on polymer concentration

Polymer concentration is the most reliable process parameter to control the morphology of electrospun fibers. (regardless the type of NFES process)

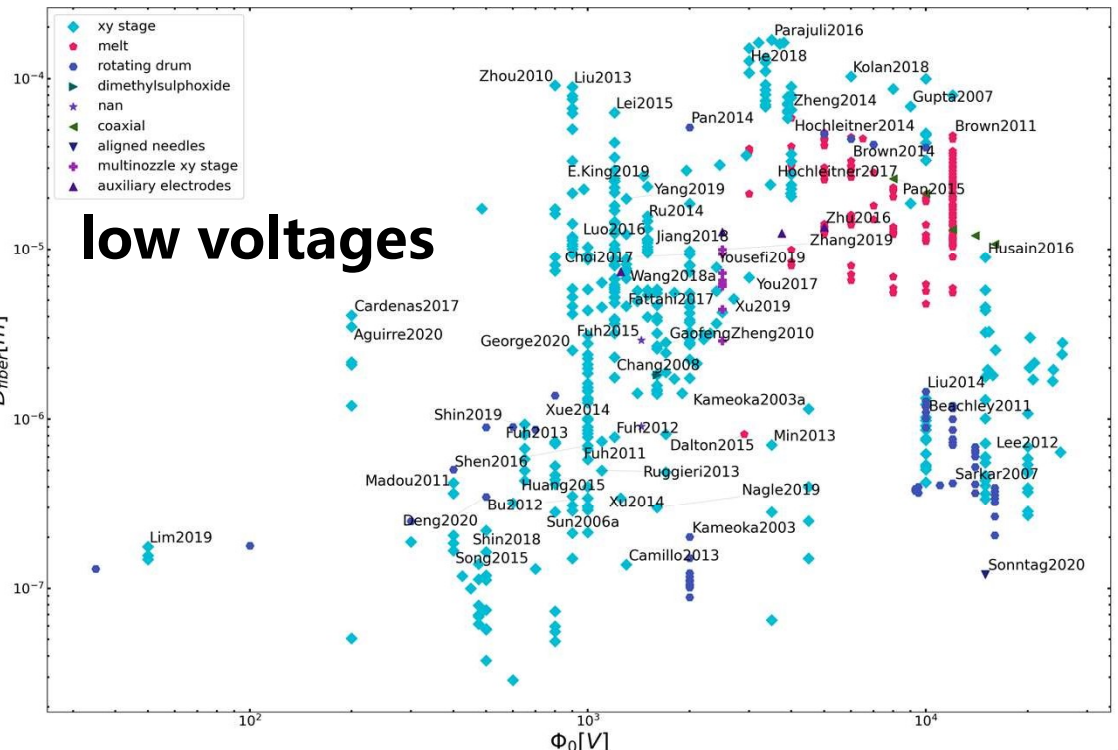
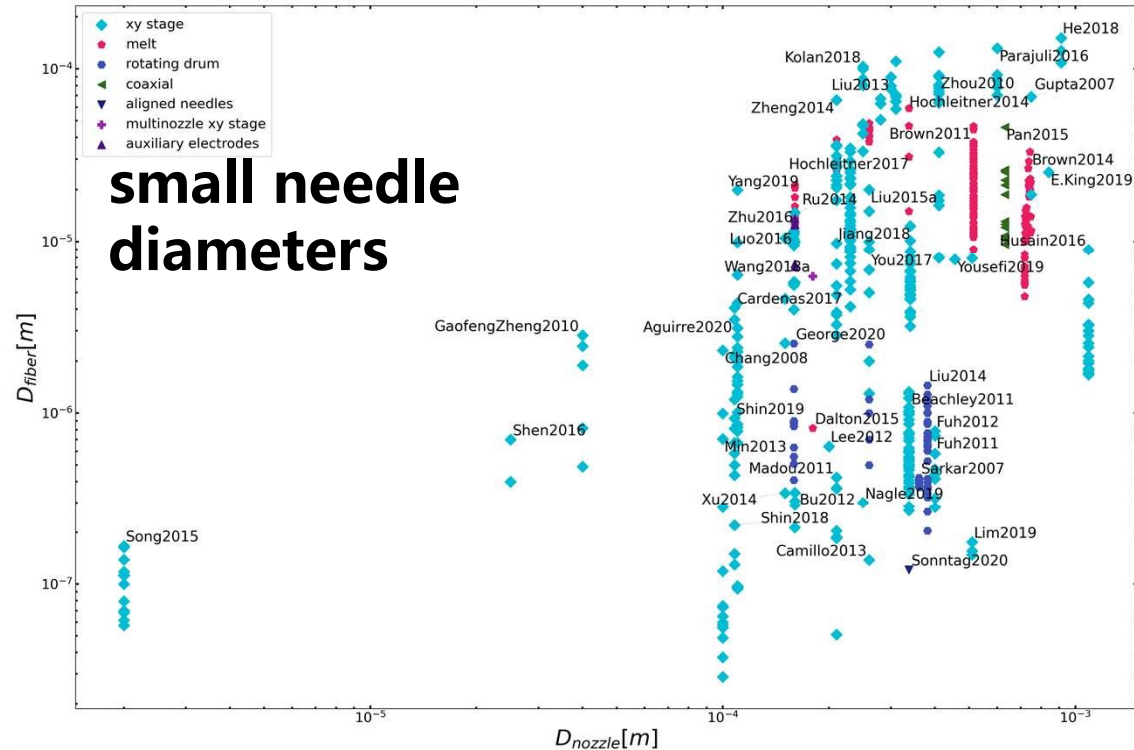
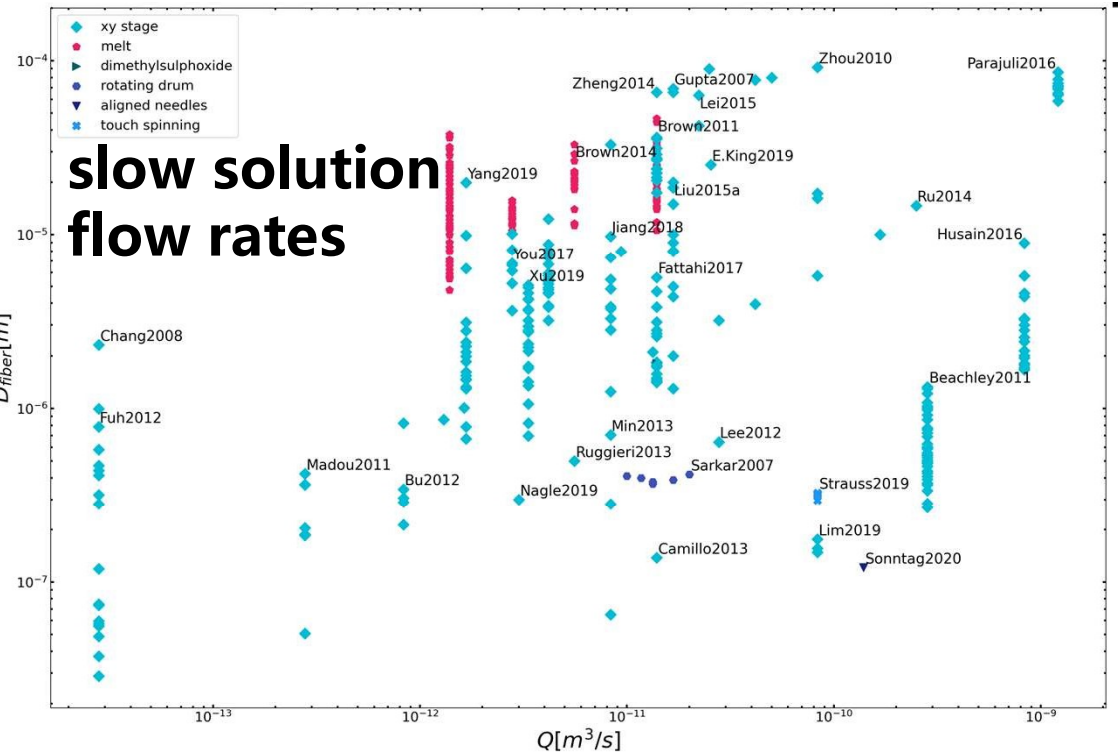
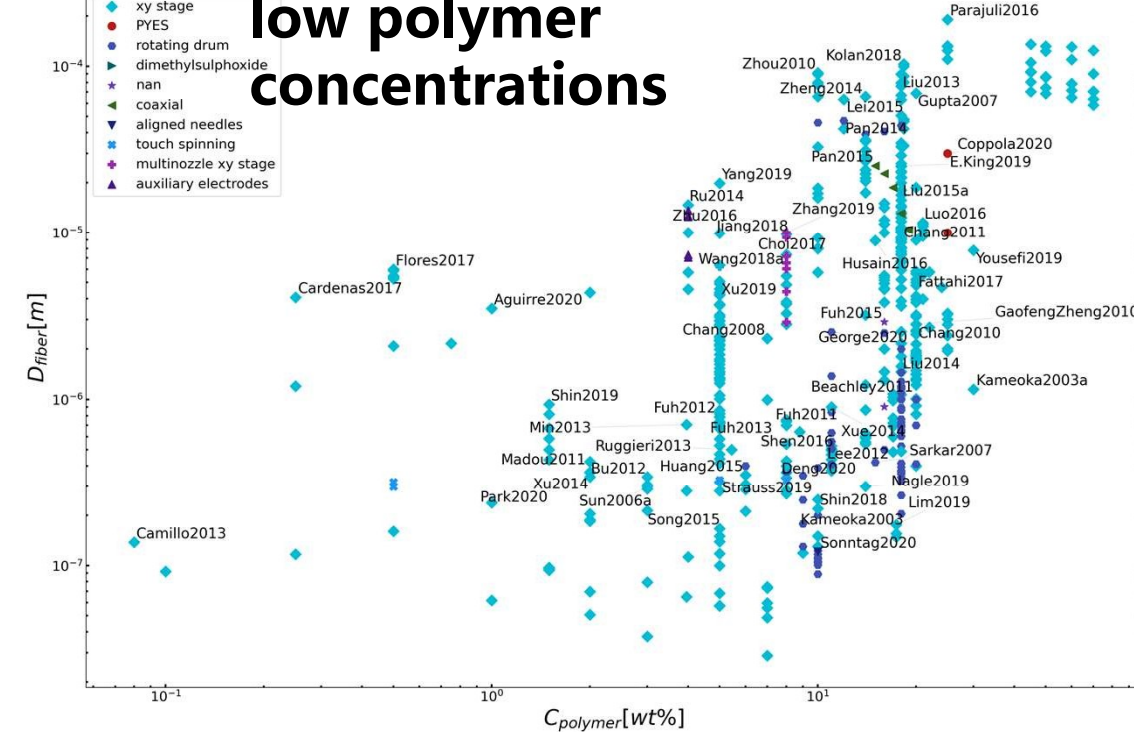
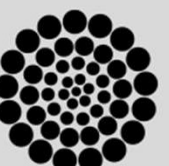


Conclusion 1.2: Let's focus on polymer concentration

Polymer concentration is the most reliable process parameter to control the morphology of electrospun fibers. (regardless the type of NFES process)



Conclusion 1.1: Process Parameters



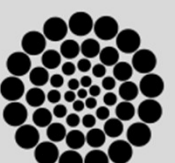
Diameter Prediction of Electrospun Fibers

The fiber morphology not only depends on the process parameters, but also on the type of electrospinning process and on polymer-solvent system.

“[...] the fiber diameter **decreases** as the applied voltage **increases.**”
Helgeson et al.

“[...] **neither** the collecting distance nor the applied voltage **has large influences** on fiber diameter [...]”
Zhang et al.

“[...] while **decreasing** the voltage could also be used to **reduce** the average fiber diameter.”
Brown et al.



The existing **interdependence** between the process and solution parameters **adds complexity and ambiguity** to the effect of each parameter

Diameter Prediction of Electrospun Fibers

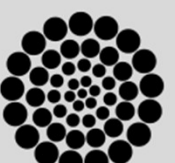
Helgeson and Wagner have presented an adimensional **analysis to predict the fiber diameter** with conservation equations of momentum, mass, electric charge and four dimensionless numbers:

Correlation between the electrostatic and viscous forces:

$$\Pi_1 = RePe\Psi = \frac{2\bar{\varepsilon}^2 \Phi_0^2}{K\eta_0 L^2}$$

Ohnesorge number (jet behaviour and capillary rupture):

$$Oh = \frac{Re^2}{We} = \frac{\eta_0}{\sqrt{\rho\gamma R_{jet}}}$$



Helgeson get rid of unknown and/or hard to measure parameters, such as the initial jet velocity.

Diameter Prediction of Electrospun Fibers

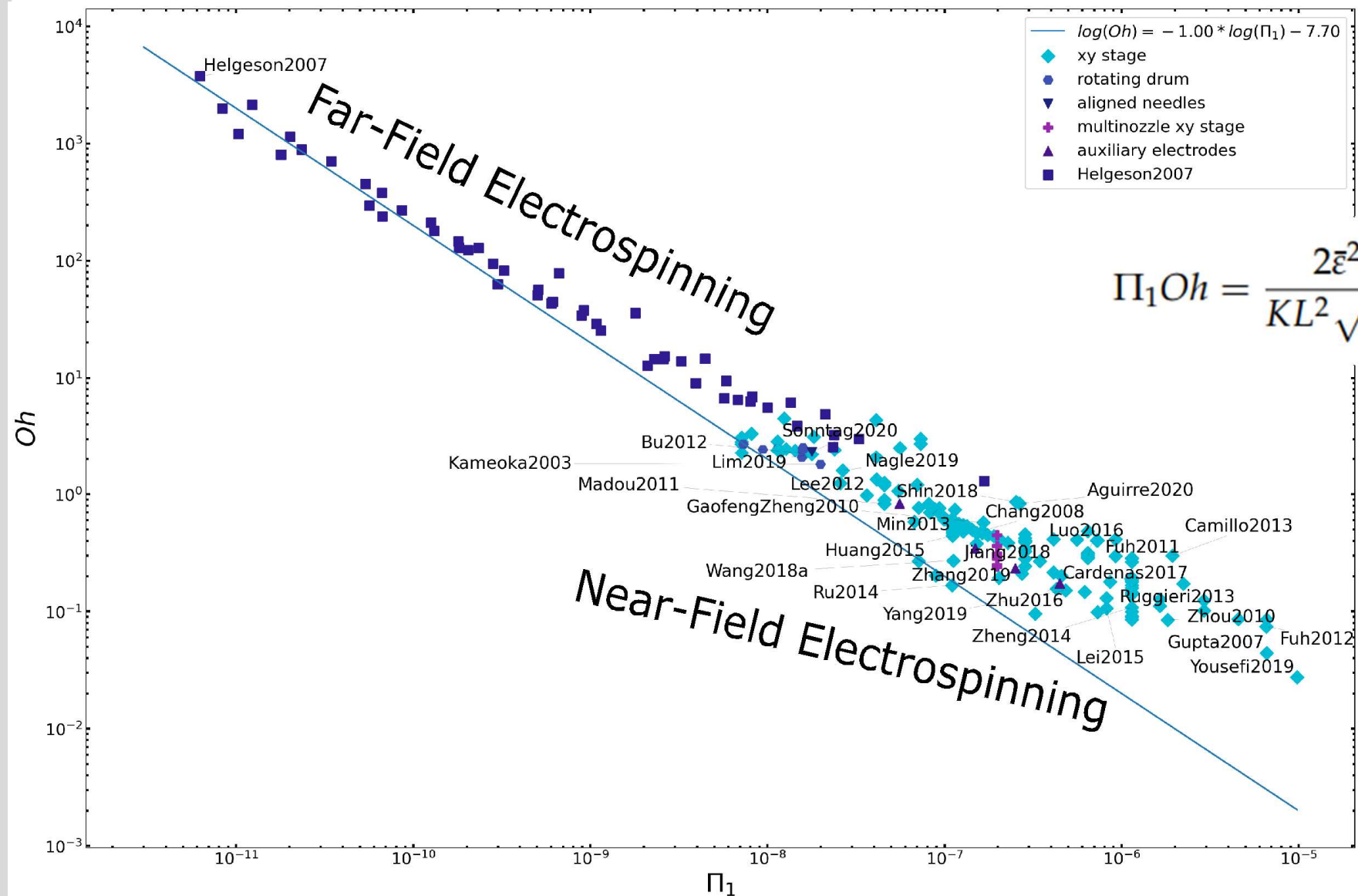
$$\text{Peclet number } Pe = \frac{2\bar{\varepsilon}v_0}{KR_0} \quad \text{Reynold number } Re = \frac{\rho v_0 R_0}{\eta_0} \quad \text{Weber number } We = \frac{\rho v_0^2 R_0}{\gamma}$$

$$\text{dimensionless electric field strength } \Psi = \frac{\bar{\varepsilon}E_0^2}{\rho v_0^2}$$

$$R_{jet} = R_f \sqrt{\frac{1}{w_s}}$$



Diameter Prediction of Electrospun Fibers

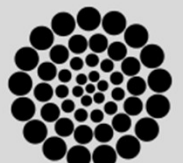


$$\Pi_1 Oh = \frac{2\bar{\varepsilon}^2 \Phi_0^2}{KL^2 \sqrt{\rho \gamma R_{jet}}} = 2.5 \pm 0.2 \times 10^{-8}$$



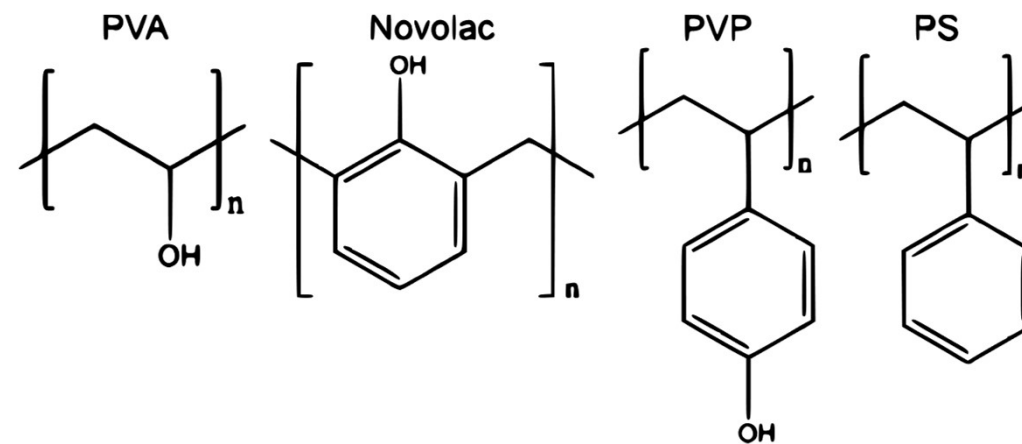
Rheology Analyses

Specific Objective 2. Through **rheological analyses**, determine if polymer solutions have comparative viscoelastic properties to those of the SU-8/PEO benchmark, and if they can be easily electrospun by NFES.

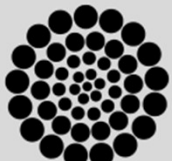


Selection of Polymer-Solvent combinations

Zhenan Bao et al. investigated the effect of the polymer chemical Structure of:

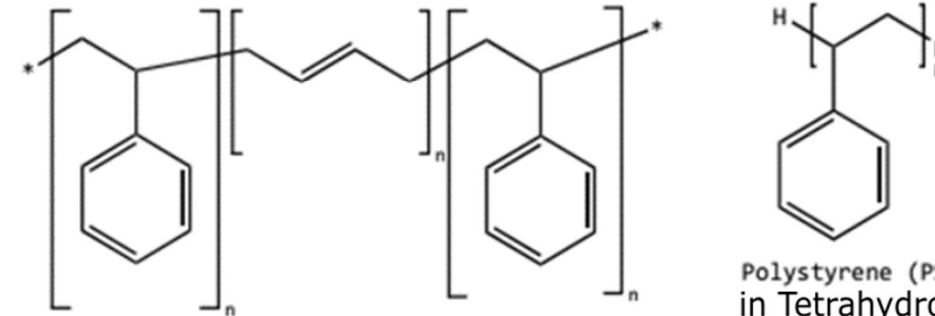


- higher **sp₂ carbon** content translates into higher graphitization degree and higher electrical conductivity
- polymers with **functional groups** are required for the creation of smooth and continuous fibers.

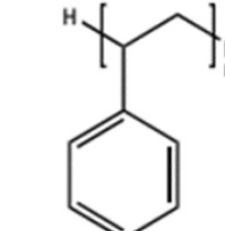


Conclusion1.3: Selection of Polymer-Solvent combinations

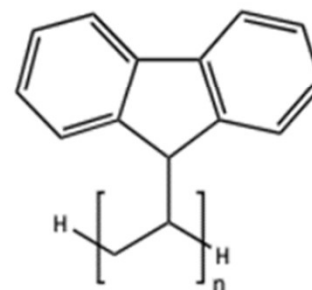
Polymers with **high carbon content relative to oxygen content**



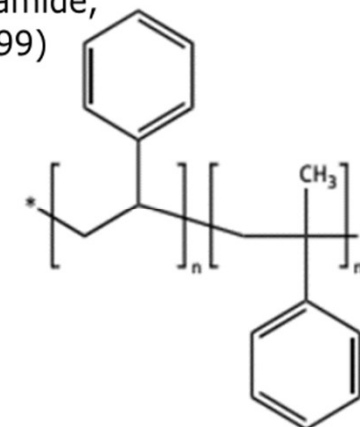
Poly(styrene-co-butadiene)
in Tetrahydrofuran, N,N-Dimethylformamide,
and 1-Methyl-2-Pyrrolidinone (Fong1999)



Polystyrene (PS)
in Tetrahydrofuran (Yousefi2019)



Poly(9-Vinyl Carbazole) (PVK)
in Chloroform (Min2013)

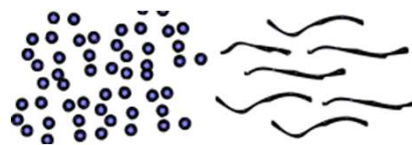


Poly(styrene-co-a-methylstyrene)
in N,N-Dimethylformamide (no records)

A.A. Yousefi, A.R. Mohebbi, S. Falahdoost Moghadam, S.A. Poursamar, L. Hao, Sol. Energy. 188 (2019) 1111–1117. <https://doi.org/10.1016/j.solener.2019.07.007>.
H. Fong, D.H. Reneker, J. Polym. Sci. Part B Polym. Phys. 37 (1999) 3488–3493. [https://doi.org/10.1002/\(SICI\)1099-0488\(19991215\)37:24<3488::AID-POLB9>3.0.CO;2-M](https://doi.org/10.1002/(SICI)1099-0488(19991215)37:24<3488::AID-POLB9>3.0.CO;2-M).
S.-Y. Min, T.-S. Kim, B.J. Kim, H. Cho, Y.-Y. Noh, H. Yang, J.H. Cho, T.-W. Nat. Commun. 4 (2013) 1773. <https://doi.org/10.1038/ncomms2785>.

Literature claims

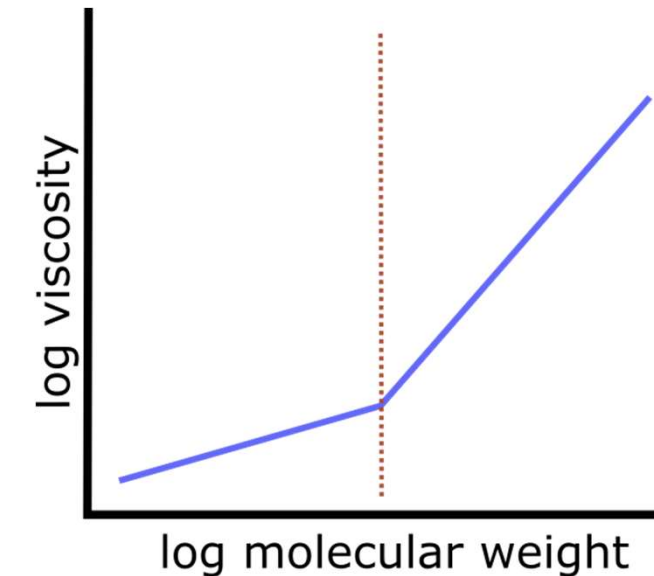
Under some critical concentration NFES yields beads or small fibres



Over some critical concentration NFES continuous fibres



Viscosity increases with molecular weight

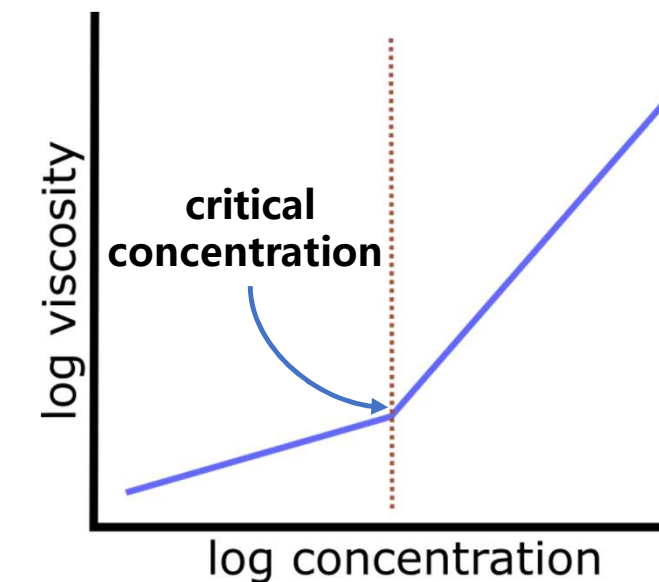
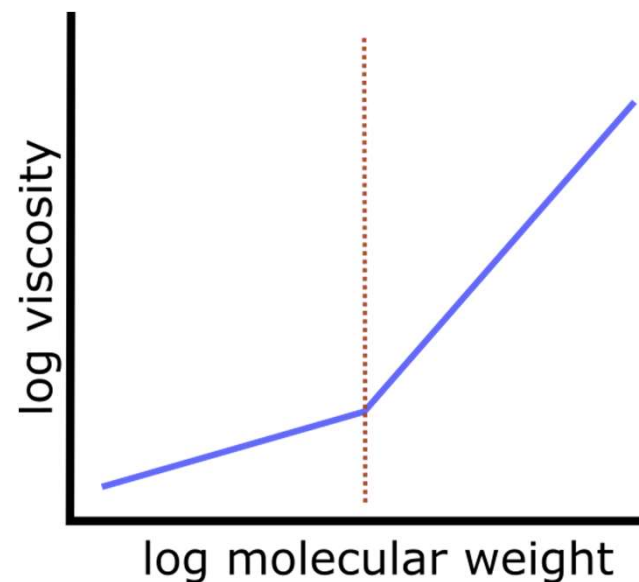


The general belief is that the molecular weight needs to be sufficient enough to create or induce **entanglements**

Literature claims

- As “electrospinnability” is determined by the **polymer chain entanglement**,
- **chain entanglement** is controlled by *molecular weight*,
- increasing *molecular weight* increases viscosity, and
- viscosity is controlled by **polymer concentration**, then

The **critical/spinnable concentration** can be found in a **viscosity vs. concentration plot**



Methods: Sample Preparation (SU8-PEO)

Sample	Weight Percent <i>wt%</i>		
	SU-8	PEO	TBF
1	99.50	0.00	0.50
2	99.25	0.25	0.50
3	99.00	0.50	0.50
4	98.75	0.75	0.50
5	98.50	1.00	0.50
density [g/ml]	1.123		

3.0 ml samples
on a heating plate at 160 rpm and 60°C, for 2 hours each.

A salt (TBF) was added to all the samples to increase the electrical conductivity



Methods: Sample Preparation (PS & PSB)

Sample	Weight Percent <i>wt%</i>		
	THF	PS	TBF
6	99.25	0.25	0.50
7	94.50	5.00	0.50
8	89.50	10.00	0.50
9	84.50	15.00	0.50
10	79.50	20.00	0.50
11	69.50	30.00	0.50
12	64.50	35.00	0.50
13	59.50	40.00	0.50
density [g/ml]		0.888	

Sample	Weight Percent <i>wt%</i>		
	NMP	PSB	TBF
14	98.50	1.00	0.50
15	95.50	4.00	0.50
16	91.50	8.00	0.50
17	87.50	12.00	0.50
density [g/ml]		1.027	

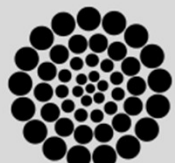
Methods: Sample Preparation (PSB & PSMS)

Sample	Weight Percent <i>wt%</i>				Sample	Weight Percent <i>wt%</i>			
	THF	DMF	PSB	TBF		DMF	PSMS	TBF	
18	70.875	23.625	5.00	0.50	25	99.00	0.50	0.50	
19	69.000	23.000	7.50	0.50	26	94.50	5.00	0.50	
20	67.125	22.375	10.00	0.50	27	89.50	10.00	0.50	
21	65.250	21.750	12.50	0.50	28	84.50	15.00	0.50	
22	63.375	21.125	15.00	0.50	density [g/ml]			0.950	
23	59.625	19.875	20.00	0.50					
24	55.875	18.625	25.00	0.50					
density [g/ml]		0.888	0.950						

Methods: Sample Preparation (PVK & SU8-PVK)

Sample	Weight Percent <i>wt%</i>		
	CHL	PVK	TBF
29	99.50	0.00	0.50
30	99.49	0.01	0.50
31	84.50	15.00	0.50
32	79.50	20.00	0.50
33	69.50	30.00	0.50
density [g/ml]	1.492		

Sample	Weight Percent <i>wt%</i>		
	SU-8	PVK	TBF
34	99.50	0.00	0.50
35	99.495	0.005	0.50
36	98.75	0.75	0.50
37	94.50	5.00	0.50
38	79.50	20.00	0.50
density [g/ml]	1.123		



Methods: Rheology – Frequency Sweeps

Geometry:

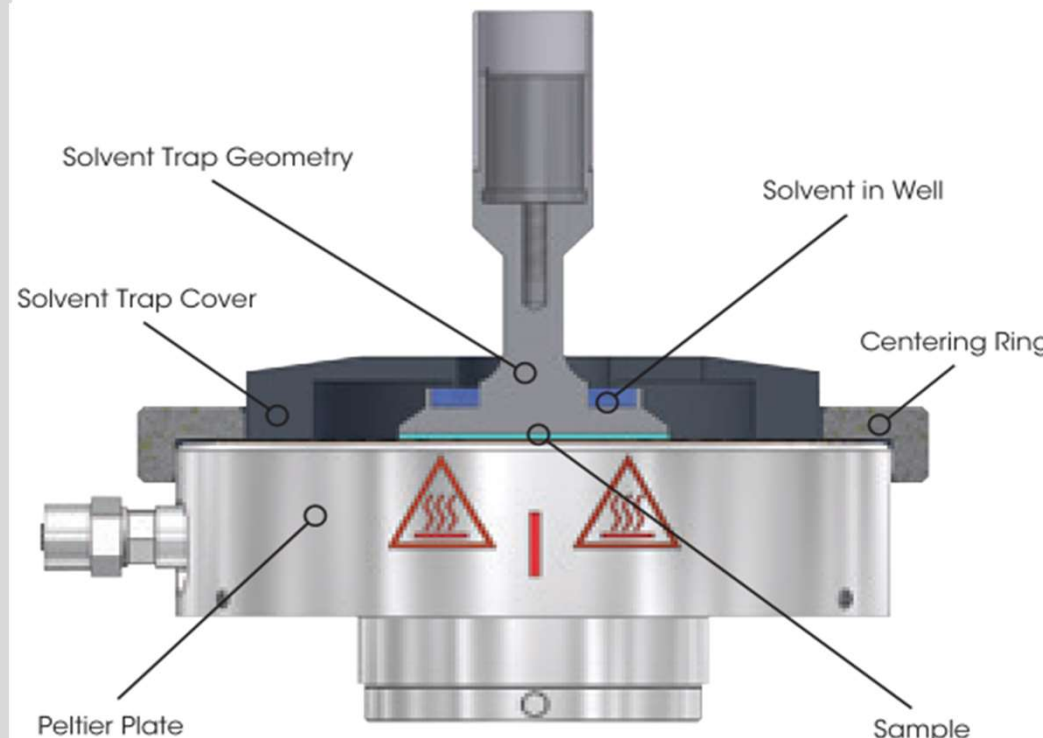
Steel cone plate, Peltier plate
(60.0 mm diameter, 0.9979° cone angle,
23 μm truncation)

Procedure:

Frequency sweep
(20°C, for 20 min
from 10^{-3} to 10^4 1/s shear rates)



Methods: Rheology – Instrumentation



Measured Parameter	Calculated Parameter
Torque	Stress
Angular displacement	Strain
Angular velocity	Shear rate

$$\text{Stress} = \text{Torque} [\text{N} \cdot \text{m}] \cdot \text{Stress constant}$$

$$\text{Strain} = \text{Angular displacement} [\text{rad}] \cdot \text{Strain constant}$$

$$\text{Shear rate} = \text{Angular velocity} \left[\frac{\text{rad}}{\text{s}} \right] \cdot \text{Strain constant}$$

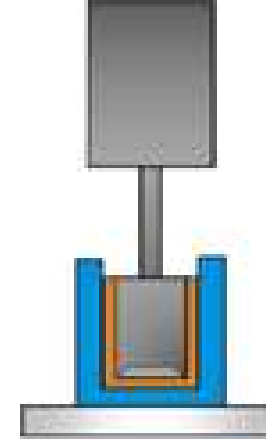
$$\text{Viscosity} = \frac{\text{Stress}}{\text{Shear rate}}$$

$$\text{Young's Modulus} = \frac{\text{Stress}}{\text{Strain}}$$

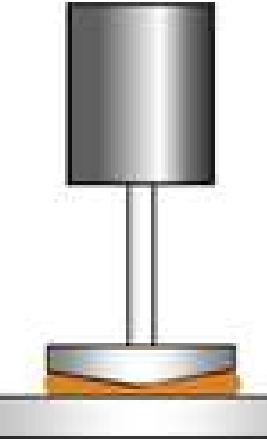
Methods: Rheology – Geometry Selection

Geometry options:

Concentric
Cylinders



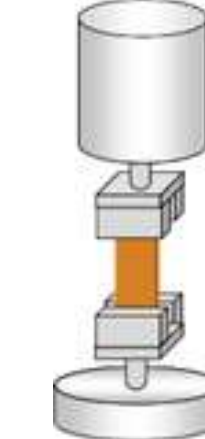
Cone and
Plate



Parallel
Plate



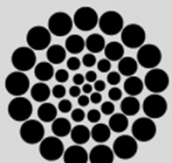
Torsion
Rectangular



Very Low Viscosity

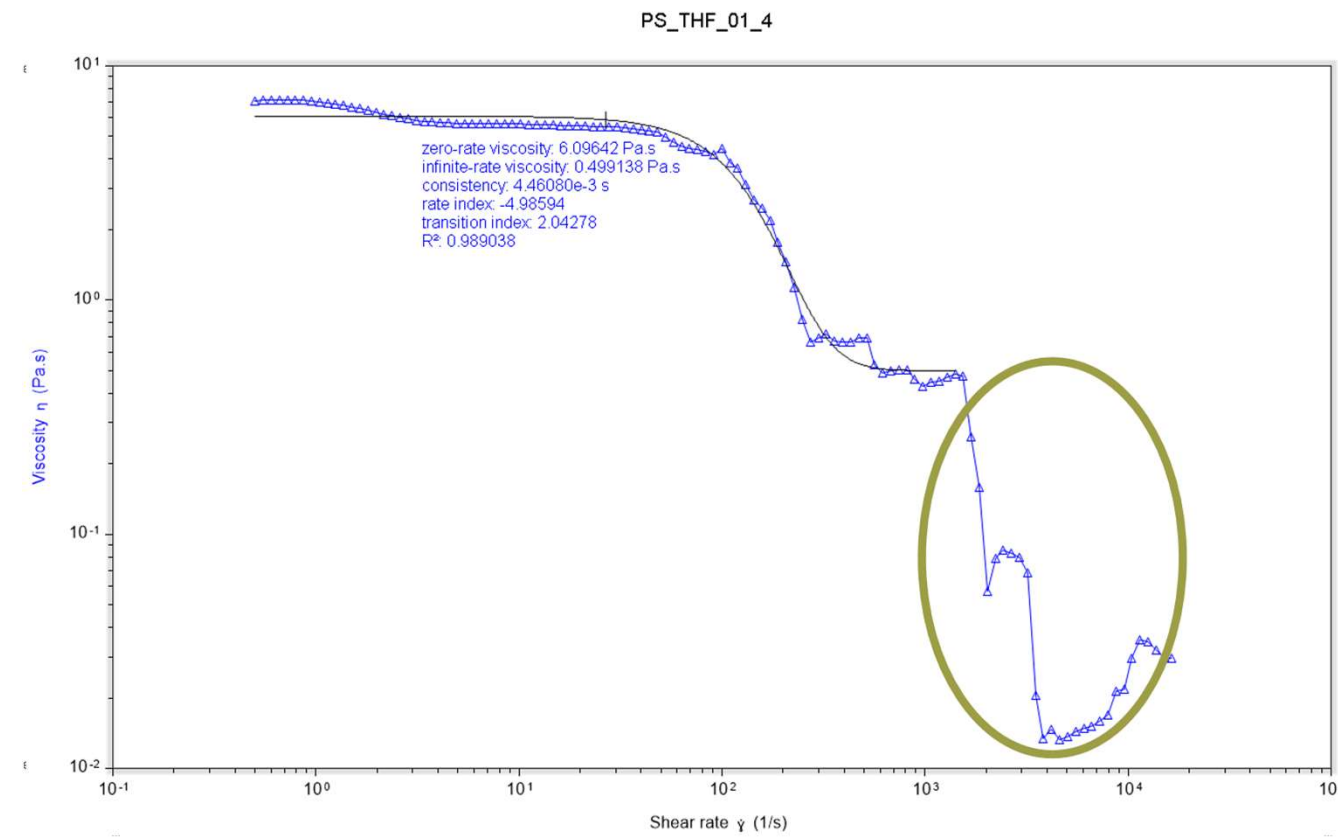


Solids



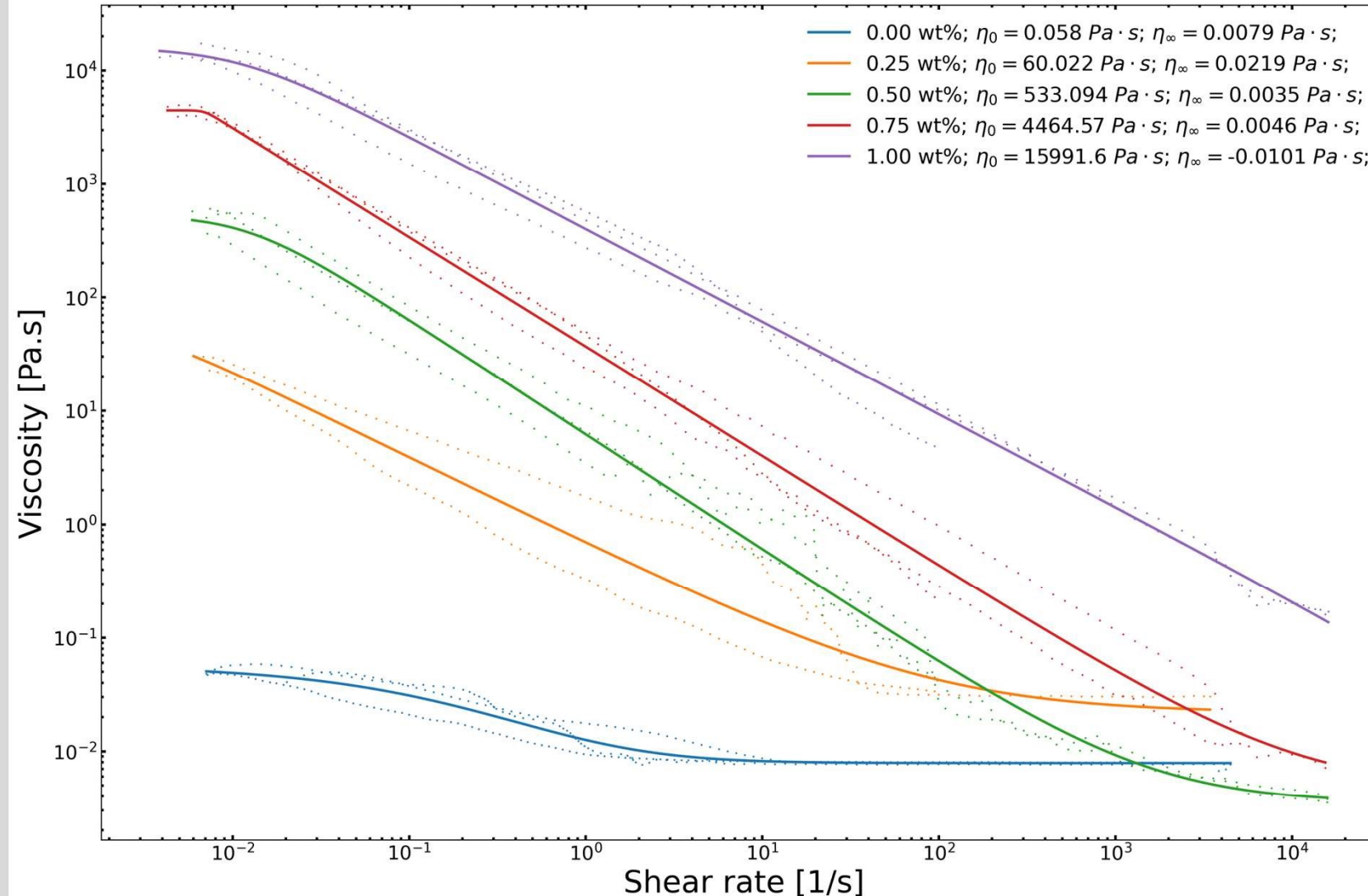
Methods: Rheology – Radial Migration Effect

High centrifugal stresses result in the sample being thrown out of the measuring area; a phenomenon known as 'radial migration effect'.



Once the 'radial migration effect' partially ejects the sample, the viscosity measurements are lower than expected due to a drop in torque.

Methods: The Carreau-Yasuda Model



$$\eta = \frac{\eta_0 - \eta_\infty}{[1 + (\kappa\dot{\gamma})^a]^{\frac{1-n}{a}}} + \eta_\infty$$

η : viscosity

$\dot{\gamma}$: shear rate

η_∞ : infinite shear rate viscosity

η_0 : zero shear rate viscosity

κ : time constant

n : Power Law index

a : width of the transition region

Methods: Other models:

Cross Model

$$\frac{\eta - b}{a - b} = \frac{1}{1 + (c\dot{\gamma})^d}$$

$$\eta = \frac{a - b}{1 + (c\dot{\gamma})^d} + b$$

where:

a = zero rate viscosity

b = infinite rate viscosity

c = consistency

d = rate index

Carreau Model

$$\frac{\eta - b}{a - b} = [1 + (c\dot{\gamma})^2]^{\frac{d-1}{2}}$$

$$\eta = \frac{a - b}{[1 + (c\dot{\gamma})^2]^{\frac{1-d}{2}}} + b$$

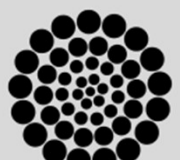
where:

a = zero rate viscosity

b = infinite rate viscosity

c = consistency

d = rate index



Methods: Other models:

Sisko

$$\eta = a + b\dot{\gamma}^{c-1}$$

where:

a = infinite rate viscosity

b = consistency

c = rate index

Williamson

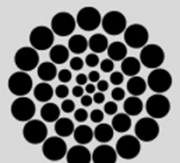
$$\eta = \frac{a}{1 + (b\dot{\gamma})^c}$$

where:

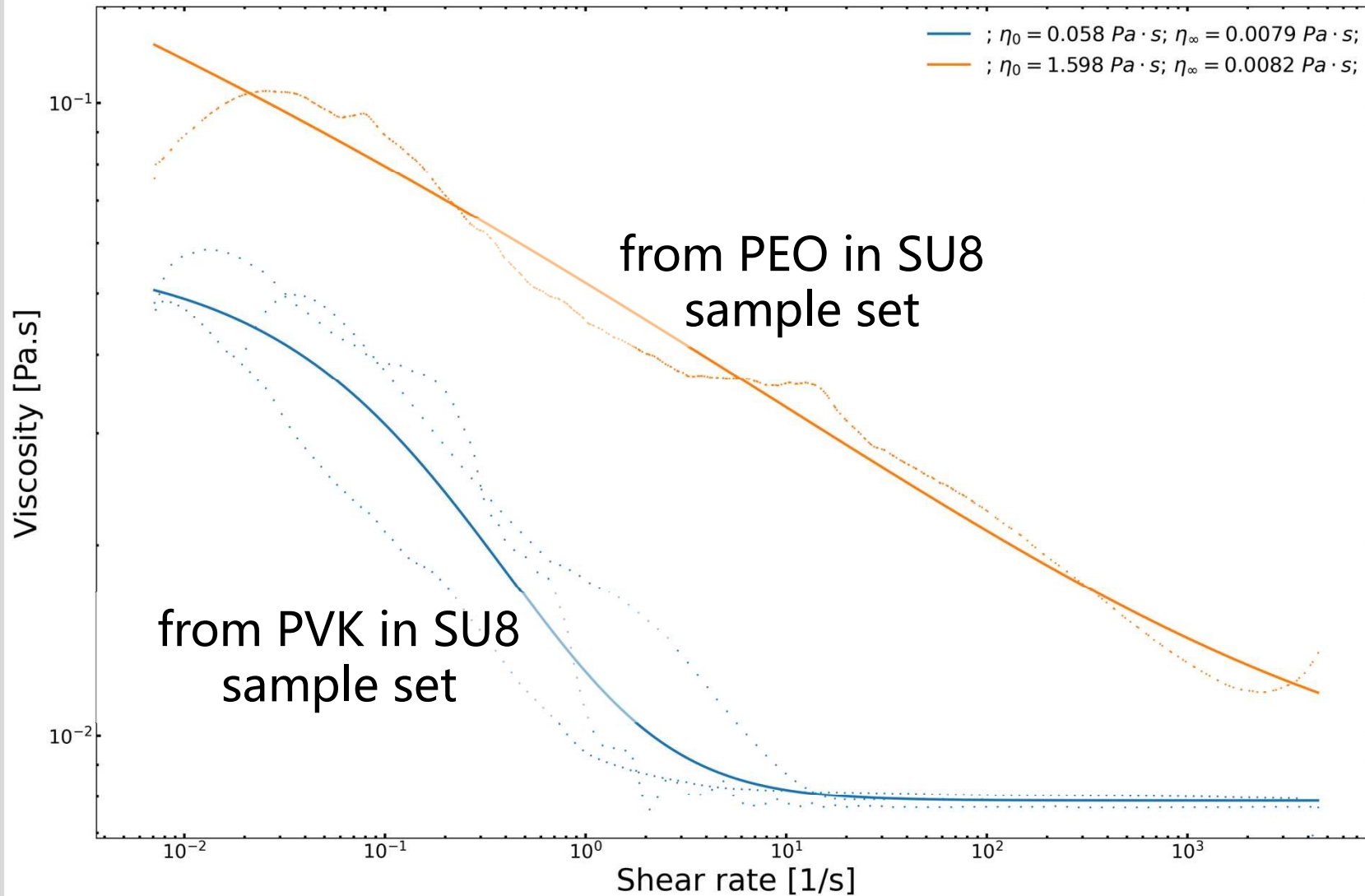
a = zero rate viscosity

b = consistency

c = rate index



Methods: Rheology results validation for 0wt% PEO and 0wt% PVK



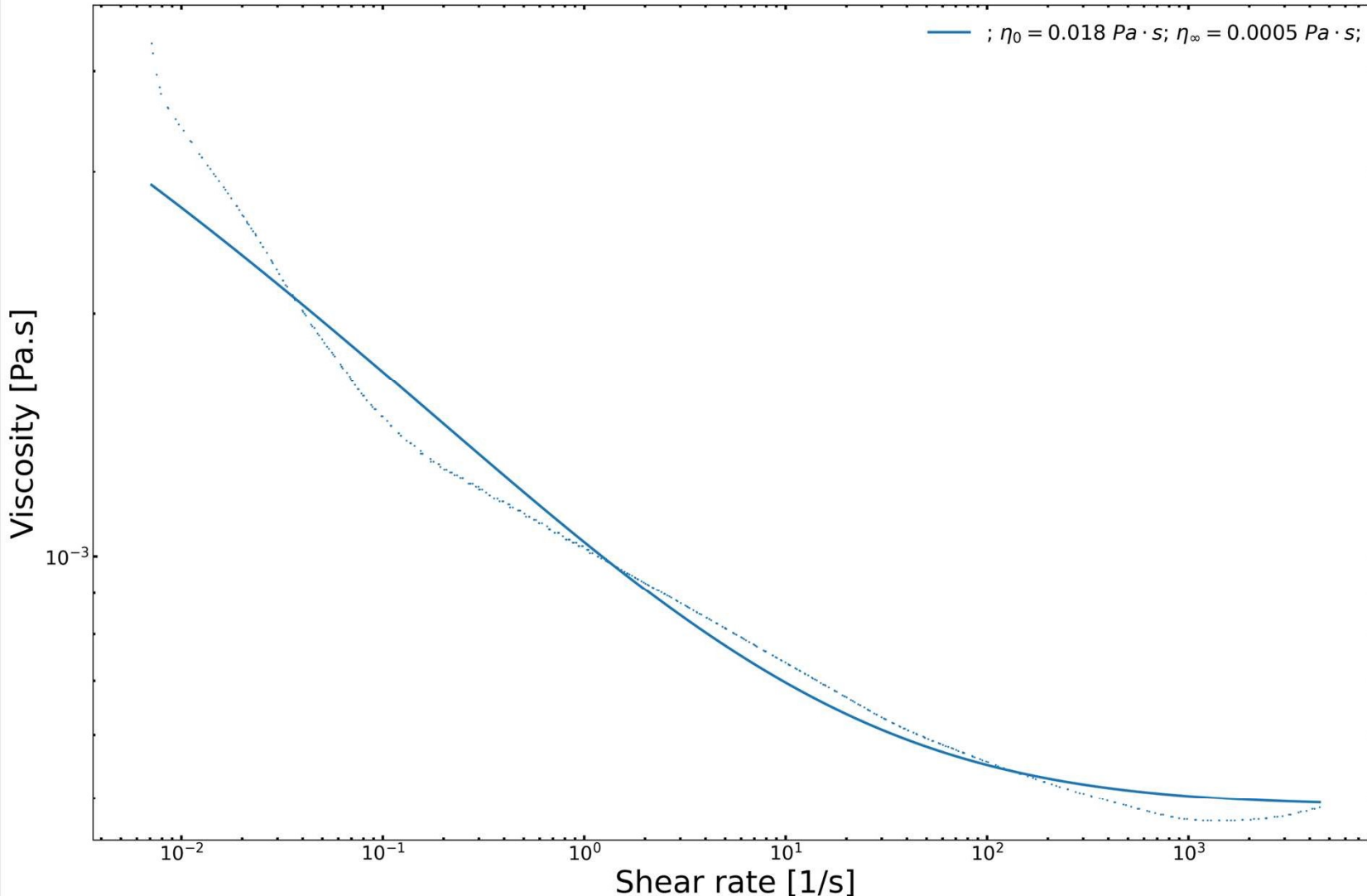
Measured:
 $(8.05 \pm 0.28) \text{ mPa} \cdot \text{s}$

vs.

MicroChem data sheet:
7.5cSt (1.123g/ml)
1000cSt · s · m · g/ml · Kg
 $= 8.422 \text{ mPa} \cdot \text{s}$

1.09 %error

Methods: Rheology results validation for 0wt% PVK



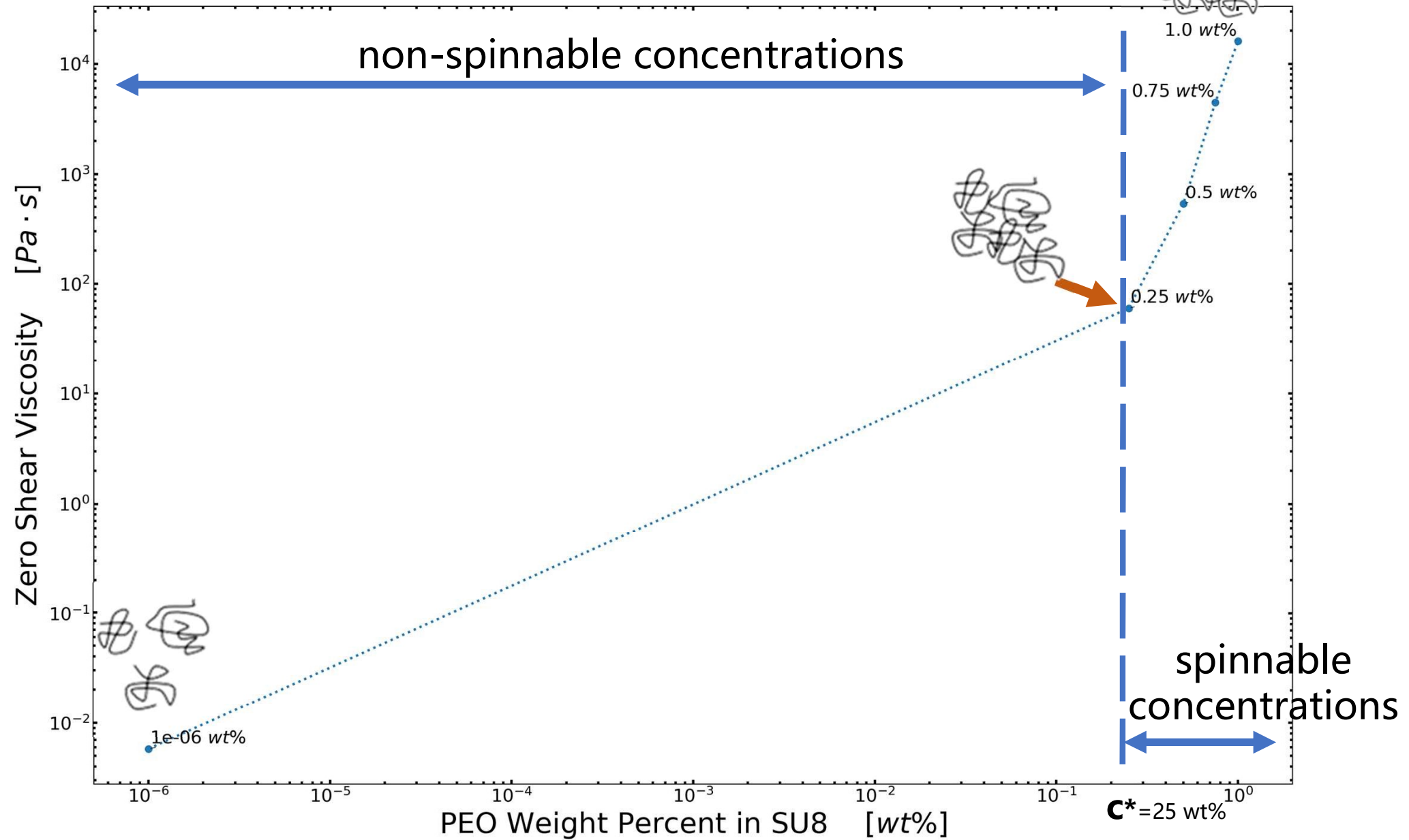
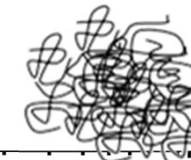
Measured CHL viscosity:
0.499 mPa · s

vs.

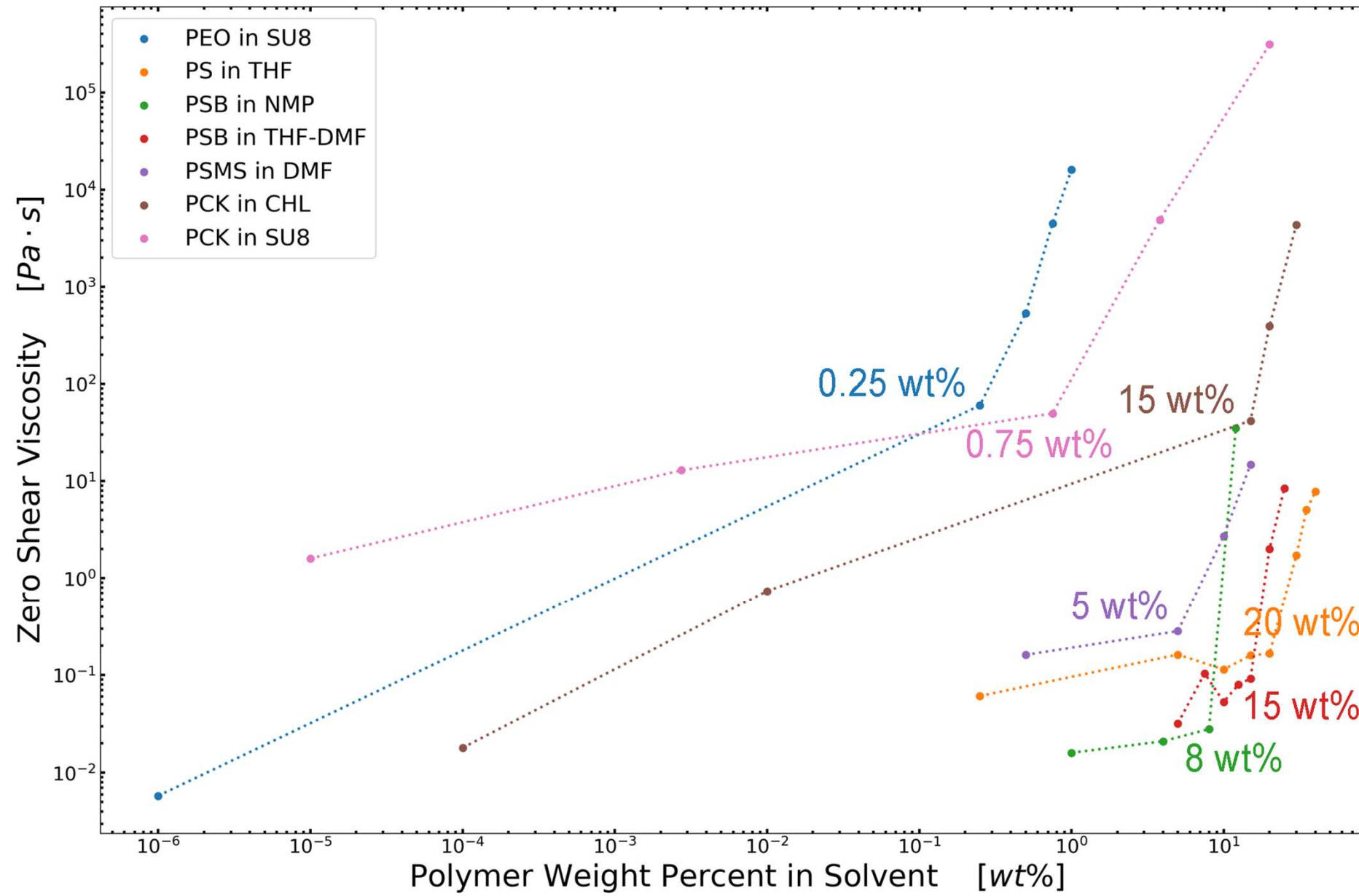
Anton-Paar data sheet:
0.563 mPa · s

11.36 %error

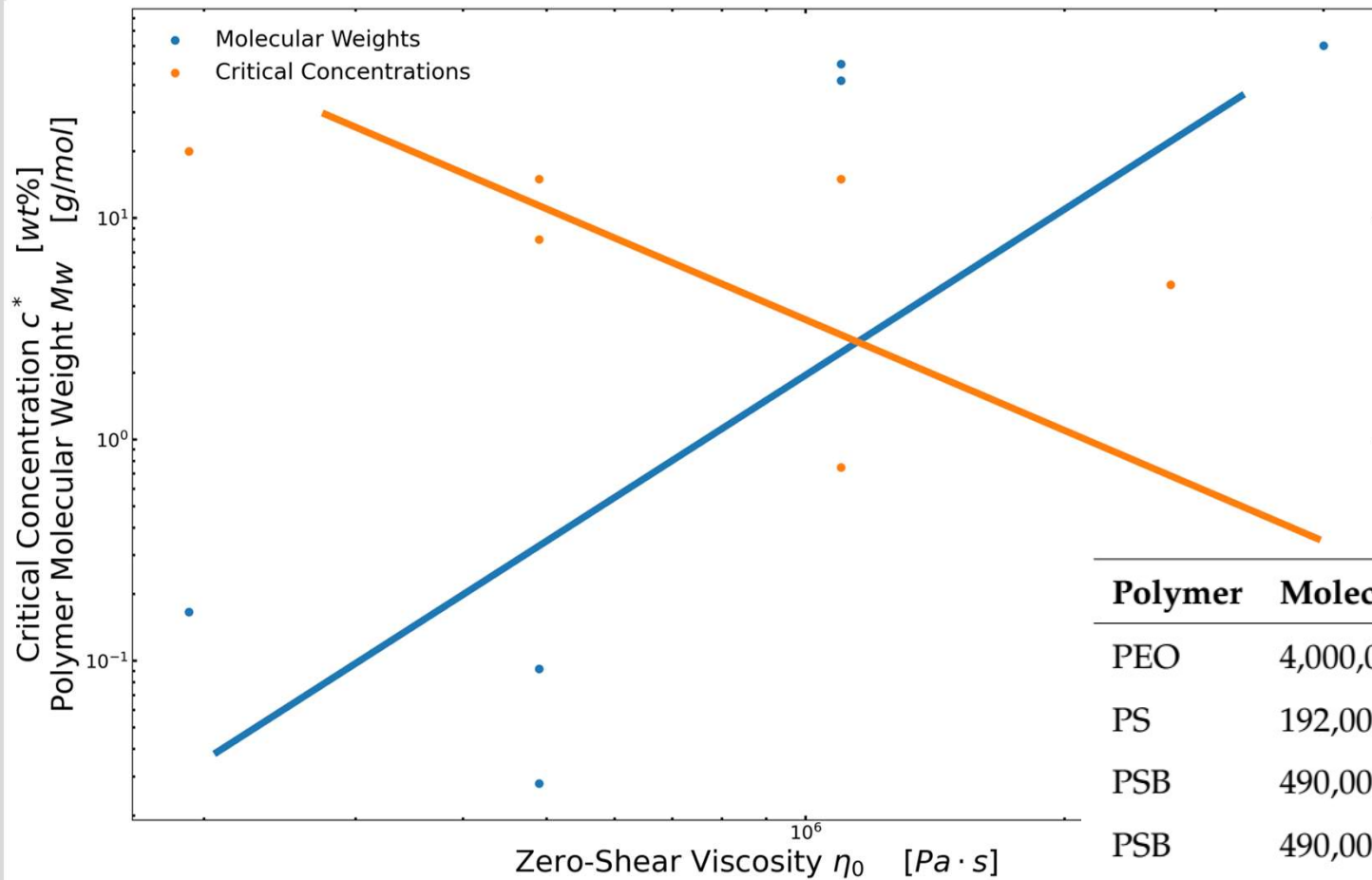
Spinnable/Critical Concentration



Spinnable/Critical Concentration

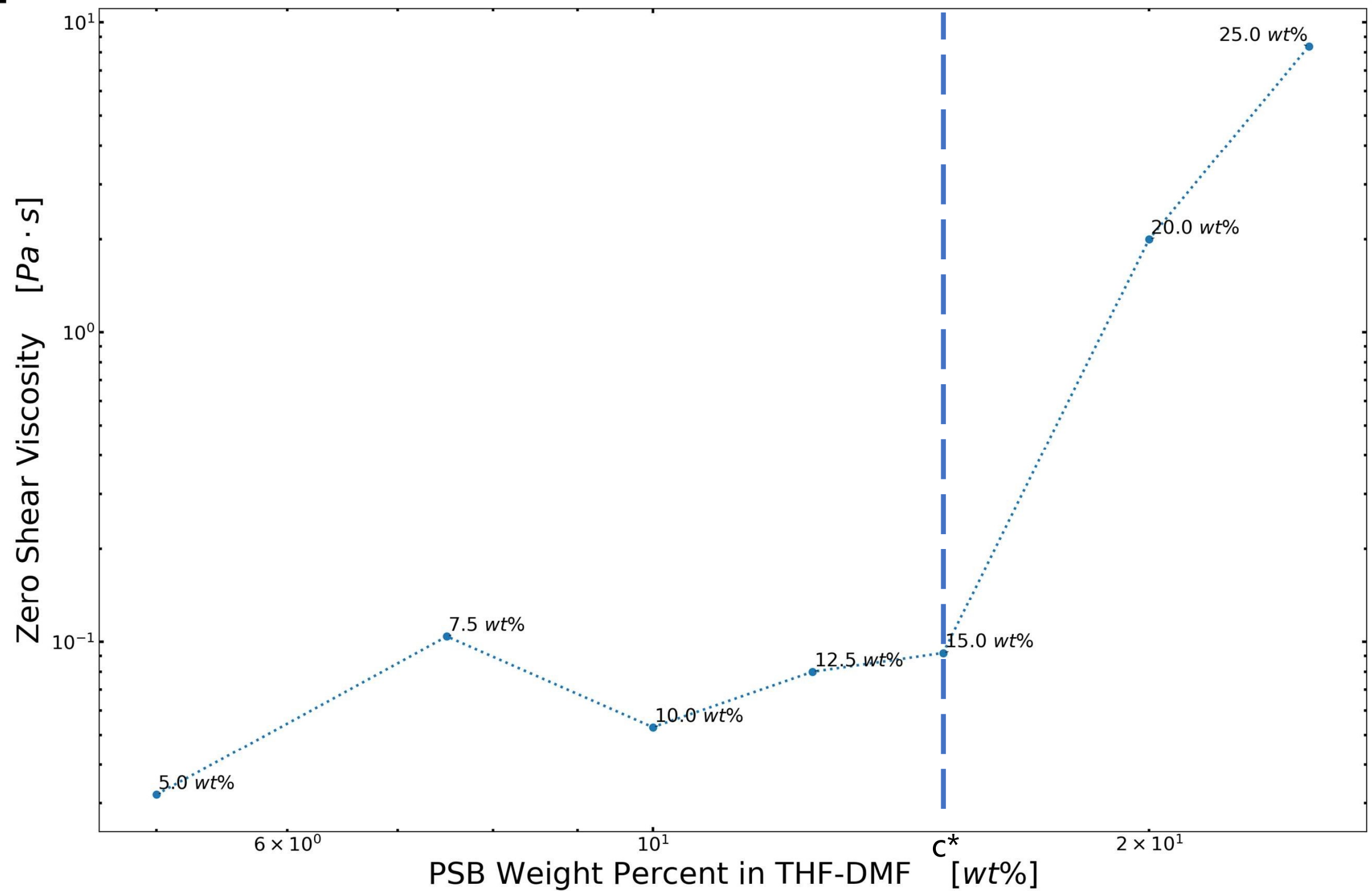


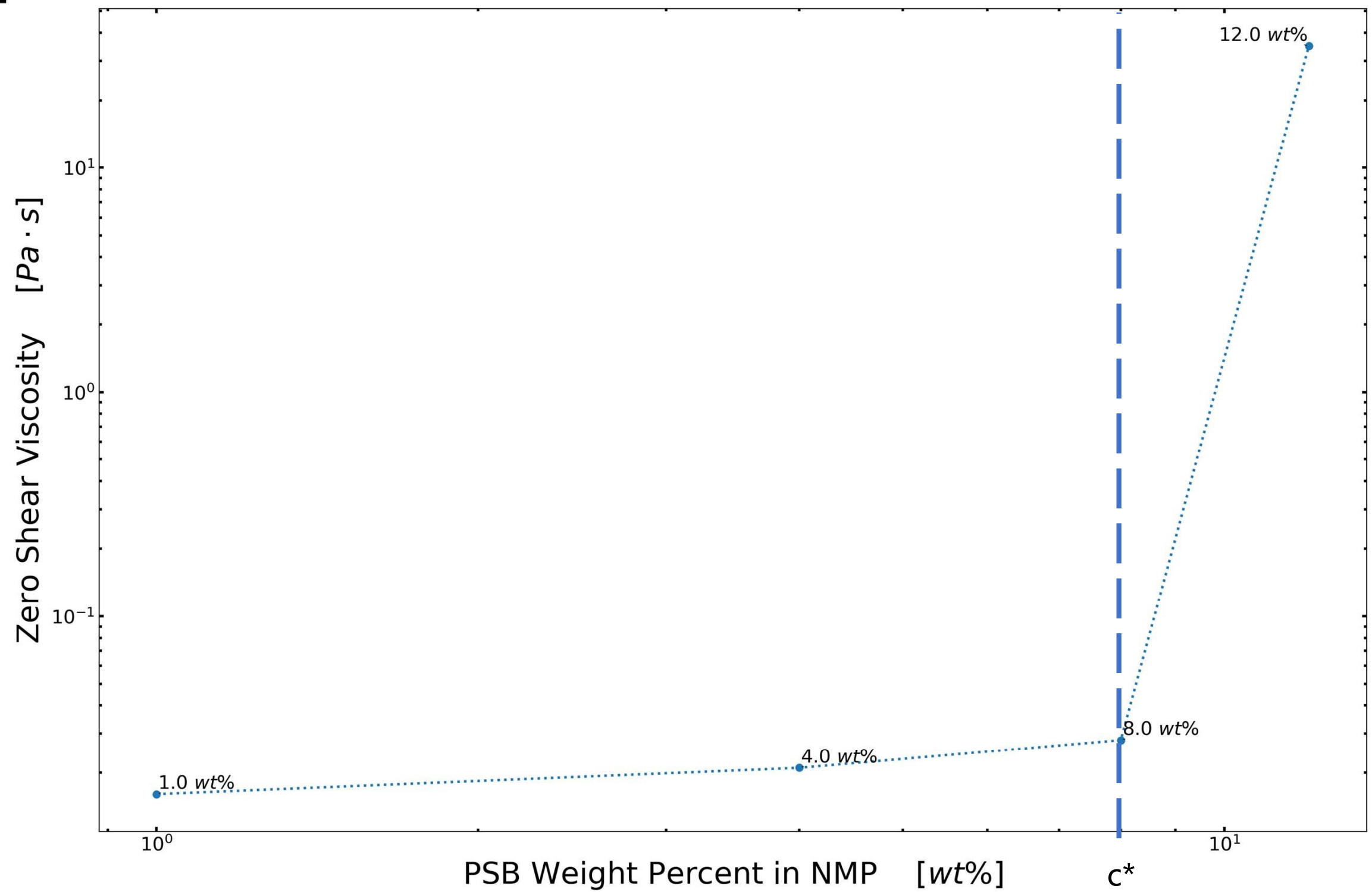
Conclusion 2.1: Spinnable/Critical Concentration

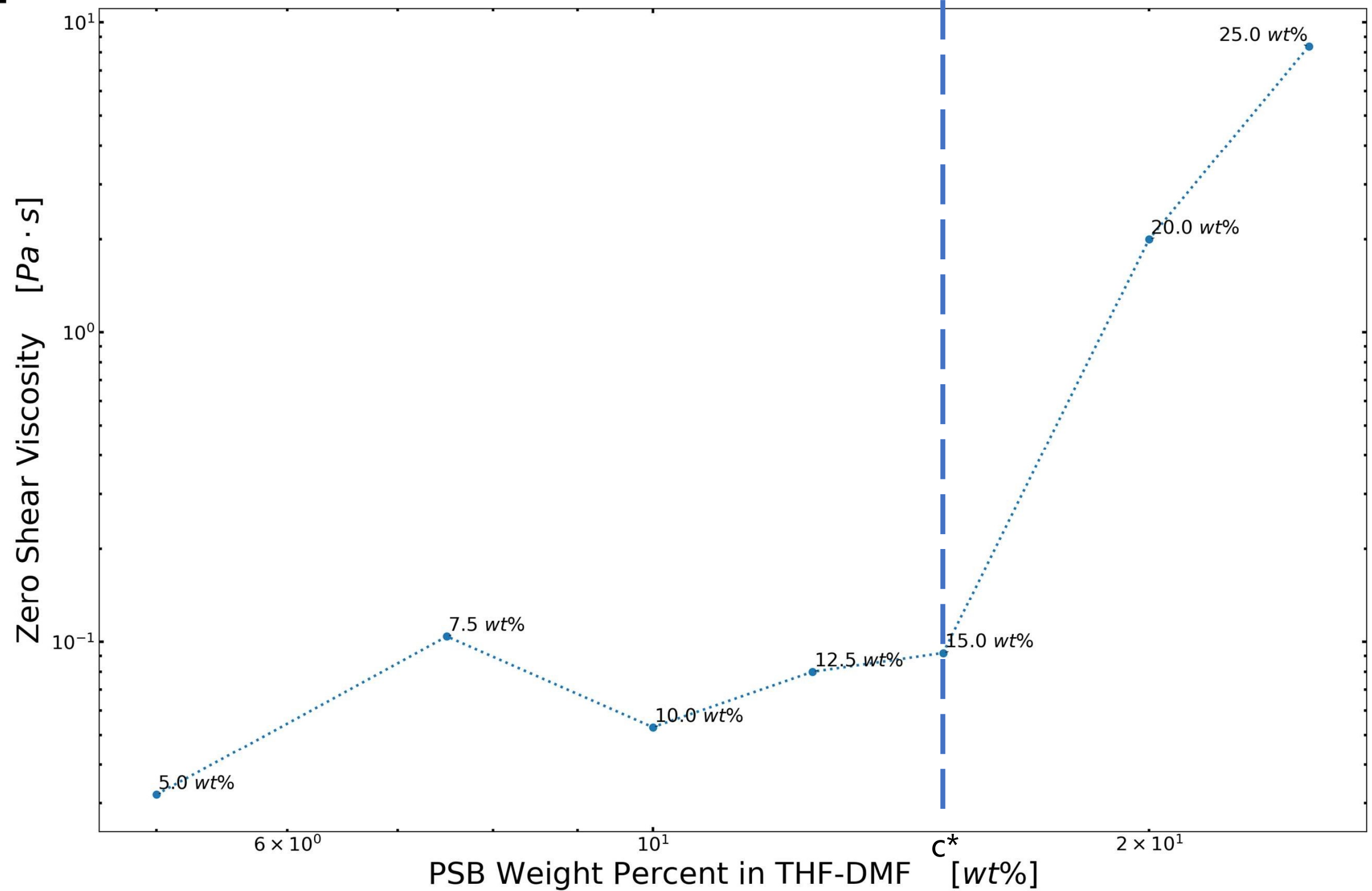


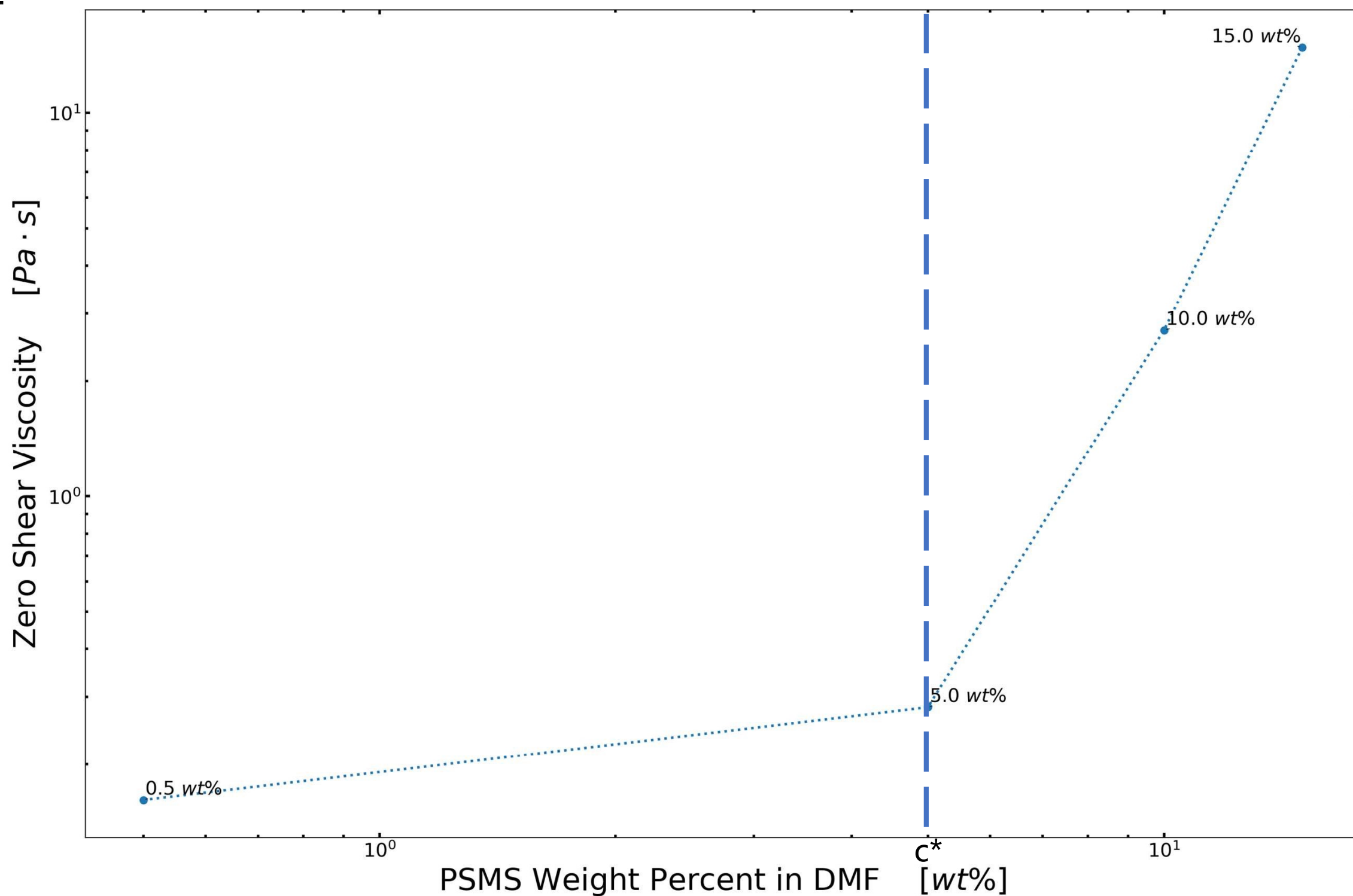
A low molecular weight shall be compensated with higher concentrations to reach a spinnable viscosity.

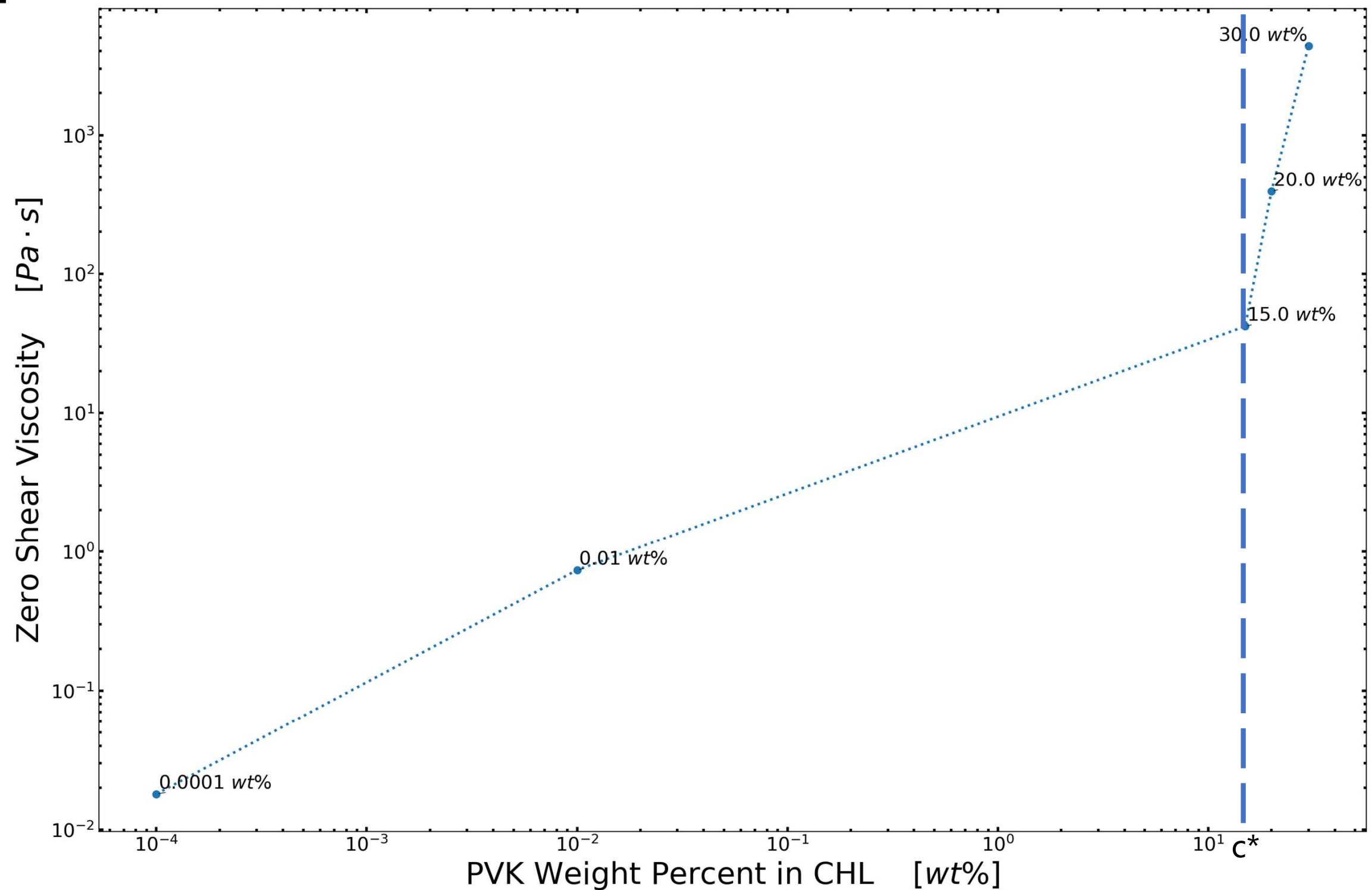
Polymer	Molecular Weight [g · mol]	Solvent	c^* [wt%]	η_0 [Pa · s]
PEO	4,000,000	CPO (SU-8)	0.25	60.022
PS	192,000	THF	20.00	0.166
PSB	490,000	NMP	8.00	0.028
PSB	490,000	THF and DMF	15.00	0.092
PSMS	2,658,076	DMF	5.00	0.282
PVK	1,100,000	CHL	15.00	41.861
PVK	1,100,000	CPO (SU-8)	0.75	49.657

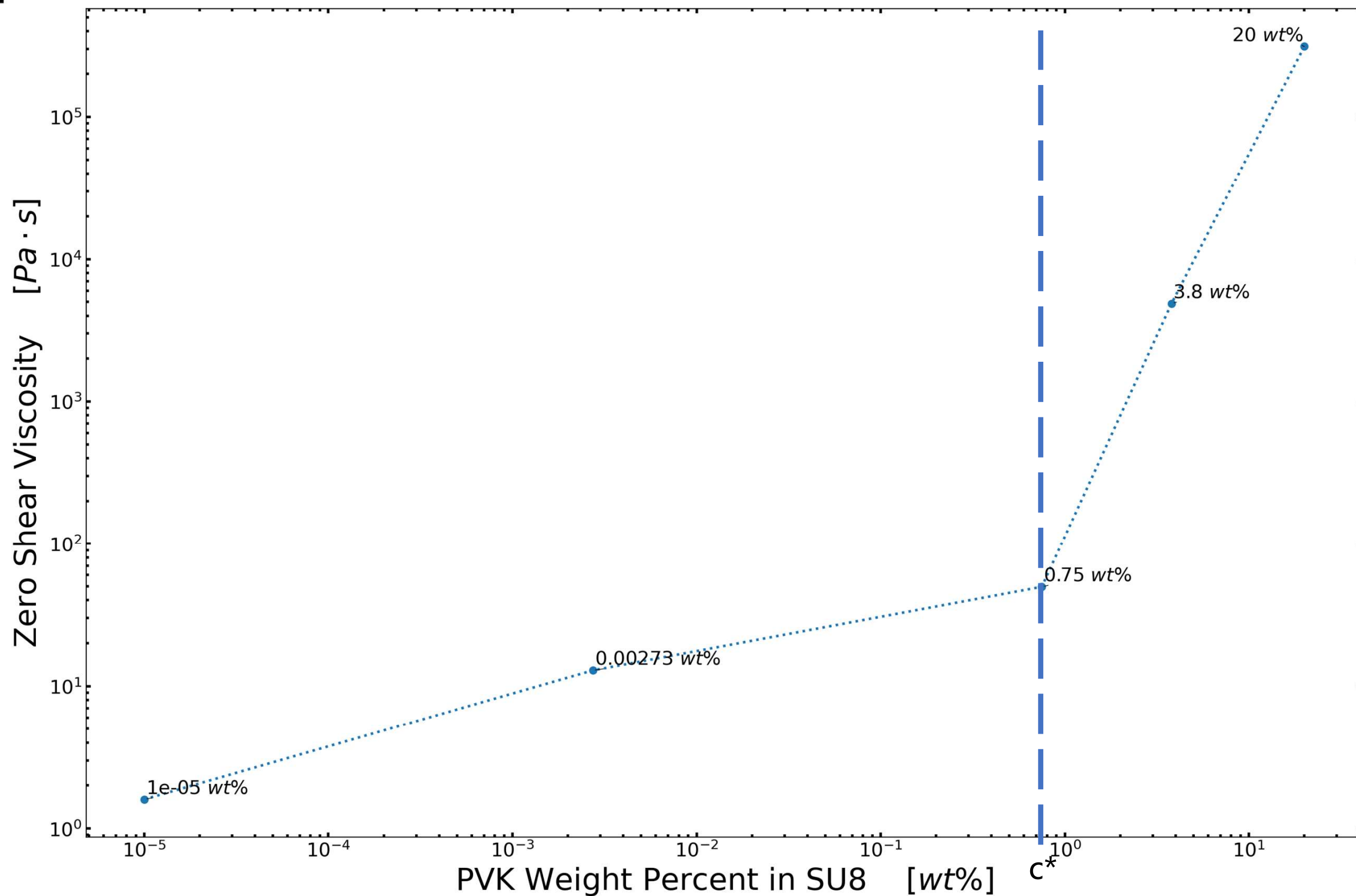






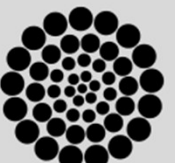






Fabrication & Characterization

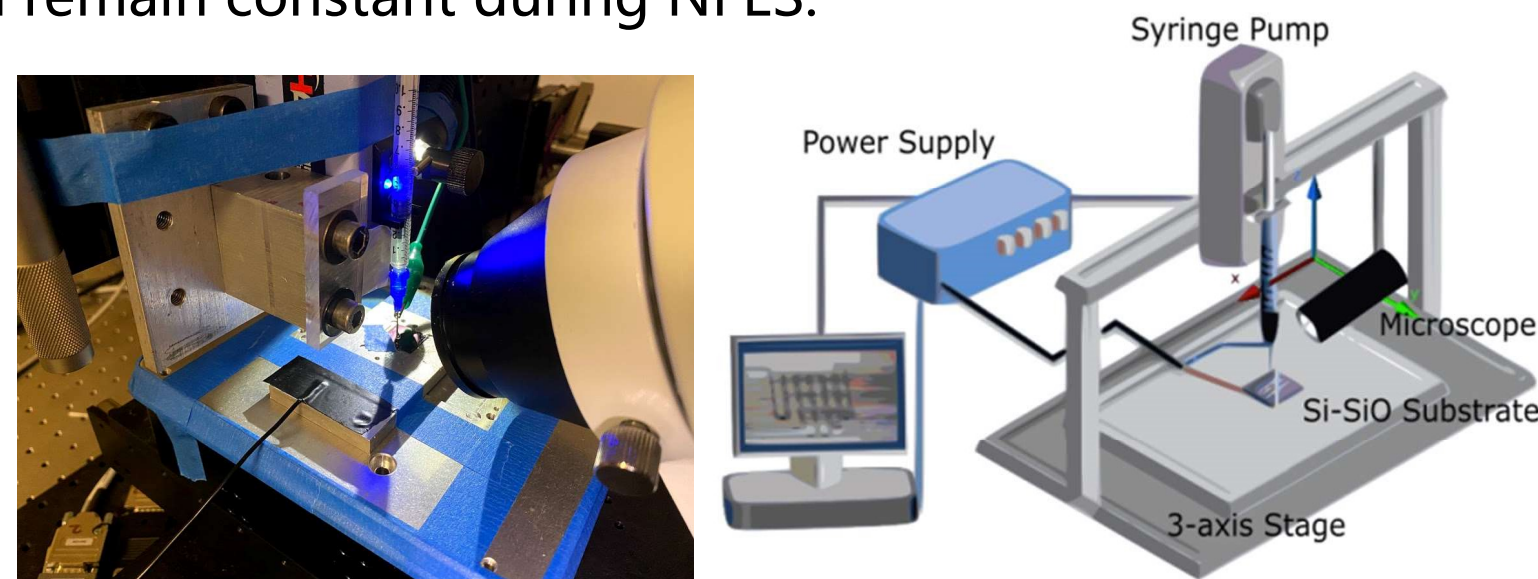
Specific Objective 3. Propose **alternatives to the SU-8/PEO benchmark** formulation for the production of microscopic polymer fibers with potential for the fabrication of carbon nano-wires.



Methods: Design of experiments / NFES

Given the results of previous work, the experiments shall reflect:

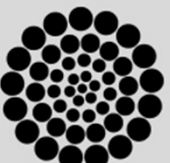
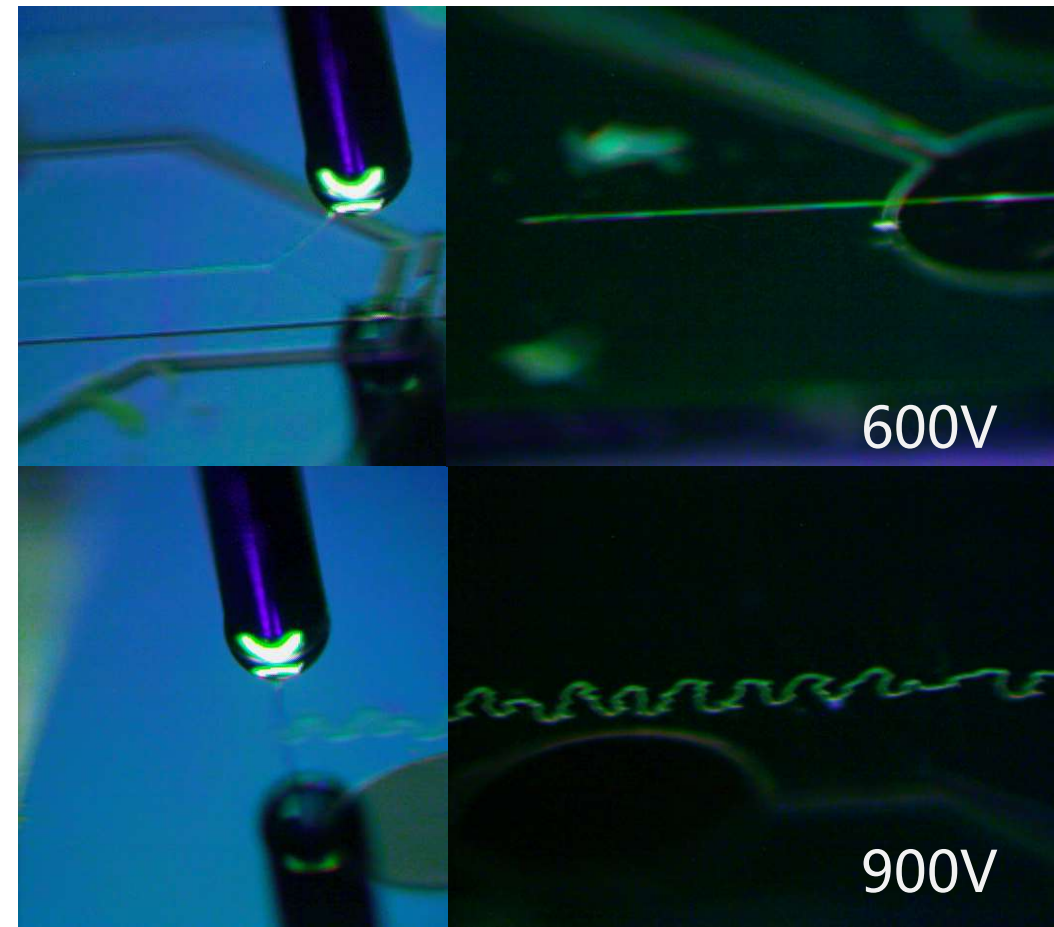
- The SU8-PEO sample set is the control
- The calculated critical concentration were used for each sample set.
- Each sample was electrospun at different applied voltages from 200 to 600V
 - Other process parameters (working distance, stage velocity, flow rate) are to be tuned and remain constant during NFES.



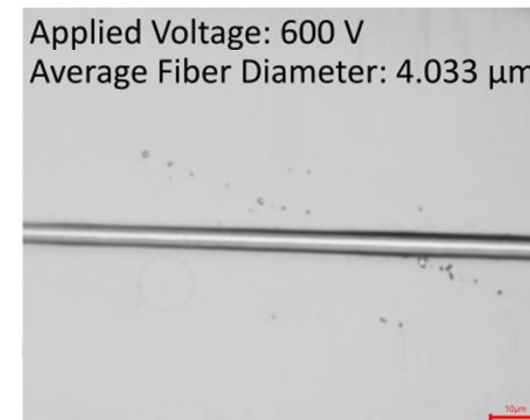
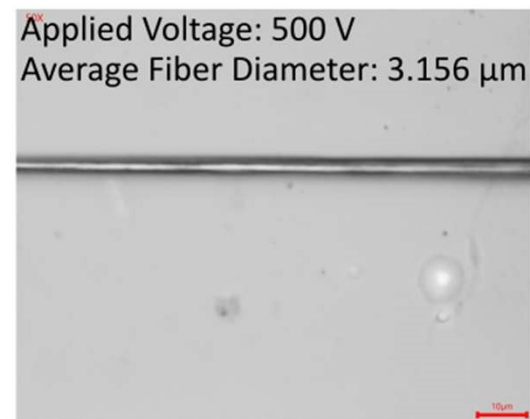
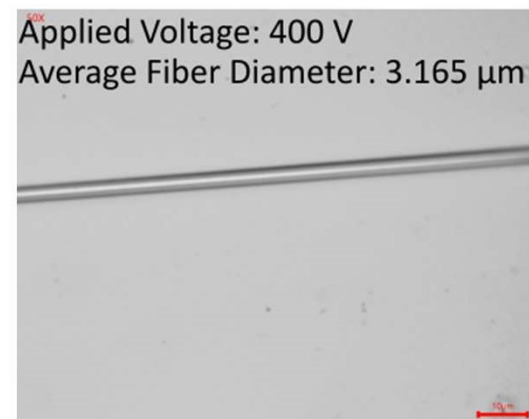
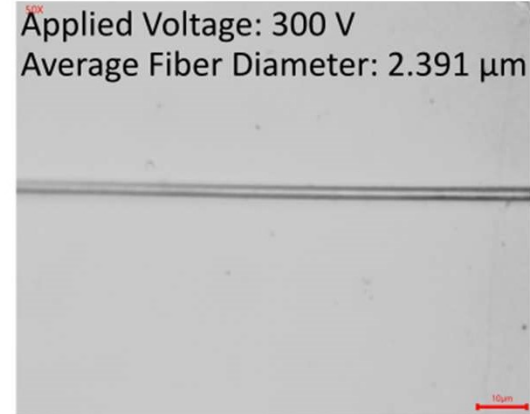
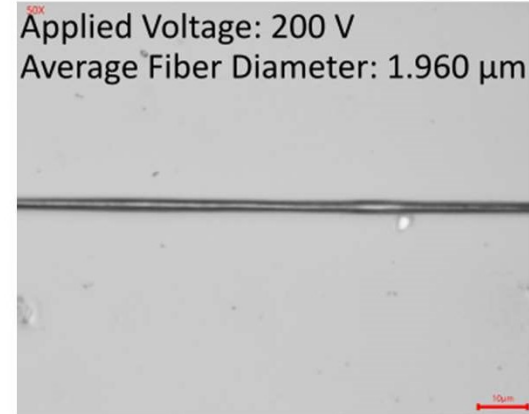
Fabrication: Process Parameters

- Fabrication velocity: 10 mm/s
- Working distance: 0.5 mm
- Applied voltage: 200V to 600V
- Applied current: 10 uA
- Flow rate: 0.04 uL/min
- Spacing: 10um

0.25 wt% PEO in SU-8



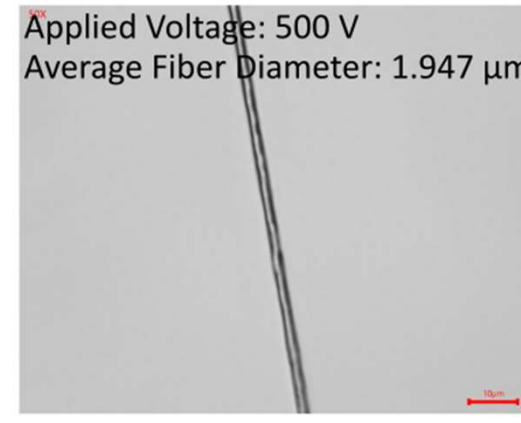
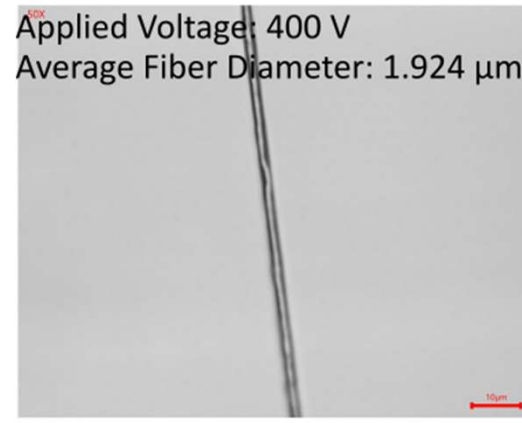
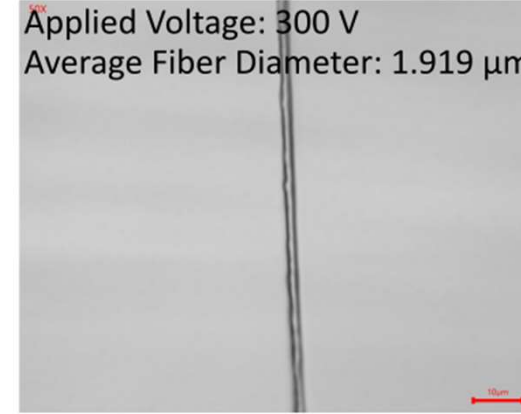
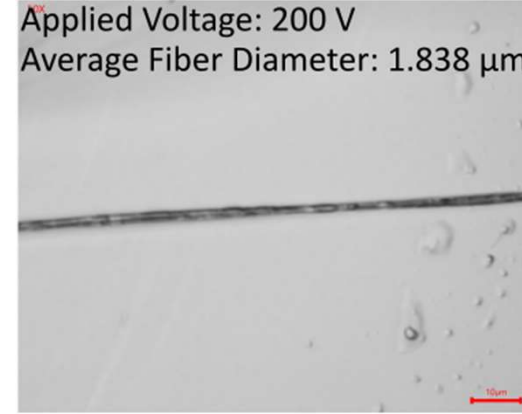
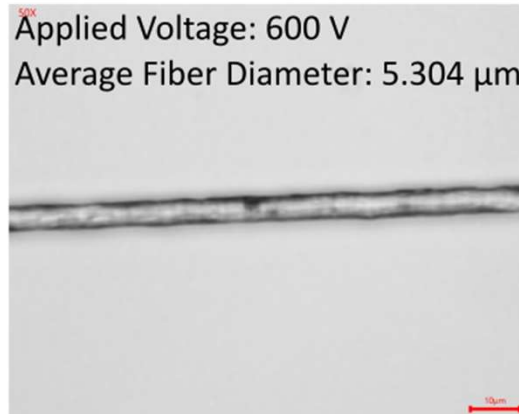
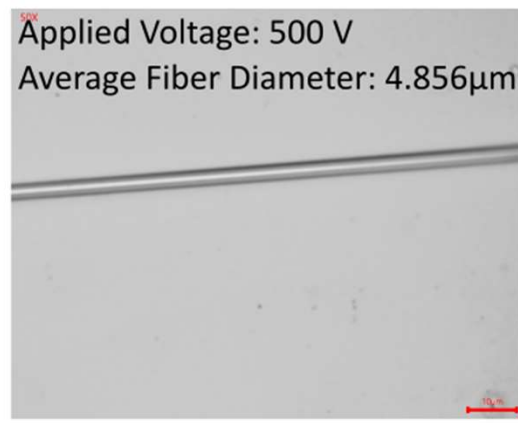
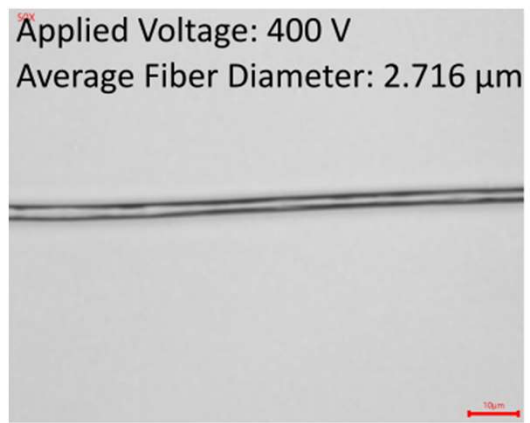
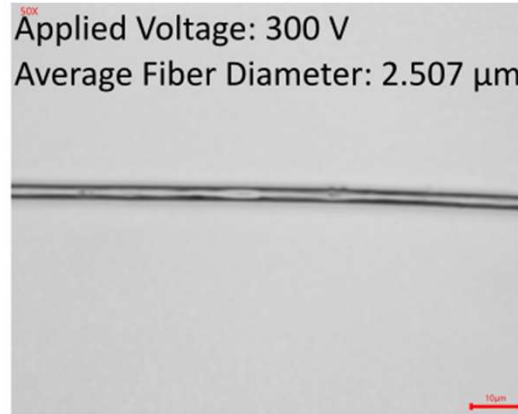
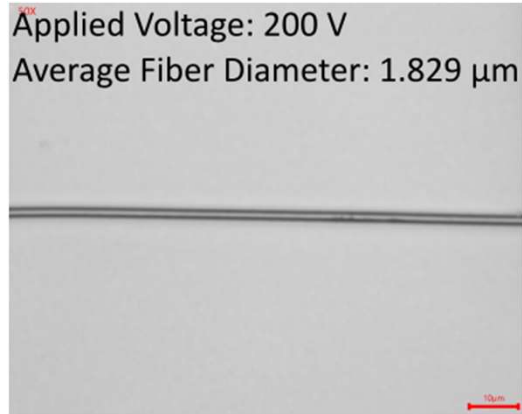
Characterization:



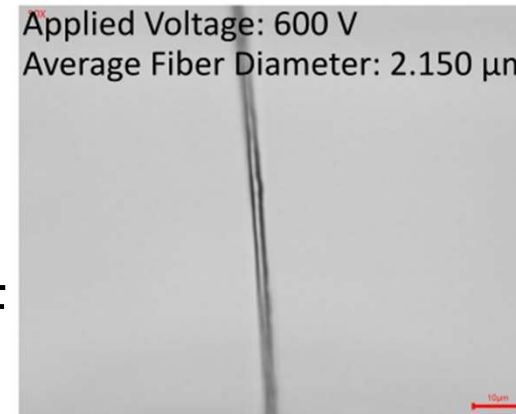
PEO in SU-8



PS in THF

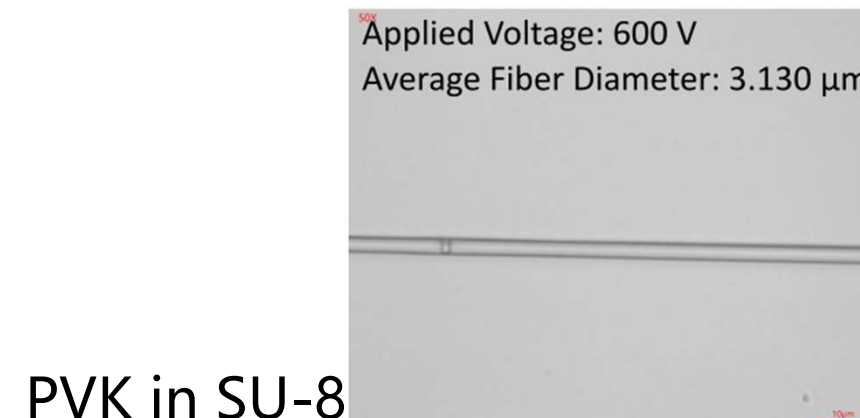
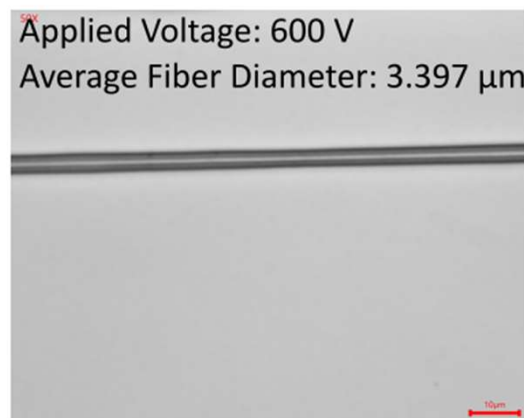
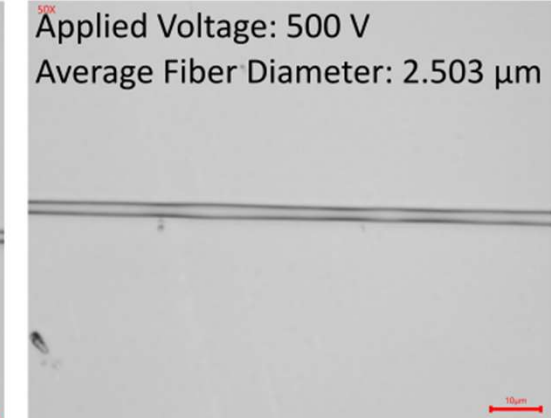
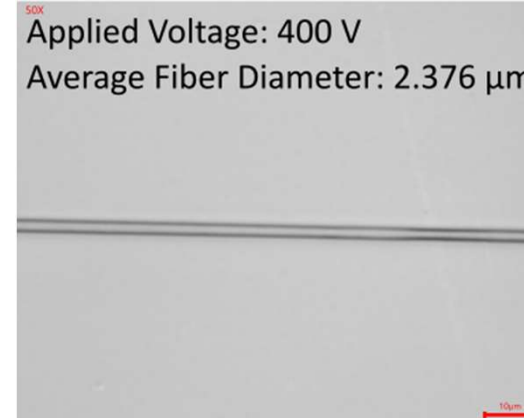
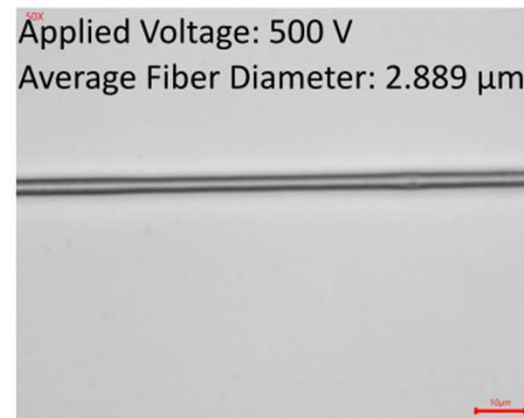
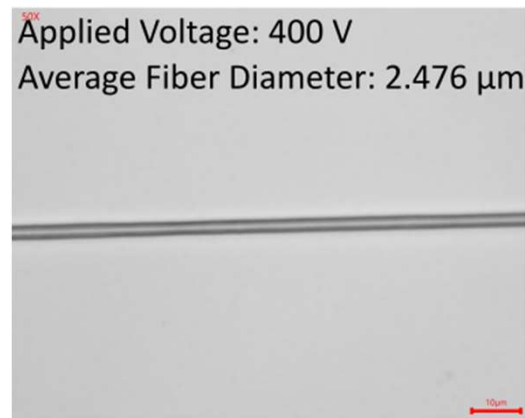
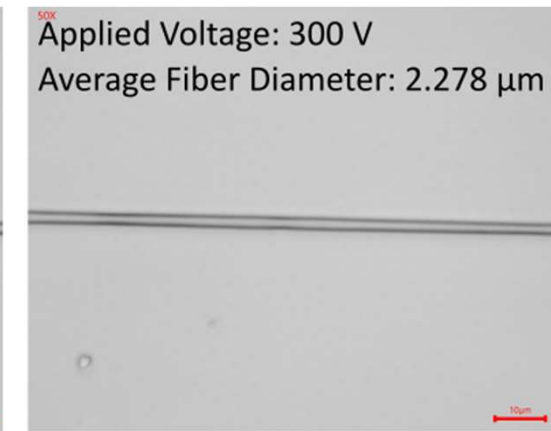
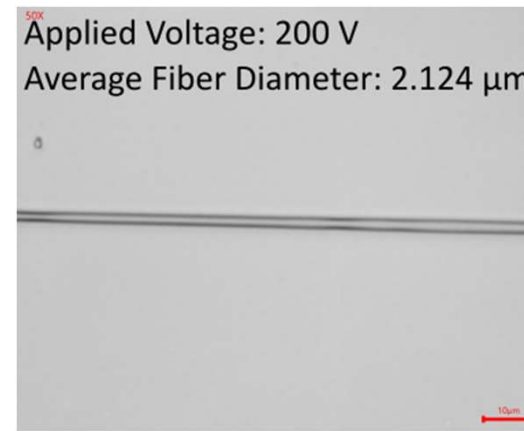
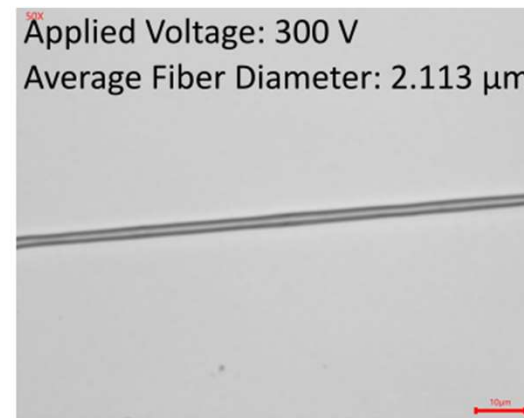
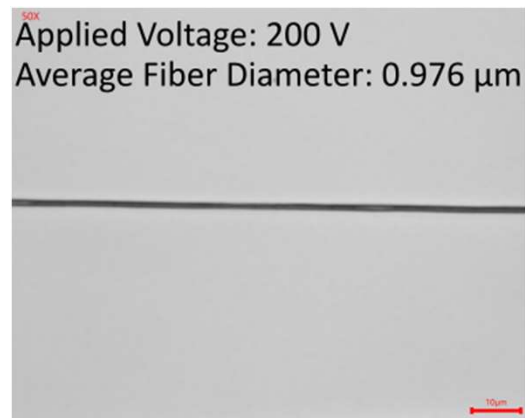


PSB in THF
and DMF





PVK in CHL



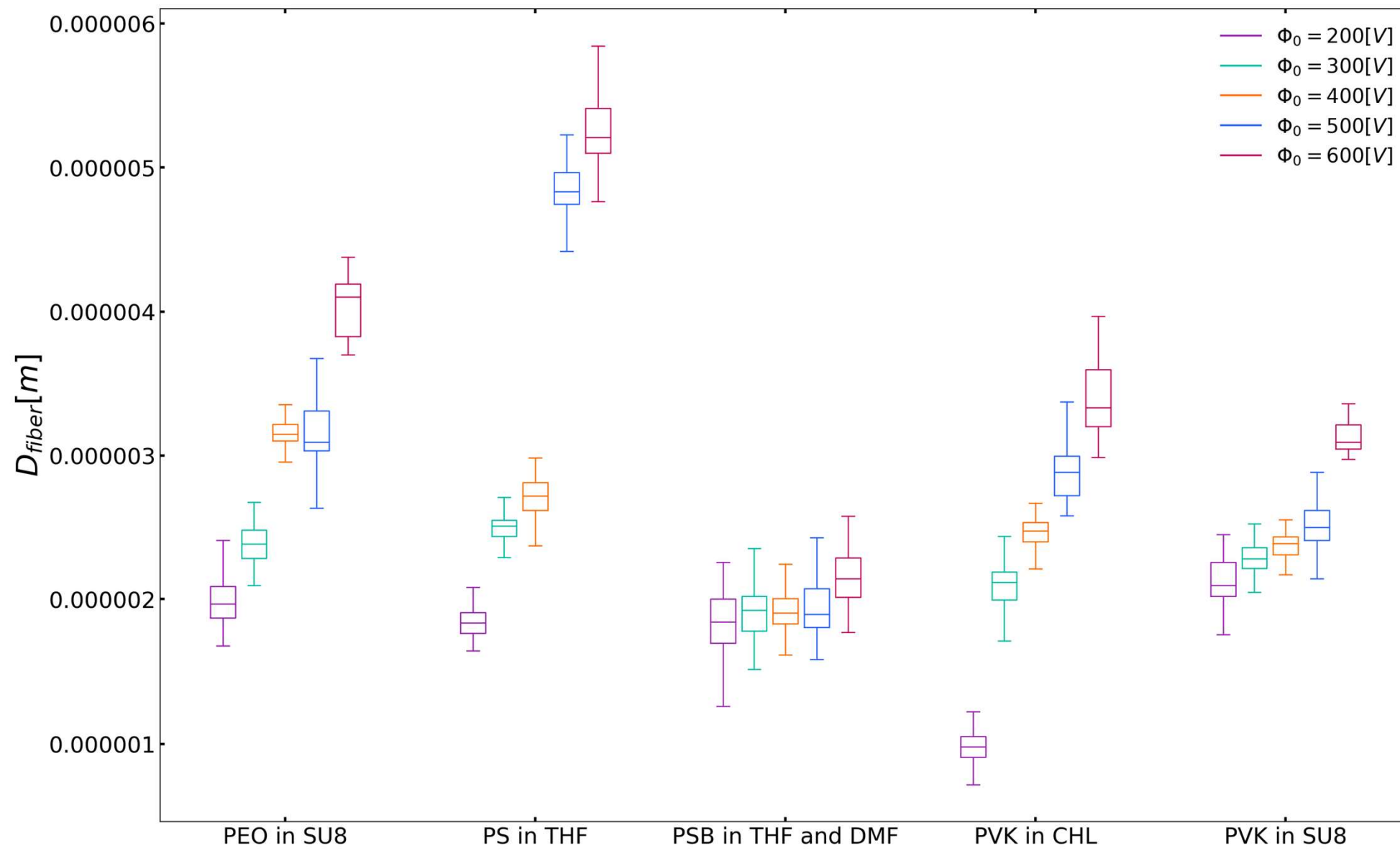
PVK in SU-8

non-spinnable solutions

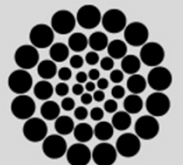
Polymer / Solvent	Critical concentration	Rationale
Poly(Styrene-co-alpha-Methylstyrene) (PSMS) in N,N-Dimethylformamide(DMF)	5 wt% (and 10, 15 wt%)	Fibres were broken into agglomerates / dust
Poly(Styrene-co-Butadiene) (PSB) in 1-Methyl-2-Pyrrolidinone (NMP)	8.00 wt%	Development of a shell around the drop.



Results: Spinnable solutions



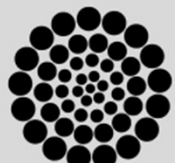
Conclusions & Future Work



Helgeson's Dimensionless analysis

Helgeson's model was thought to work with **far-field electrospinning**, hence the deviation of the NFES data from the model trend.

For an accurate NFES fiber diameter prediction, the **mechanical stresses** introduced by the moving stage shall be considered in the model

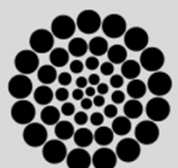


Pyrolysis Process

This work verifies the electro-spinnability of four new formulations and one modification to the PEO/SU-8 solution, however **fibers were not carbonized** into carbon structures.

Further work shall **study the pyrolysis process** of the proposed fibers to get carbon structures with good electrical conductivity.

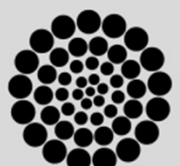
A photo-polymerization process could be introduced before pyrolysis to increase the order of the molecules and achieve carbon with higher conductivity.



Process Parameters

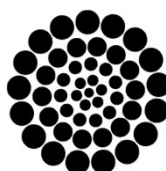
The viscosity-concentration plot is a helpful tool to estimate the critical spinnable concentration of a polymer-solvent system as NFES solutions require specific viscosities to initiate a polymer jet. However there is room for improvement as this method **only considers rheological data.**

Other methods could be adopted to better **tune other process parameters** such as stage velocity, and applied voltage.





Tecnológico
de Monterrey



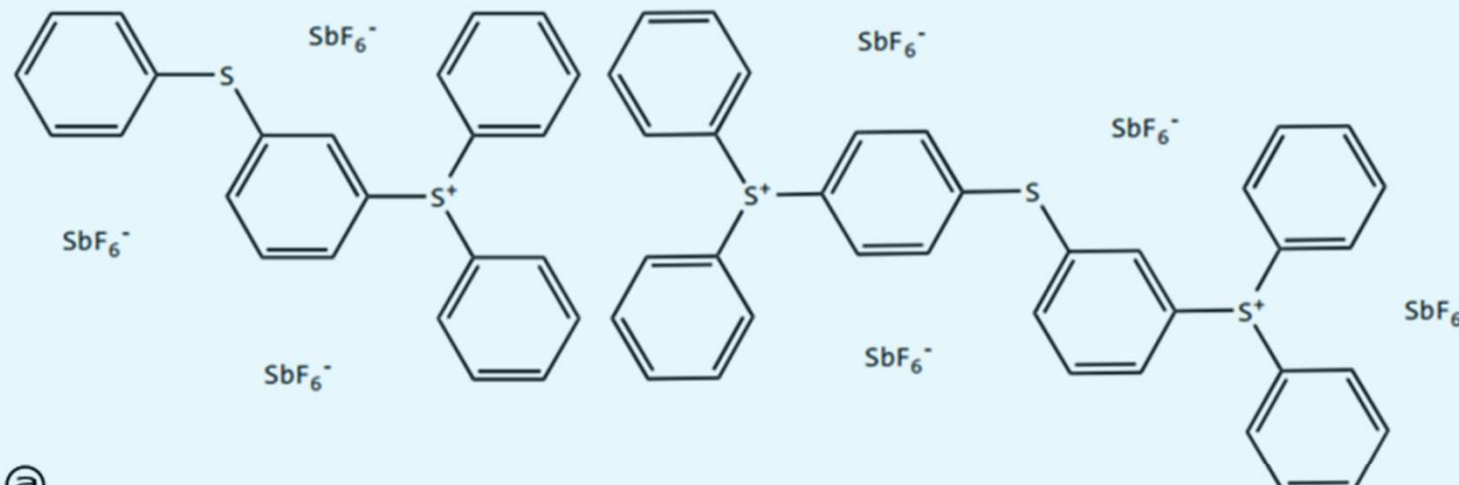
CONACYT
Consejo Nacional de Ciencia y Tecnología



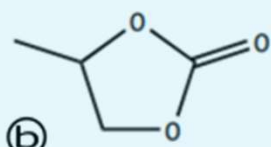
A landscape photograph featuring a calm lake in the foreground, a dense forest of green trees in the middle ground, and majestic mountains with snow-capped peaks in the background under a clear blue sky.

Any Questions?

SU-8 (MicroChem, US)



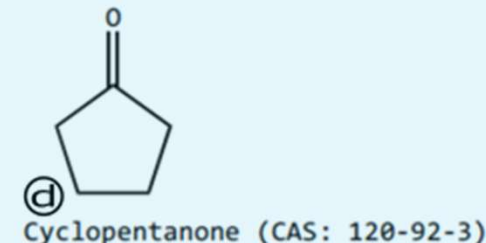
a Mixed Triarylsulfonium/Hexafluoroantimonate Salt (CAS: 89452-37-9)/(CAS: 71449-78-0)



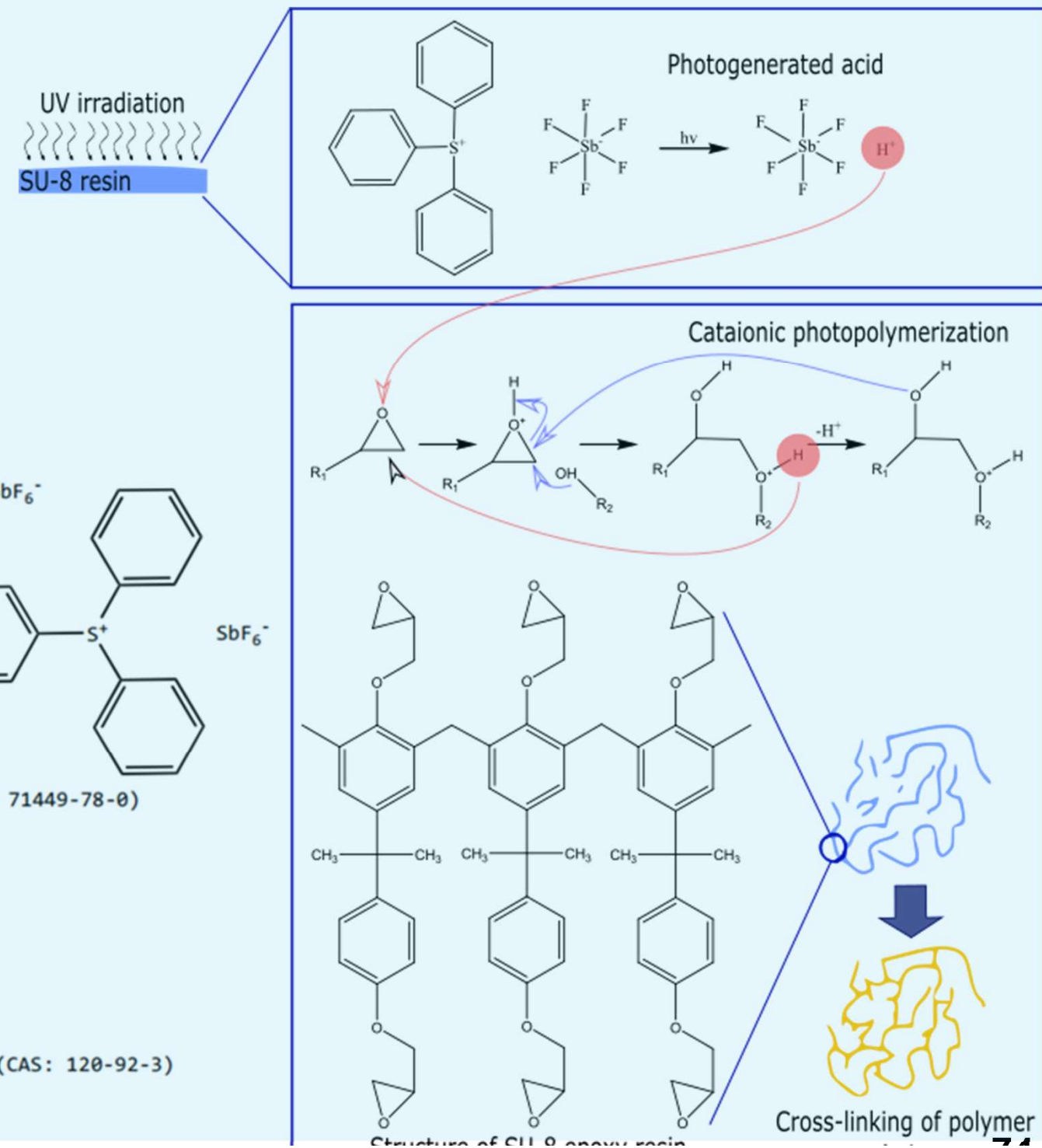
b Propylene Carbonate (CAS: 108-32-7)



c Epoxy Resin (CAS: 28906-96-9)



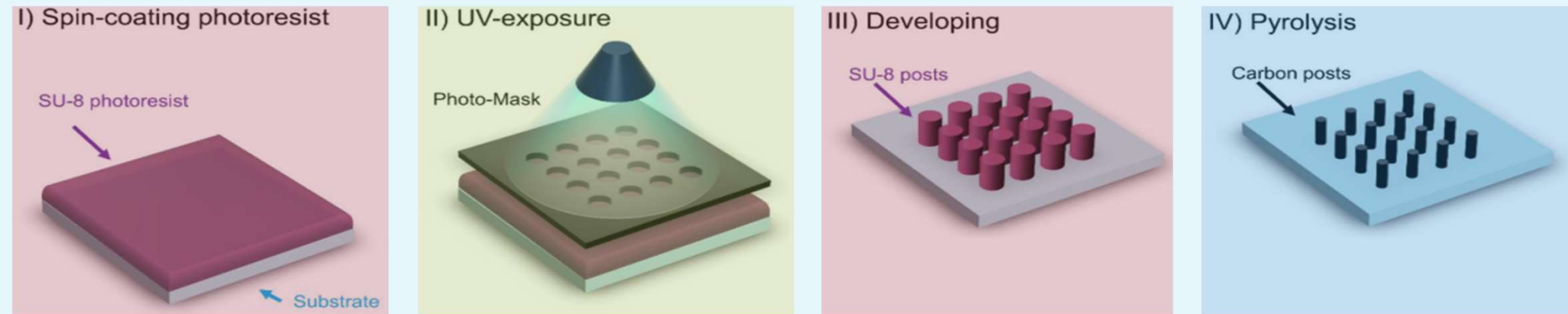
d Cyclopentanone (CAS: 120-92-3)



Carbon nanostructures via Lithography

The production of C-MEMS:

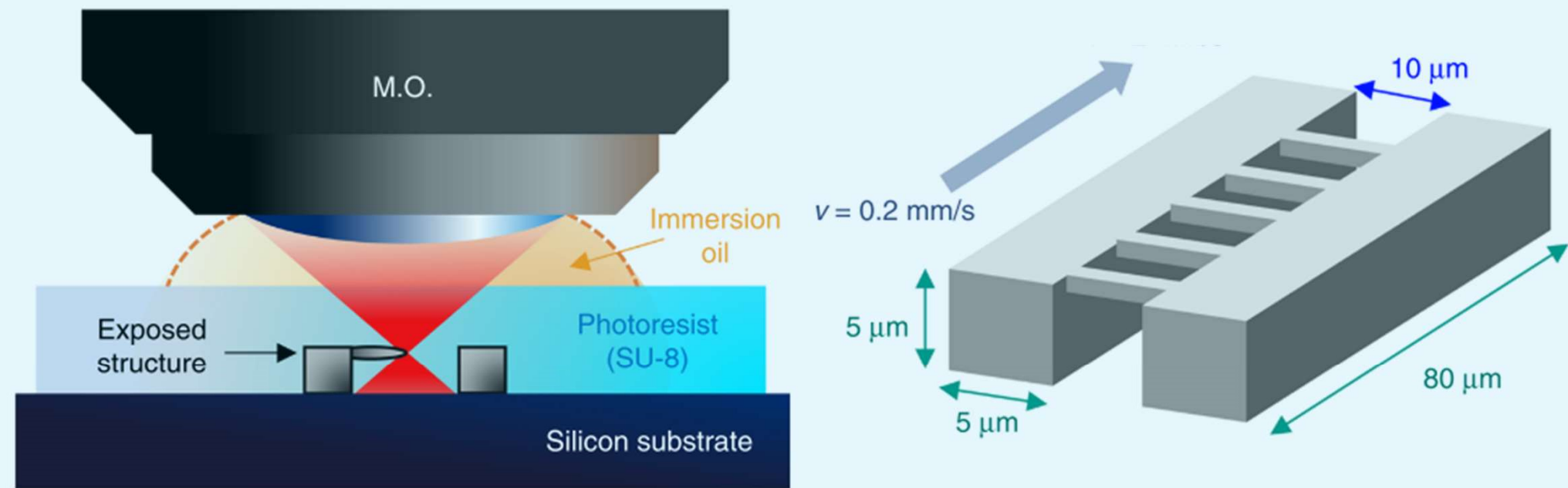
1. Polymer patterning through ~~photolithography~~
electrospinning
2. Carbonization through **pyrolysis**



photolithography
process

- SU-8 Waste
- Physical & Optical Limitations
- Structure Limitations

TPP – Two-Photon Polymerization

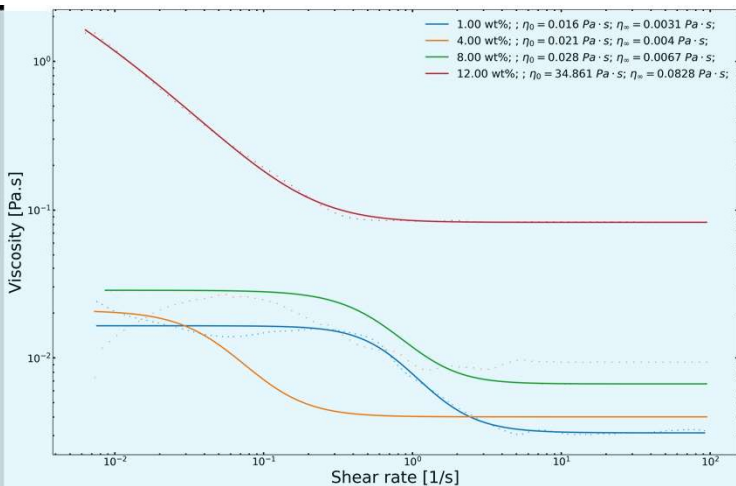


B. Cardenas-Benitez, C. Eschenbaum, D. Mager, J.G. Korvink, M.J. Madou, U. Lemmer, I. De Leon, S.O. Martinez-Chapa, Pyrolysis-induced shrinking of three-dimensional structures fabricated by two-photon polymerization: experiment and theoretical model, *Microsystems Nanoeng.* 5 (2019). <https://doi.org/10.1038/s41378-019-0079-9>.

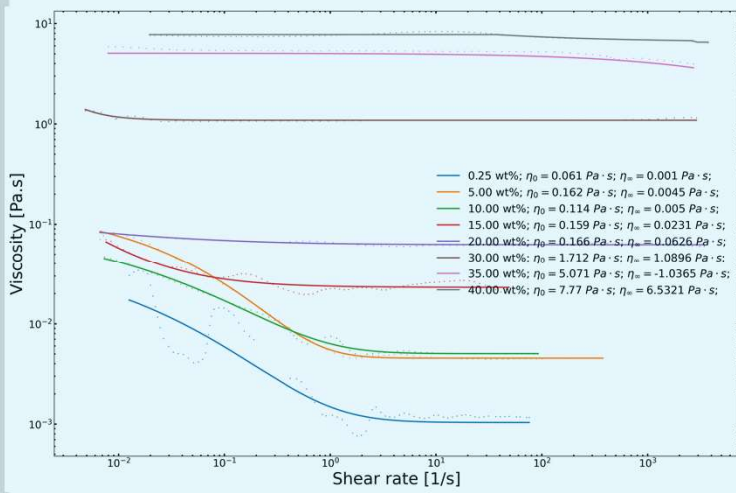
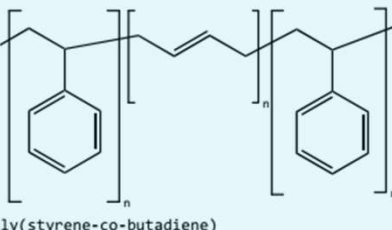
Characterization of the 0.25 wt% PEO Solution



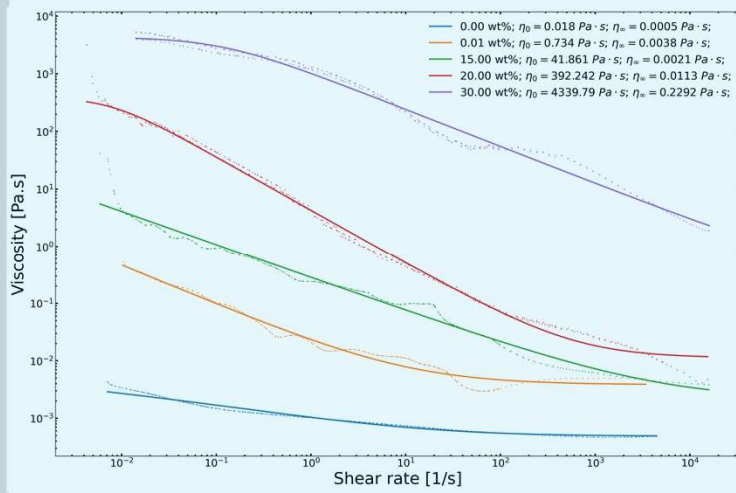
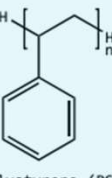




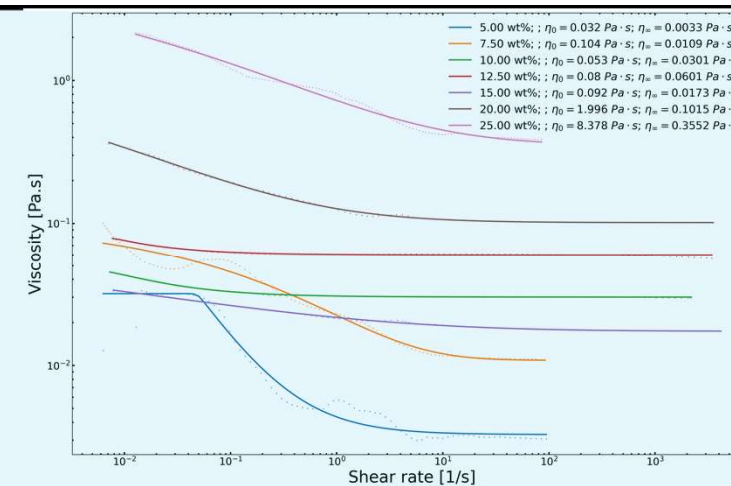
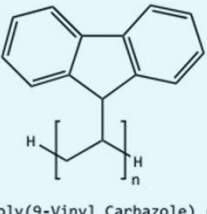
wt% in NMP



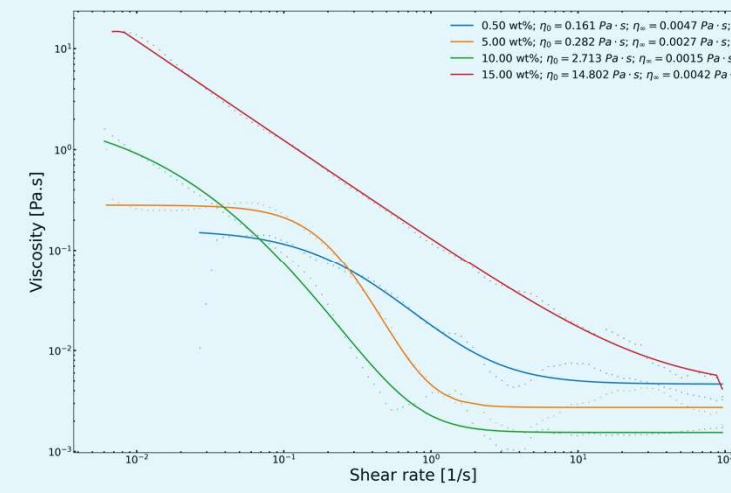
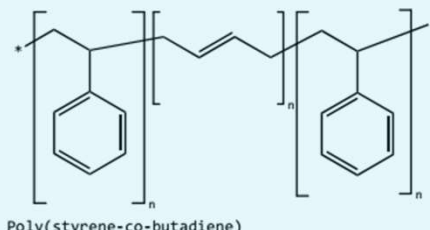
wt% in THF



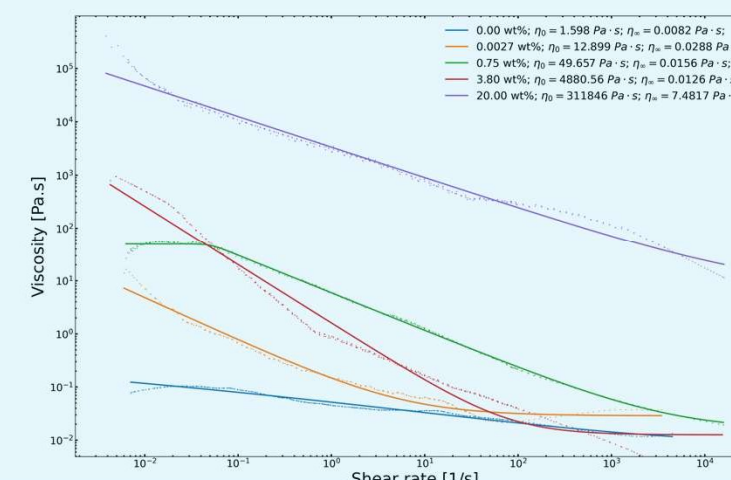
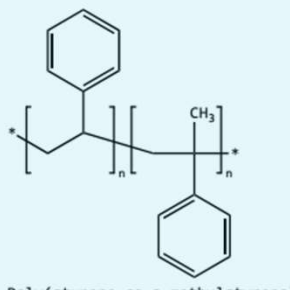
wt% in CHL



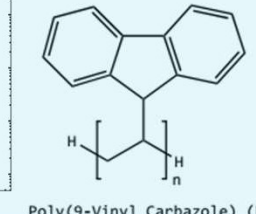
wt% in THF & DMF



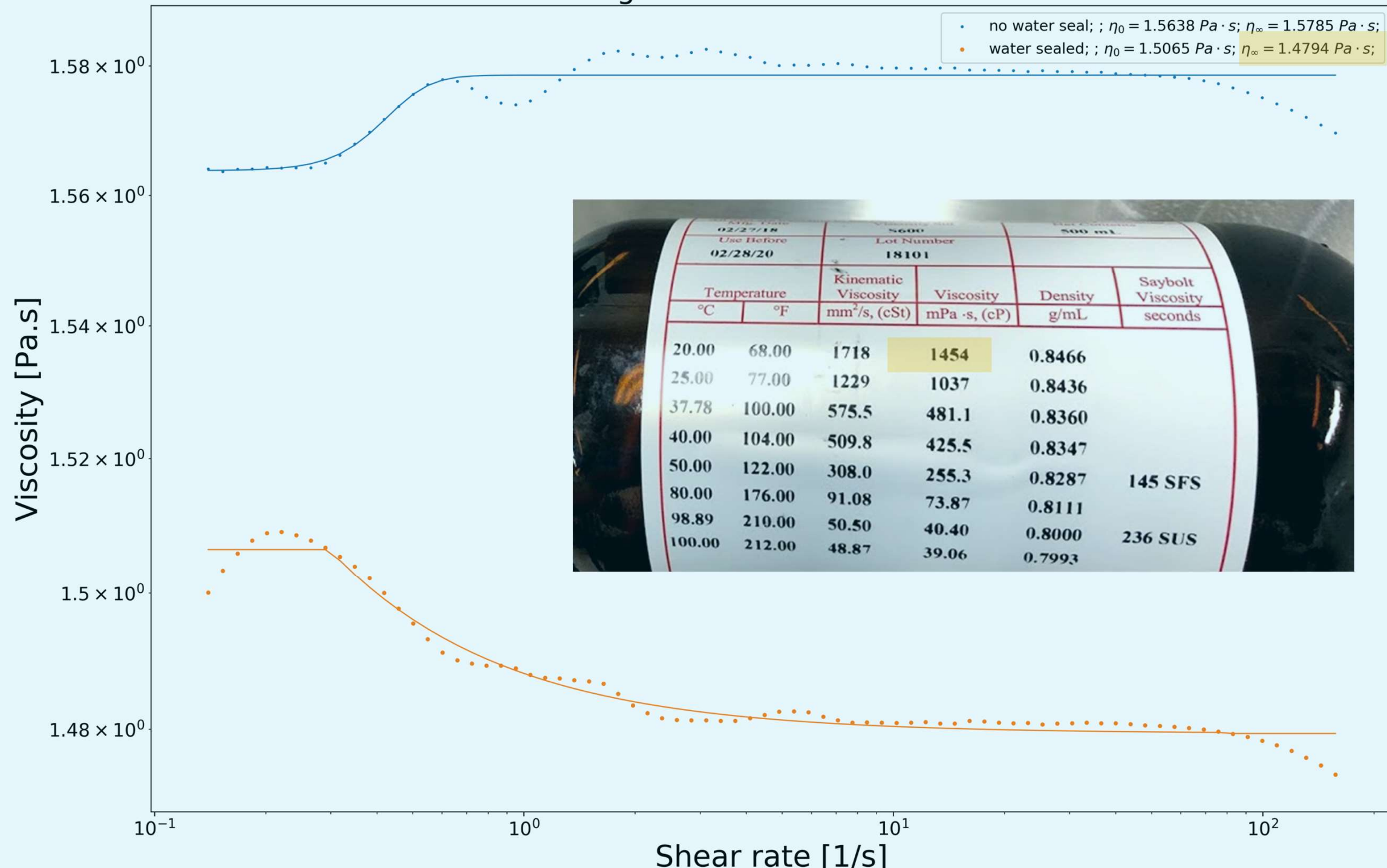
wt% in DMF



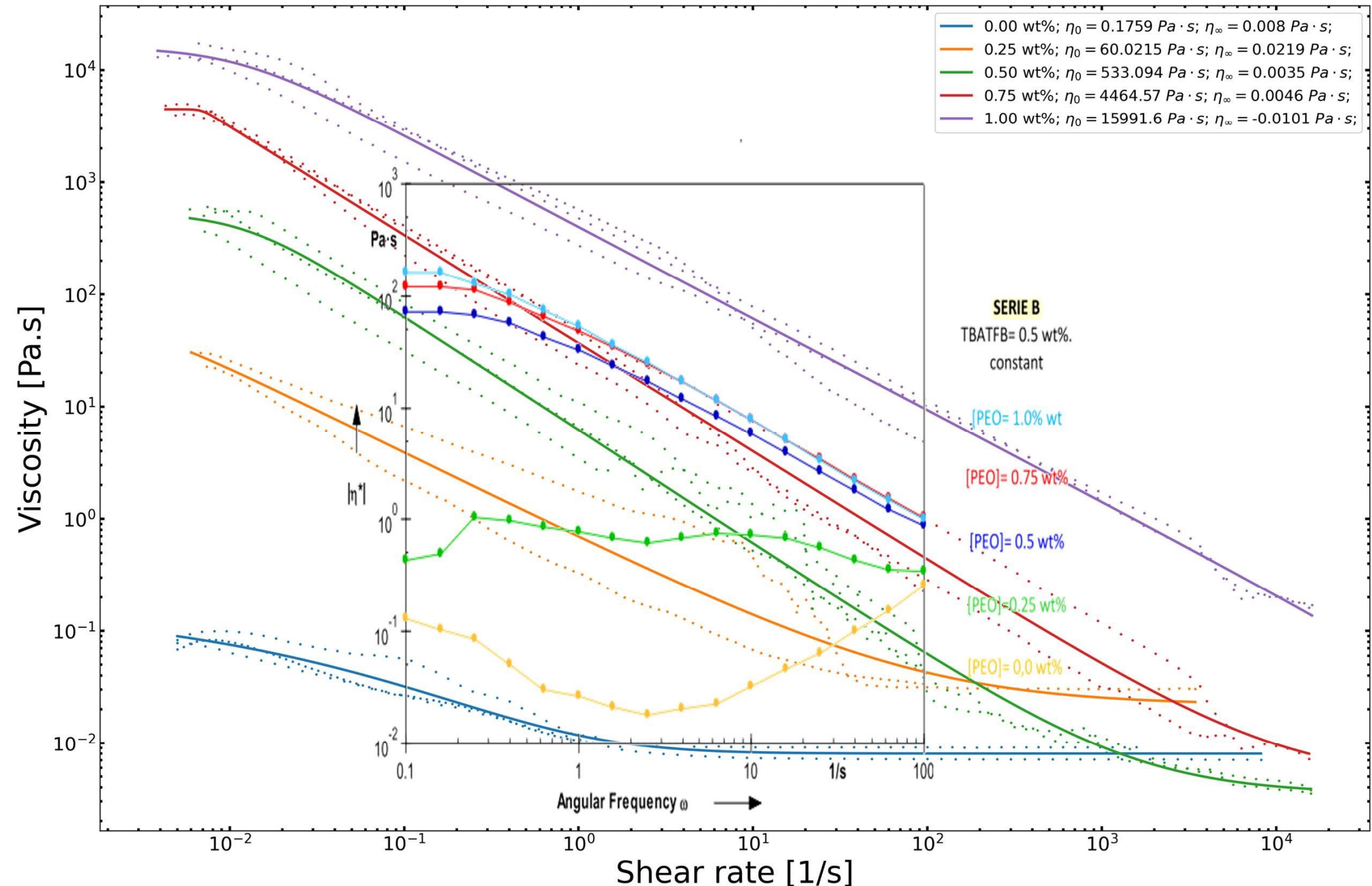
wt% in SU-8



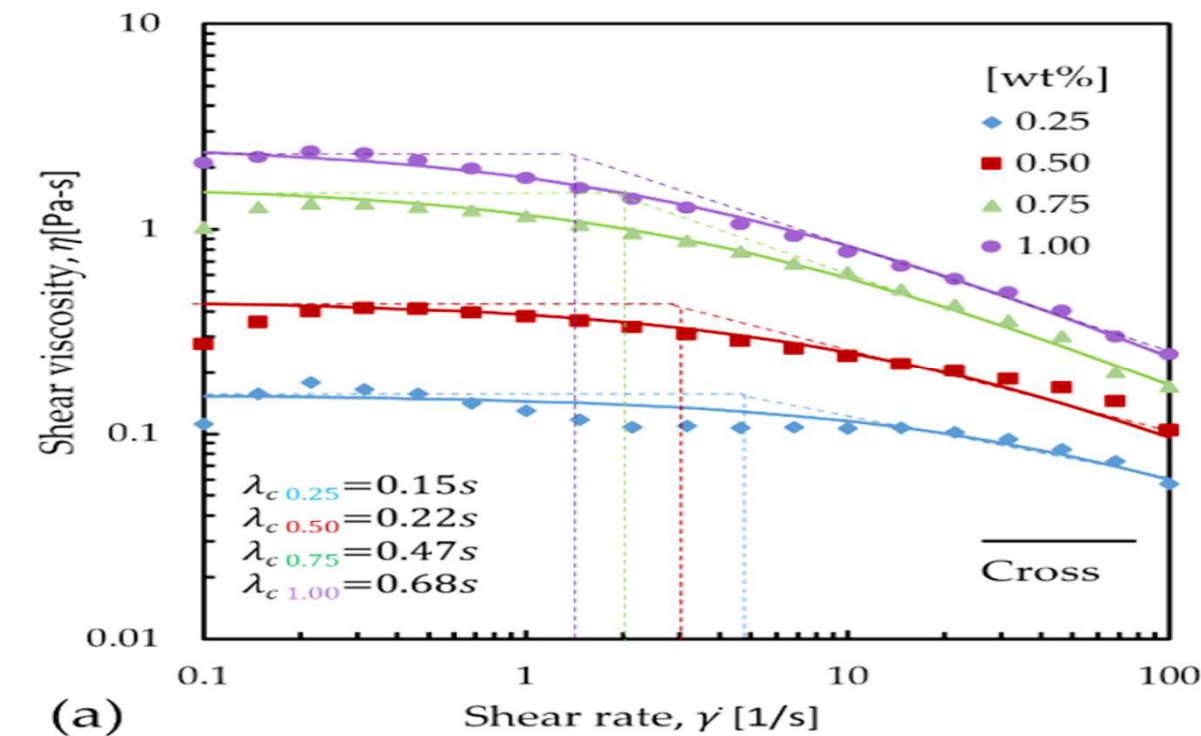
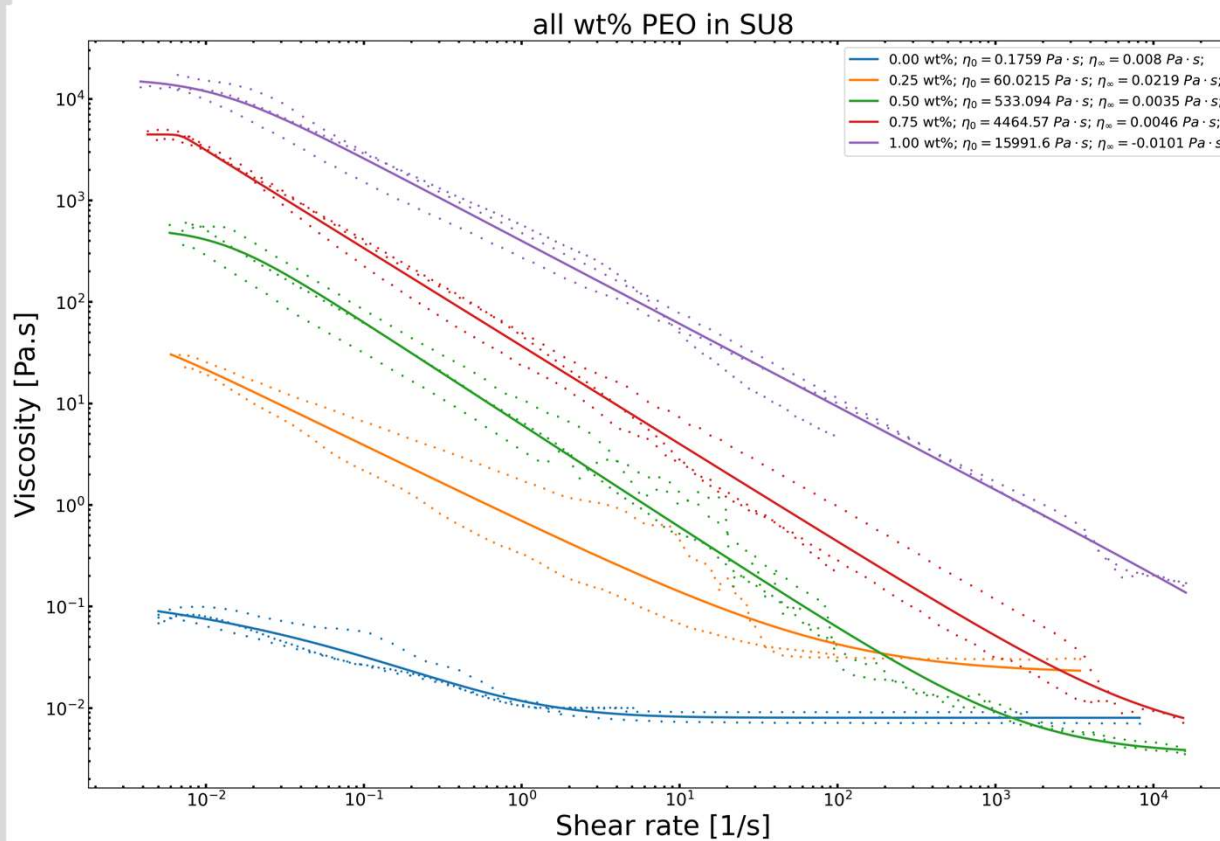
Standard Conforming to ASTM Oil Standard - Water Seal Test



all wt% PEO in SU8



Methods: Rheology results validation



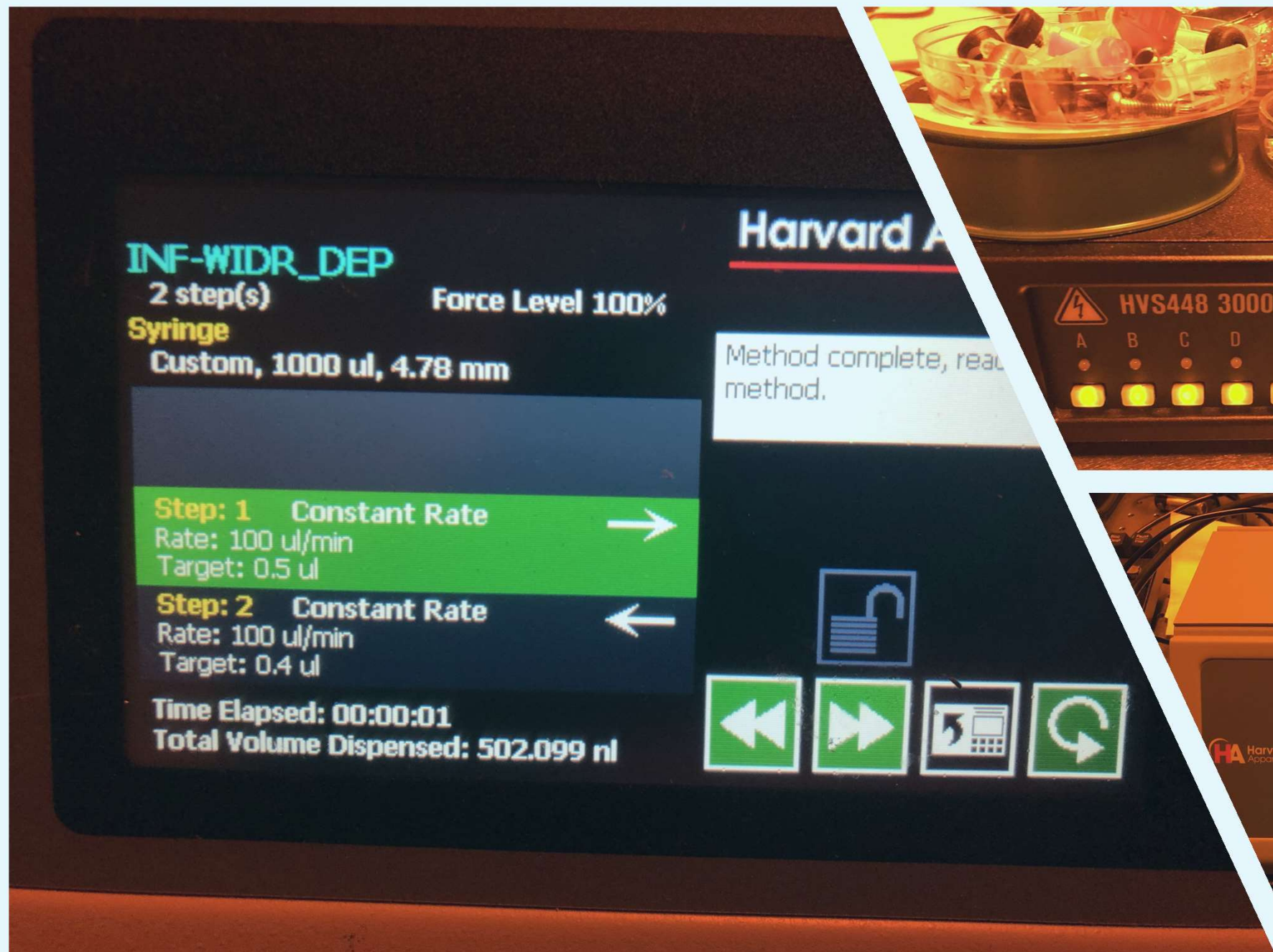
Methods: Rheology results validation

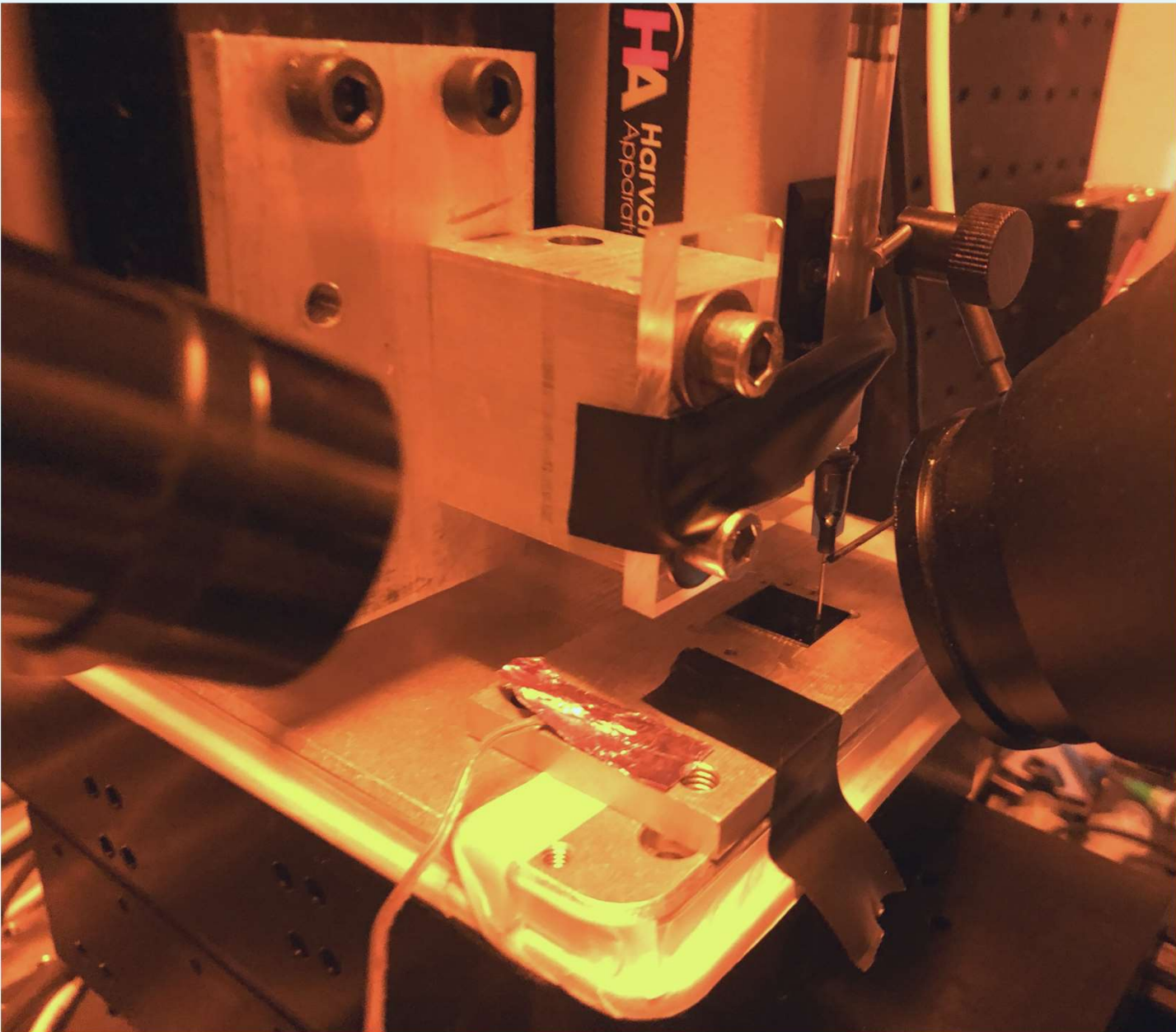
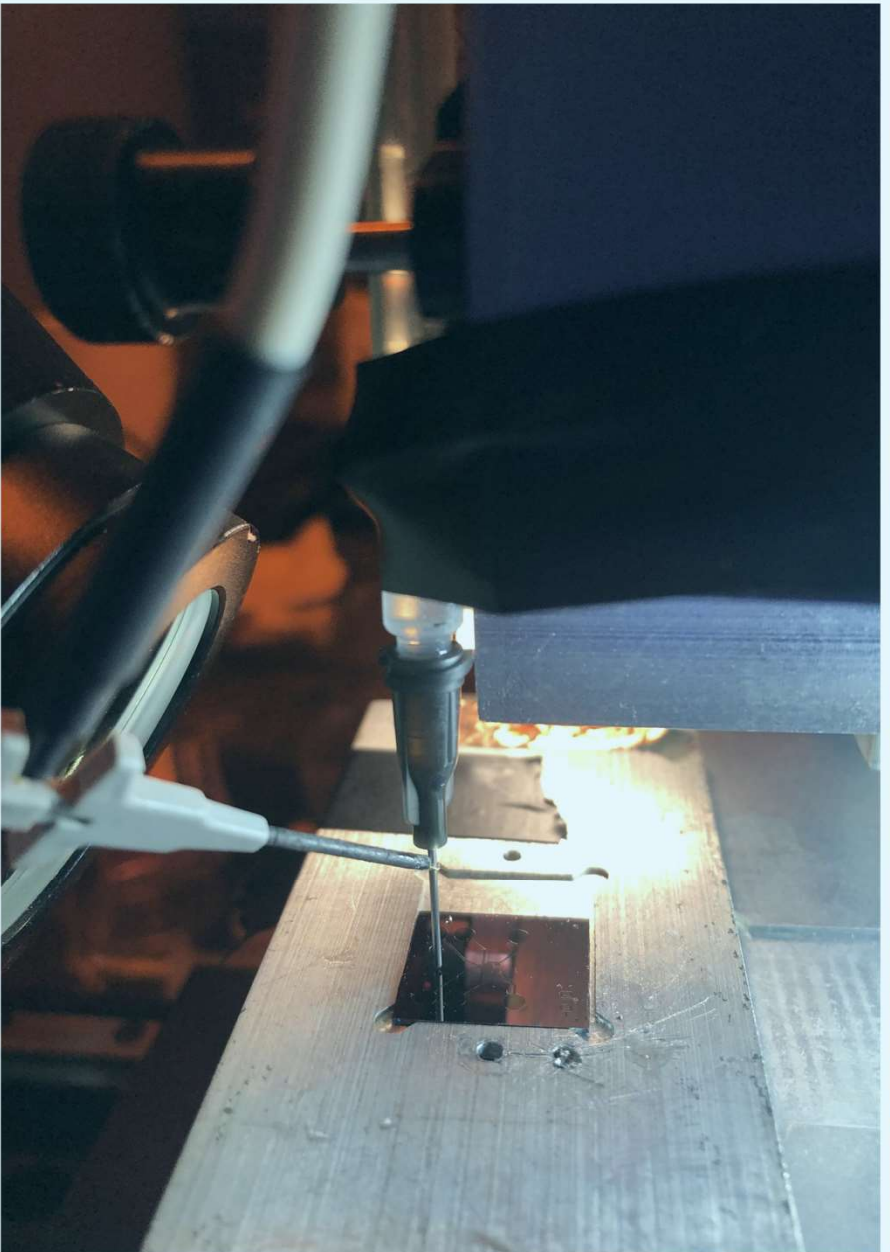
Sample	Weight Percent <i>wt%</i>		
	SU-8	PEO	TBF
1	99.50	0.00	0.50
2	99.25	0.25	0.50
3	99.00	0.50	0.50
4	98.75	0.75	0.50
5	98.50	1.00	0.50
density [g/ml]	1.123		

0.00 wt%; $\eta_0 = 0.058 \text{ Pa} \cdot \text{s}$; $\eta_\infty = 0.0079 \text{ Pa} \cdot \text{s}$;
0.25 wt%; $\eta_0 = 60.022 \text{ Pa} \cdot \text{s}$; $\eta_\infty = 0.0219 \text{ Pa} \cdot \text{s}$;
0.50 wt%; $\eta_0 = 533.094 \text{ Pa} \cdot \text{s}$; $\eta_\infty = 0.0035 \text{ Pa} \cdot \text{s}$;
0.75 wt%; $\eta_0 = 4464.57 \text{ Pa} \cdot \text{s}$; $\eta_\infty = 0.0046 \text{ Pa} \cdot \text{s}$;
1.00 wt%; $\eta_0 = 15991.6 \text{ Pa} \cdot \text{s}$; $\eta_\infty = -0.0101 \text{ Pa} \cdot \text{s}$;

Table 1. Zero-Shear Viscosity and Relaxation Time Calculated for Different PEO Concentrations

	Zero-Shear Viscosity η_0 (Pa·s)	Relaxation Time λ (s)
1% PEO	1.33	0.7
2% PEO	28.70	10.0
3% PEO	111.00	25.0





SU-8 (MicroChem, US)

MICROCHEM CORP SU-8 2002 500ML

encompass

Manufacturer: MICROCHEM CORP Y111029

Catalog No.	NC0702370
\$628.71 / Each	
Qty	<input type="text"/> Check Availability
	Add to cart

<https://www.fishersci.com/shop/products/NC0702370/nc0702370#?keyw ord=MICROCHEM+CORP+PHOTORESIST+SU-8>

MICROCHEM CORP SU-8 DEVELOPER 4L

encompass

Catalog No. NC9901158

\$172.90 / Each

INGREDIENTS:

Cyclopentanone (CAS: 120-92-3); 23-78%.
Mixed Triarylsulfonium/ Hexafluoroantimonate Salt;
(CAS: 89452-37-9)/(CAS: 71449-78-0); 1-5%
Propylene Carbonate (CAS: 108-32-7); 1-5%
Epoxy Resin (CAS: 28906-96-9); 25-75%

<https://www.fishersci.com/shop/products/NC9901158/nc9901158#?keyw ord=SU-8++developer>

Materials

Safety Solvents		CAS Number	Presentation
	1-Methyl-2-pyrrolidinone (NMP)	872-50-4	anhydrous, 99.5% 328634-100ML 328634-1L
	Dichloromethane (Methylene chloride)	75-09-2	anhydrous, ≥99.8%, 40-150 ppm amylene as stabilizer 270997-100ML 270997-1L
	Dimethylacetamide (DMAc)	127-19-5	anhydrous, 99.8% 271012-100ML 271012-1L
250 ml	Dimethylformamide (DMF)	68-12-2	anhydrous, 99.8% 227056-100ML 227056-1L
1 L	Tetrahydrofuran (THF)	109-99-9	anhydrous, ≥99.9%, inhibitor-free 401757-1L
	Dihydrolevoglucosenone (Cryene)	53716-82-8	807796-100ML 807796-1L
Polymers			
	Polystyrene (PS)	9003-53-6	average Mw 192,000 430102-1KG
	Poly(styrene-co-butadiene)	9003-55-8	butadiene 4 wt. %, melt index 6 g/10 min (200°C/5kg) 430072-1KG
	Poly(styrene-co- α -methylstyrene)	9011-11-4	457205-250G
	Polybenzimidazole (PBI)	26985-65-9	rod, diam. 9.5 mm, L 25 mm, black GF31259527-1EA
	Polyaniline (PANI / emeraldine salt)	25233-30-1	average Mw >15,000, powder (Infusible), 3-100 μ m particle size 428329-5G
	Polyvinylcarbazole (PVK)	25067-59-8	average Mw ~1,100,000, powder, 182605-5G

title:

- <a point>
- <another point>

<content> <**key concept**> <**key concept**>

